Bioactive Materials 39 (2024) 74–105

Contents lists available at ScienceDirect

Bioactive Materials

journal homepage: www.keaipublishing.com/en/journals/bioactive-materials

Review article

Structure-function integrated biodegradable Mg/polymer composites: Design, manufacturing, properties, and biomedical applications

Xianli Wang [a,b,c], Cheng Wang [a,b], Chenglin Chu [a,b], Feng Xue [a,b], Jun Li [c,**], Jing Bai [a,b,*]

[a] School of Materials Science and Engineering, Southeast University, Jiangning, Nanjing, 211189, Jiangsu, China
[b] Jiangsu Key Laboratory for Advanced Metallic Materials, Jiangning, Nanjing, 211189, Jiangsu, China
[c] Department of Biomedical Engineering, College of Design and Engineering, National University of Singapore, Singapore, 119276, Singapore

ARTICLE INFO

Keywords:
Mechanical property
Interface
Biodegradation
Stimuli-responsiveness
Tissue engineering

ABSTRACT

Mg is a typical biodegradable metal widely used for biomedical applications due to its considerable mechanical properties and bioactivity. Biodegradable polymers have attracted great interest owing to their favorable processability and inclusiveness. However, it is challenging for the degradation rates of Mg or polymers to precisely match tissue repair processes, and the significant changes in local pH during degradation hinder tissue repair. The concept of combining Mg with polymers is proposed to overcome the shortcomings of materials, aiming to meet repair needs from various aspects such as mechanics and biology. Therefore, it is essential to systematically understand the behavior of biodegradable Mg/polymer composite (BMPC) from the design, manufacturing, mechanical properties, degradation, and biological effects. In this review, we elaborate on the design concepts and manufacturing strategies of high-strength BMPC, the "structure-function" relationship between the microstructures and mechanical properties of composites, the variation in the degradation rate due to endogenous and exogenous factors, and the establishment of advanced degradation research platform. Additionally, the interplay among composite components during degradation and the biological function of composites under non-responsive/stimuli-responsive platforms are also discussed. Finally, we hope that this review will benefit future clinical applications of "structure-function" integrated biomaterials.

1. Introduction

With the development of modern society, the incidence of various tissue injuries caused by accidents and population aging is on the rise. Researchers are dedicated to advancing tissue engineering for the repair and replacement of damaged and/or lost tissues and structures [1]. To minimize damage to autologous tissues and mitigate adverse reactions such as immune rejection caused by allogeneic grafts, extensive researches are conducted on biomaterials to overcome these challenges. Among various biomaterials, metals are one of the oldest and most widely studied material categories. Currently, the most commonly used metal biomaterials in clinical practice include mechanically superior titanium alloys, cobalt alloys, and stainless steel.

However, traditional biologically inert metal materials face challenging issues, including slow tissue repair rates and the need for secondary surgeries for removal. In contrast, biodegradable metals exhibit biological activity, and their degradation by-product (mainly metallic ions) facilitate the acceleration of local tissue healing. Moreover, the metabolized products can be excreted from the body, alleviating the contradiction between patients and outdated medical devices. In 2016, the American Society for Testing and Materials (ASTM) released ASTM-F3160 as a reference standard for the development and testing of biodegradable metal materials. Biodegradable metals are defined as "initially apparent foreign substances or substances that can be metabolized or assimilated directly or indirectly by cells and/or tissues through expected degradation [2]". Currently, the main biodegradable metals that meet this standard are Mg, Zn, Fe (iron), and their alloys. These biodegradable metals are considered revolutionary medical materials due to two significant advantages. (i) They do not require secondary surgeries for removal, reducing the burden on patients. (ii) Their comprehensive mechanical properties are superior to other biodegradable materials such as polymers, ceramics, and bio-glass. Their

Peer review under responsibility of KeAi Communications Co., Ltd.
* Corresponding author. School of Materials Science and Engineering, Southeast University, Jiangning, Nanjing, 211189, Jiangsu, China.
** Corresponding author.
E-mail addresses: jun-li@nus.edu.sg (J. Li), baijing@seu.edu.cn (J. Bai).

https://doi.org/10.1016/j.bioactmat.2024.05.024
Received 14 April 2024; Received in revised form 10 May 2024; Accepted 11 May 2024

mechanical properties are closer to natural bone than other non-degradable metals. Therein, Mg has relatively weaker mechanical properties but a modulus closer to that of natural cortical bone than other biodegradable metals, thereby reducing "stress shielding" effects. Therefore, Mg has garnered significant attention from researchers in the field of bone repair. By alloying or deformation processing, Mg alloys with Young's modulus in the range of 37.5–65.0 GPa and ultimate tensile strength in the range of 190–250 MPa can be obtained [3]. Zn alloys have slightly higher mechanical properties, with Young's modulus ranging from 90.0 to 105.0 GPa and ultimate tensile strength ranging from 100 to 520 MPa [4,5]. Fe alloys exhibit the strongest mechanical properties, with Young's modulus and ultimate tensile strength fluctuating within the range of 200–205 GPa and 540–1000 MPa, respectively [6] (Fig. 1A).

In addition to biodegradable metals, biodegradable polymers are extensively utilized in the medical field due to their wide availability of source materials and ease of processing. Biodegradable polymers are defined as "polymers that degrade into normal metabolites or products both *in vitro* and *in vivo* that can be eliminated from the body with or without further metabolic transformation" [7]. Biodegradable polymers can be classified into natural biodegradable polymers and synthetic biodegradable polymers based on their sources. At present, the commonly used natural biodegradable polymers in the medical field include cellulose, starch, alginate, chitosan, hyaluronic acid, and collagen. Synthetic biodegradable polymers include esters, amides, ethers, urethanes, or hybrid systems [8]. Among them, poly (lactic acid) (PLA) is derived from plant sources such as corn stalks, and it is processed through ring-opening polymerization. PLA finds widespread use in surgical sutures, drug encapsulation, tissue engineering scaffolds, organ anti-adhesion protection, and other fields. Its biocompatibility is also certified by the U.S. Food and Drug Administration (FDA).

Although biodegradable metals or polymers have their respective advantages, their individual disadvantages are also quite evident. Taking Mg for example, the major issue with Mg metal is its rapid degradation rate (standard electrode potential −2.37 V vs. SCE). Its structural integrity is compromised before tissue repair, leading to poor mechanical compatibility [9,10]. Additionally, the rapid degradation of Mg results in adverse reactions such as the release of large amounts of H_2 gas and strong alkalinity around Mg. Therefore, proper protection strategies are required to improve the corrosion resistance [11,12]. Compared to Mg metals, Zn and Fe metals exhibit better corrosion resistance, but they often degrade too slowly in the body, potentially persisting after tissue repair. For biodegradable polymers, their mechanical strength is relatively low (Young's modulus less than 7.0 GPa), making it challenging to meet the mechanical compatibility needs for some tissue repair (e.g. cortical bone: Young's modulus ranges from 14.0 GPa to 20.0 GPa) [13]. Furthermore, their degradation products often consist of small molecules with acidic groups, causing local pH imbalance and inflammation in physiological environments [14]. More importantly, most synthetic polymer materials exhibit bioinert and lack cell recognition signals on their surfaces, thus hindering cell adhesion, proliferation, and differentiation [15].

To overcome their respective shortcomings, previous researchers borrowed the design concept of composites, allowing biodegradable metals and polymers to complement each other's characteristics and maximize their functionality (Fig. 1B). Combining the advantages of both metals and polymers, composites attract widespread attention globally. As shown in Fig. 1C, according to the Web of Science database, the number of publications related to biodegradable metal/polymer composites has sharply increased over the past decade. Among them, the number of papers related to BMPC is significantly larger than those related to biodegradable Zn (or Fe)/polymer composites. Therefore, topics related to biodegradable Mg and their composites are relatively new and hot, and we mainly discussed BMPC in this review. The visual network graph in Fig. 1D illustrates the prominent research areas in the field of BMPC. Most studies revolve around the interface bonding, mechanical properties, corrosion, degradation, ion release, as well as biocompatibility and tissue engineering applications of Mg/polymer composites. These areas also represent the future development trends of biodegradable metal/polymer composites.

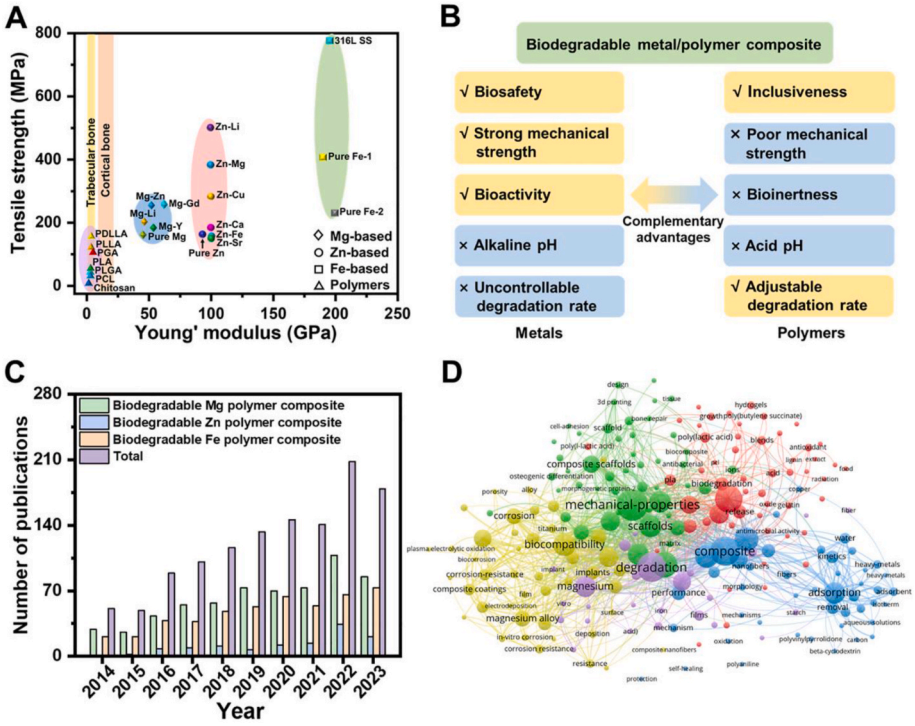

Fig. 1. (A) Comparison of mechanical properties of biodegradable metals and polymers with natural trabecular bone and cortical bone [3,5,6,16–22]. (B) Design concepts for biodegradable metal/polymer composites. (C) A total number of publications since 2013 on biodegradable metal/polymer composites retrieved from Web of Science databases. (D) Network visualization plot of hot research words in the field of BMPC.

Although BMPC are increasingly widely used in tissue engineering, most of the work in this field lacks well-established material composite strategies and comprehensive evaluation systems for material performance in tissue engineering applications. This deficiency leads to a lack of systematic analysis regarding the interactions and mechanisms between implanted degradable materials and cells/tissues. Therefore, it is crucial to establish a comprehensive understanding of the factors influencing the performance of BMPC at various stages, from processing to biological applications.

In this review paper, based on our expertise in composite design, we first introduced representative enhancement methods and processing techniques for biodegradable Mg/composites, elucidating the toughening mechanisms of these composites. Subsequently, we discussed endogenous and exogenous factors influencing the mechanical properties, local environmental composition, and degradation rates of composites, revealing the interactions and mechanisms among composite components during degradation. Especially, considering the disparities between *in vitro* platforms and *in vivo* physiological environment [23], we introduced a real-time degradation research platform, which better mimicked *in vivo* environmental factors in evaluating biodegradable materials degradation. Furthermore, we reviewed the potential molecular mechanisms of these biodegradable composites in repairing various tissues in the body, including bone, cartilage, blood vessels, nerves, and other tissues. Finally, building on the existing biological activity of these BMPC, we discussed strategies for constructing intelligent platforms that enhance tissue repair capabilities through their stimuli-responsiveness.

2. Design, manufacturing, and strengthening mechanism

Although biodegradable materials have their advantages, their disadvantages are also obvious. Combining biodegradable polymers with Mg allows the achievement of various functionalities by adjusting their components, structures, and forms. The composite of these two materials can leverage their strengths and compensate for their weaknesses. This approach not only addresses the poor mechanical compatibility issue in composites but also overcomes the problems caused by the overly alkaline or acidic local microenvironments resulting from their respective degradation products. It maximally meets the requirements for tissue repair.

The development of BMPC with high strength involves three aspects: the Mg reinforcement phase, the polymer matrix, and the interface between the two components. Our research group has accumulated some experience in these areas, leveraging precise microfabrication of Mg and synthesizing various microstructures, including micro or nanoparticles, ultrafine fibers, fiber networks, rods, sheets, etc. Additionally, techniques like severe plastic deformation are employed to enhance the mechanical compatibility of the composites during the preparation of BMPC (Fig. 2). In the following section, we will elaborate on three parts including the preparation of the Mg reinforcement phase, processing of the polymer matrix, and the interface bonding of BMPC.

2.1. Reinforcement phase design

Considering the perspective of the reinforcement phase in composites, Mg with densely packed hexagonal structures, unlike other metals, have limited slip systems, making it challenging to obtain high-quality, micro-scale reinforcement metals through convenient processing or synthesis methods. Take Mg as an example; due to its highly reactive nature, it is difficult to achieve highly precise micro-nano reinforcement phases through bottom-up approaches. Unremitting efforts are paid to

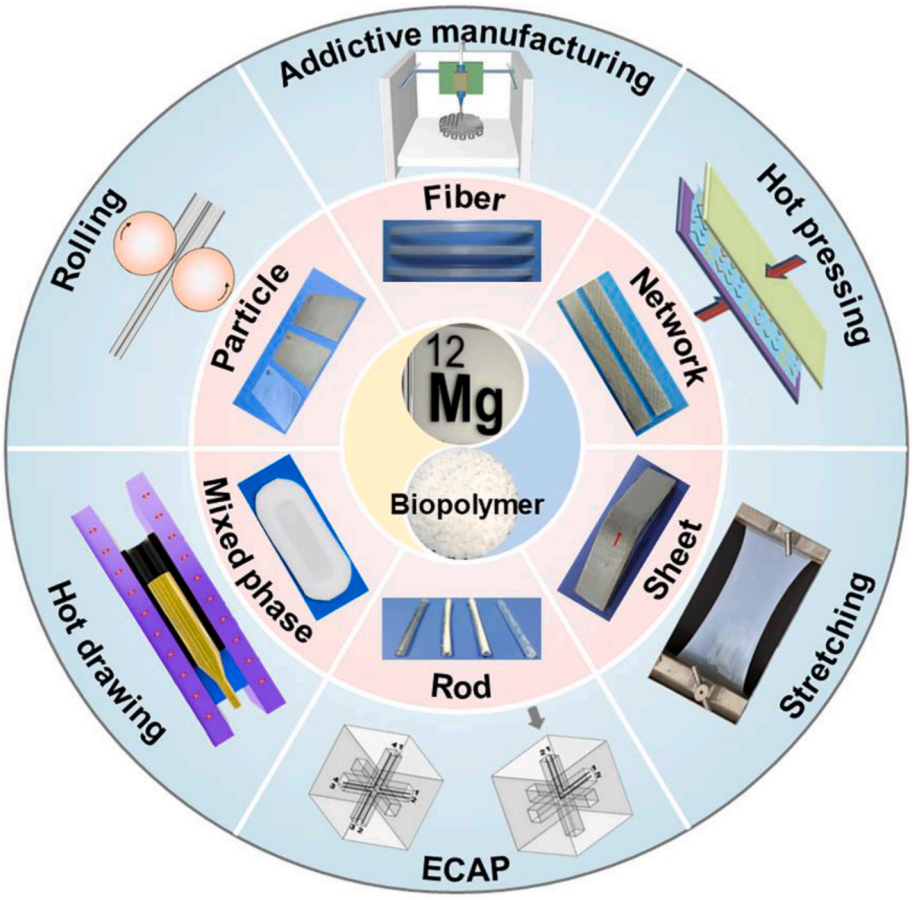

Fig. 2. Shape and processing method of reinforcement phase in BMPC with high strength and toughness.

overcome the processing bottleneck of Mg microstructures and contribute to the production of Mg/polymer composites with reinforcement phase morphologies primarily including particle, fiber, network, sheet, rod, and mixed forms. Examples of these will be discussed below.

2.1.1. Particle reinforcement

Particle reinforcement is one of the most common methods for strengthening composite. It achieves the isotropic formation of composites through the non-continuous enhancement of discrete particles. Specifically, the proportion of Mg particles in the composite can be flexibly adjusted, allowing easy molding adjustments based on existing processing techniques. The particle reinforcement method is widely applied in various polymer-based materials, enhancing both the mechanical performance and biological functionality of composites simultaneously [24,25]. Unlike other reinforcements, small particles are more prone to agglomeration, leading to a decrease in the mechanical properties of the composites. Reportedly, the addition of Mg micro/-nanoparticles to PLA resulted in changes to the PLA crystal structure. A small amount of Mg could be uniformly dispersed in the PLA matrix, acting as a heterogeneous nucleating agent. It resulted in an increment of the PLA crystallinity. However, an excess of Mg could lead to partial agglomeration, which was detrimental to PLA crystallization. Particularly during PLA processing, when the molecular chains were in an amorphous state and needed to rearrange to form an ordered crystalline structure, Mg impeded this process, leading to a decrease in the crystallinity of the PLA [26]. Therefore, it is not advisable to incorporate excessive amounts of particles in composites.

2.1.2. Fiber reinforcement

Fibers are a common reinforcement in composites, notably, carbon fibers used in resin composites, offering strength comparable to steel but with a significantly lower strength-to-weight ratio. In the field of degradable materials, continuous Mg microfibers also serve as reinforcements for polymer materials. For example, Ali et al. [27] utilized continuous AZ31 Mg alloy fibers to create a unidirectionally reinforced PLA composite, mimicking the microstructure of natural “bamboo”. These materials exhibit remarkable bending strength, holding substantial value in the field of orthopedic fixation devices.

2.1.3. Network reinforcement

Compared to unidirectionally reinforced polymers by fibers, two-dimensional or three-dimensional fiber networks can enhance the anisotropy of composites, addressing fixation issues essential for their use in orthopedic devices. For instance, Li et al. [28] employed two-dimensional fiber weaving techniques, incorporating rational AZ31 Mg alloy fiber weaving angles (15°, 30°, 45°, and 60°) to ensure fiber continuity. This approach mitigated problems related to decreased load-bearing capacity caused by perforations in composite bone plates, enabling the plate to exhibit exceptional resistance to impact loads. When the weaving angle of the AZ31 Mg alloy fiber network was set at 30° with a volume fraction of 12 %, the composite plate achieved maximum tensile and shear strengths of ~82.0 MPa and ~82.4 MPa, respectively.

2.1.4. Sheet reinforcement

Compared to fiber reinforcement methods, Mg sheets used as reinforced phases offer a convenient way to achieve high-strength composite plates. As the volume percentage of Mg sheets increases, their strength gradually approaches the mechanical strength of pure Mg. This not only imparts excellent mechanical properties to the composite but also slows down the corrosion rate of the Mg due to the protection of polymers. For instance, Cai et al. [29] utilized the Mg-2Zn sheet as a reinforcing phase and hot press method to prepare the Mg-2Zn/PLA composite plate. When the volume percentage of the Mg-2Zn sheet reached 80 %, the tensile strength and bending strength of Mg-2Zn/PLA composite plates (120 mm × 12 mm × 2.5 mm) reached their maximum values, ~116 MPa, and ~230 MPa, respectively.

2.1.5. Rod reinforcement

In addition to sheet reinforcement, which significantly improves mechanical properties by increasing the proportion of Mg in composites, transforming the shape of the reinforcing Mg and employing appropriate processing techniques can yield rod-shaped composites to meet diverse requirements. For instance, Muhammad et al. [30,31] utilized AZ31 Mg alloy rods with a diameter of 2.44 mm as a reinforcing phase in composites. By combining injection molding techniques, they obtained AZ31 Mg alloy/PLA composite rods with a diameter of 4 mm. Through appropriate surface modifications, the tensile strength and bending strength of the composite rods increased from ~60 MPa to ~118 MPa to about ~131 MPa and ~245 MPa, respectively.

2.1.6. Mixed reinforcement

To meet the mechanical and biological requirements for tissue repair, it is necessary to composite two or more reinforcing phases with polymers. For instance, to address the need for bone defect repair in oral bacterial growth environments, we integrated pure Mg sheets and MgO nanoparticles into poly(caprolactone) (PCL) [32]. We employed a combination of “casting method + electrospinning” for composite processing, sandwiching Mg sheets in the middle and exposing MgO nanoparticles on the surface. This resulted in an Mg-MgO/PCL-guided bone tissue regeneration membrane with a Janus structure. Leveraging the plastic deformation advantage of Mg sheets, the composite membrane provided ~0.91 N mm^{-1} of supportive force to the flexible PCL membrane, aiding in maintaining the growth space for oral bone tissues. Furthermore, the embedded MgO nanoparticles not only further increased the supportive force of the composite membrane (~0.94 N mm^{-1}) through heterogeneous nucleation but also provided its membrane with long-lasting broad-spectrum antibacterial capabilities, owing to their inherent chemical properties. Furthermore, Ali et al. [33] developed a BG/Mg/PLA hybrid composite by incorporating AZ31 Mg wires (with diameters of 313 μm) and bioactive glass (BG) fibers (with diameters of 20–40 μm) into PLA (Fig. 3A, B). In this case, the Mg wires with high elongation limited the cluster formation of BG fibers and the expansion of cracks in the composite, a phenomenon referred to as the “positive hybrid effect”. The resulting hybrid composite exhibited mechanical strength comparable to cortical bone (tensile strength: ~137 MPa; elastic modulus: ~13.4 GPa; at a BG fiber content of 25 vol% and Mg wire content of 30 vol%). The composite also had a good maintenance of mechanical properties during the degradation process.

Among the various Mg metal reinforcement phases, it is undeniable that the presence of reinforcement phases in the form of fibers, sheets, or rods can significantly improve the mechanical properties of BMPC, and the improvement degree in mechanical properties is positively correlated with the volume percentage of Mg metal. In contrast, the improvement degree in the form of micro/nanoparticles or short fibers is smaller, and it may even lead to a decrease in BMPC performance due to the presence of agglomeration phenomena. Therefore, the reinforcement phase should be flexibly selected according to the usage conditions.

2.2. Manufacturing methods

From the perspective of the polymer matrix in composites, although increasing the polymer’s molecular weight can significantly enhance the mechanical properties of the composite, there is a direct correlation between polymer molecular weight and cost. Therefore, it is economically impractical to increase the strength of composites by improving the molecular weight of polymers. To overcome this challenge, utilizing physical methods for further processing of Mg/polymer composites to achieve high strength and toughness is a more ideal approach. Adhering to this concept, several famous research groups worldwide developed

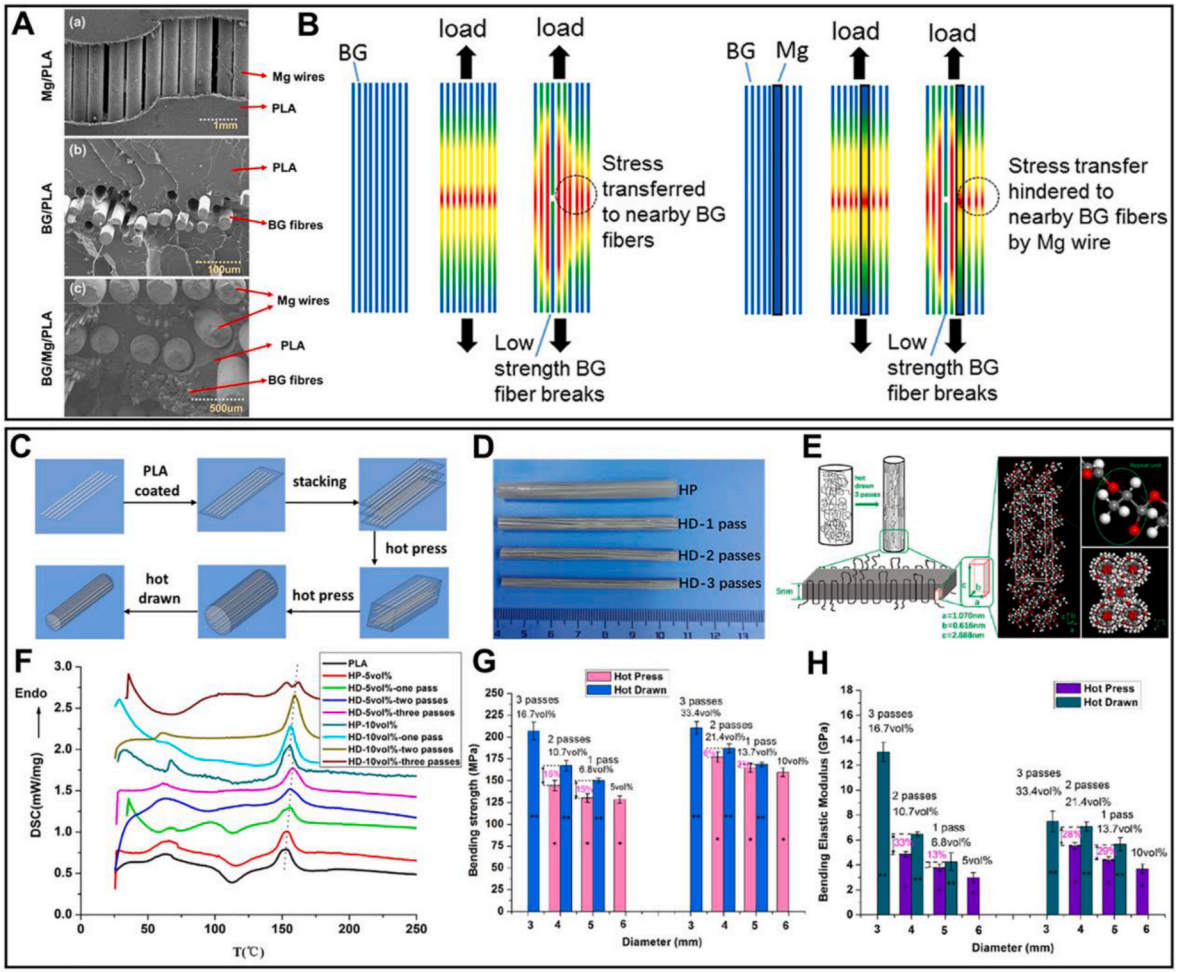

Fig. 3. The manufacturing process, strengthening/toughening mechanism of Mg/polymer composites. (A) Fractured surface of different composites. (B) Schematic of failure development upon breakage of low-strain BG fibers: stress transfer to nearby BG fibers and stress transfer to nearby BG fibers hindered by Mg wire [33]. (C) Illustration of the hot-drawn preparation process of Mg alloy fibers/PLA composite rod. (D) 10 vol% Mg/PLA composite rods prepared by hot pressing and hot drawing from one pass to three passes. (E) The changes of orientation and molecular conformation of PLA chains during the hot drawn process. (F) DSC curves of PLA at different states. (G) The bending strength and (H) bending elastic modulus of the composite rods for hot pressed and hot drawn states with initial fibers content of 5 vol% and 10 vol% [40]. Copyright 2020, 2018, Elsevier.

innovative methods including injection molding, equal channel angular extrusion (ECAP), hot pressing, hot drawing, stretching, rolling, additive manufacturing, etc. These methods enable the BMPC with high strength and toughness.

2.2.1. *Injection molding*

Injection molding is one of the most utilized methods to transform thermoplastic polymers into complex and high-precision products. The primary process involves the reciprocating motion of the screw in the barrel of an injection molding machine, utilizing frictional heating to melt the incoming thermoplastic resin. Subsequently, the polymer melt is forced into the mold cavity and then cooled for shaping [34]. Injection molding can process granules and powders, with the final shape of the product determined by the mold, such as cylinder, plate, rod, and film [35]. Differing from common injection molds, Muhammad et al. [30,31] designed a cylindrical mold chamber containing an AZ31 Mg alloy rod. When the PLA pellet melt flowed into the mold chamber from the injection machine, the chamber also applied pressure around the rod. After cooling, a composite rod wrapped with a PLA coating was obtained. When the diameter of the AZ31 Mg alloy rod was 2.44 mm and the composite rod's diameter was 4 mm, the tensile strength and bending strength of the Mg-MgF_2/PLA composite rod reached ~131 MPa and ~245 MPa, respectively.

2.2.2. *ECAP*

In the field of metallurgy, ECAP is a process of shearing deformation that compresses polycrystalline samples into specialized molds, achieving high strain levels. It primarily refines the material's grains through pure shearing effects during deformation, thereby significantly enhancing the material's mechanical and physical properties. Thermoplastic polymers can also undergo shear deformation to achieve molecular orientation through ECAP processing. The controllable orientation of polymer molecular chains can be induced with ECAP without altering the sample's geometric shape [36].

To effectively enhance the mechanical strength of PLA, Li et al. [37] designed a multi-channel mold to induce shear deformation in PLA through ECAP techniques. This not only resulted in varied preferred orientations of molecular chains in the crystalline and amorphous regions of PLA but also created distinct microstructures. After two rounds of ECAP processing, PLA's bending strength increased from ~98 MPa to ~167 MPa. Meanwhile, the fracture toughness of PLA processed three times with ECAP rose from ~1.6 MPa $m^{1/2}$ to ~3.3 MPa $m^{1/2}$. After 16 weeks of *in vitro* degradation in phosphate buffer saline (PBS), the bending strength of the ECAP-processed PLA samples remained significantly higher than the initial strength of the unprocessed PLA samples. Despite numerous studies that report significant mechanical improvements in polymers post-ECAP, research on the polymer channel design

and the mechanism of shear deformation under ECAP still requires further exploration.

2.2.3. Hot pressing

Hot pressing refers to a process of manufacturing powdered or flake materials under heated and pressurized conditions. This powder integration process has a long history in the powder metallurgy industry. For Mg/polymer composites, the polymer materials are first heated to their melting point. Then, the polymer materials bridge and adhere to each other across the Mg under pressure, ultimately achieving monolithic molding of the composite.

In the study of Li et al. [38], high-strength AZ31 Mg alloy/PLA composite was first calculated by finite element analysis to optimize the distribution manner for obtaining the highest bending strength of AZ31 Mg alloy fibers in PLA matrix under the same volume percentage. Subsequently, they bonded the unidirectionally arranged Mg alloy fibers and PLA through thermal pressing. After pressurizing for 15 min at 5 MPa and 190 °C, they obtained a composite plate with relatively consistent theoretical and actual bending strengths. When the volume percentage of AZ31 Mg alloy fibers was 40 %, the tensile strength, bending strength, and impact strength of the composite were ~108 MPa, ~190 MPa, and ~150 kJ m^{-2}, respectively. Ali et al. [39] also conducted similar work to Li's but with some differences. To enhance the mechanical strength of the Mg/PLA composite further, they increased the average molecular weight of PLA to a range of 90,000–120,000 g/mol, and the Mg fiber content reached up to 50 vol%. After being subjected to higher heating temperature (190 °C) and insulation, the tensile strength and flexural strength of the Mg/PLA composite sheet were ~164 MPa and ~245 MPa, respectively. The elastic modulus and flexural modulus were ~12.9 GPa and ~12.3 GPa, respectively.

2.2.4. Hot drawing

Although the use of fibers or fiber network reinforcement has yielded composites with high bending strength, there remains a gap in meeting the strength requirements of load-bearing human bones. To achieve higher strength in bone fixation devices, Cai et al. [40] obtained Mg-2Zn alloy fibers unidirectionally reinforced PLA (Mg/PLA) composite plates based on their earlier works. They further obtained tougher composite rods enhanced by Mg-2Zn fibers through multiple passes of hot drawing at 80 °C (Fig. 3C). As shown in (Fig. 3D, E), the diameter of the composite rod gradually decreased with each drawing pass, and the molecular chains inside the PLA became more orderly. The heating process, concurrent with the drawing process, not only forced the molecular chains in the non-crystalline areas of PLA to orientate but also induced reorientation and recrystallization in the crystalline areas due to their rubbery state at 80 °C. The crystallinity of PLA in the composite rod also increased with each drawing pass. With an initial fiber content of 10 vol %, the crystallinity surged from an initial 13.30 %–86.00 % after three drawing passes (Fig. 3F).

Utilizing this cooperative enhancement technique involving fiber reinforcement and self-enhancement of PLA, when the volume percentage of Mg-2Zn alloy fiber was 16.7 %, the Mg/PLA composite rod reached a bending strength of ~211 MPa and a bending modulus of ~13.0 GPa (Fig. 3G, H) following three hot-drawing passes. This far exceeded the bending strength of cortical bone (~176 MPa), or was comparable to the bending strength of degradable fixation products produced by some well-known domestic and international manufacturers (e.g. Jiangsu Dikang Medical Technology Co., Ltd from China: ~110 MPa; Inion Freedom Screw from Finland: ~150 MPa; Tianjin Boshuobei Biotechnology Co., Ltd from China: ~210 MPa; GRAND FIX from Japan: ~215 MPa).

2.2.5. Stretching

Stretching technology is common in the processing of plastic resins or plastics such as polypropylene, poly (ethylene terephthalate), poly (ethylene terephthalate), polyoxymethylene, polytetrafluoroethylene, and PLA. It is widely used in the formation of thin films for areas including product packaging, insulation materials, and decorative materials. Stretching methods encompass uniaxial and biaxial stretching processes, with biaxial stretching techniques further subclassified into tube film (blow molded film) bidirectional stretching and flat film bidirectional stretching. The optical and mechanical performances of the obtained film are significantly impacted by the type of plastic substrate, stretching process, and material compounding methods.

Shi et al. [41] discovered that uniaxial stretching significantly affected the crystalline melting behavior, phase blending, crystal structure, and mechanical properties of the poly (L-lactide)/poly (vinyl acetate) (PLLA/PVAc) blend a lot. Post-stretching, the PLLA/PVAc blend displayed a fully blended phase system, with a stretching ratio significantly promoting molecular chain orientation and crystallization, thus enhancing the crystallization. Combining a suitable ratio of PLLA to PVAc and a stretching ratio could significantly improve PLLA's mechanical performance. When the stretching ratio was 6 and PVAc accounted for 5 wt%, a blend with Young's modulus, tensile strength, and elongation at break of ~3923 MPa, ~190 MPa, and ~31.7 %, respectively, could be obtained. This research provided theoretical support for the large-scale practical application of PLLA.

2.2.6. Rolling

Contrary to the stretching method, which only applies tension to the material, the rolling process exerts compressive forces concurrently, leaving a gradual thinning in thickness and a denser structure. From the perspective of the rolling direction, it can be divided into unidirectional and bidirectional rolling. Classified by processing temperature, rolling methods include cold rolling and hot rolling.

Cold rolling refers to a manufacturing method performed at temperatures below the glass transition temperature of the polymer. Research results illustrated that cold rolling of PLA-based composite at room temperature significantly affected its crystal morphology, crystallinity, density, molecular orientation, microhardness, and mechanical properties [42]. Although the orientation of PLA molecular chains increased with the rolling ratio, the crystallinity decreased gradually. This was primarily due to the highly oriented PLA molecular chains in the amorphous region during the rolling process at room temperature, which resulted in the destruction of the quasi-crystal and subsequently lowered the crystallinity. Static and dynamic mechanical analyses indicated that PLA exhibited anisotropy during the rolling process.

Hot rolling, for metal materials, refers to the rolling performed above their recrystallization temperature. For composites containing thermoplastic polymers, the hot rolling temperature is usually controlled above the glass transition temperature of the polymer and below its melting point temperature. During this phase, the thermoplastic polymer is in a rubber state with a great deformation capacity. Simultaneously, the plasticity of the metal during hot rolling is high and the deformation resistance is low, greatly reducing the energy consumption of metal deformation. During hot rolling, deformation microstructures or orientation structures may appear in the composite, thereby significantly improving its mechanical properties in the rolling direction. Building on this, our previous study proposed an accumulative rolling method to overcome the uneven Mg microparticle distribution in particle-reinforced PLLA composite membranes [43]. Initially, composite membranes were stacked in the designed sequence and hot pressed into a whole piece. Then, a hot-rolling process with a rolling ratio of 50%–87.5 % was performed at 140 °C. This novel accumulative rolling method not only overcame the uneven spatial distribution of Mg microparticles in PLLA composite membranes but also yielded a composite membrane with an order of magnitude improvement in mechanical properties. When the mass percentage of Mg was 5 wt% and the rolling ratio was 75 %, the resulting composite membrane achieved a tensile strength, Young's modulus, and fracture elongation of ~104 MPa, ~2.6 GPa, and ~53 %, respectively, comparable to some metallic materials such as pure Mg or Zn metal membranes.

Compared to the cold rolling method, hot rolling can result in PLA molecular orientation and a substantial increase in crystallinity. This is primarily because the molecular chains cannot reorganize and crystallize during cold rolling at room temperature, and only the molecular chains in the amorphous region are forced to orient. However, when hot rolling at temperatures above the PLA glass transition temperature, PLA is in a rubbery state and the mobility of molecular chains in both the crystalline and amorphous regions is enhanced, allowing them to reorient and recrystallize.

2.2.7. Other methods

Besides the proposed mechanical processes, high-strength PLLA and its composites with a bending strength ranging from ~200 MPa to ~450 MPa can also be achieved by forging and pressing or extrusion methods [44]. To achieve a uniform dispersion of Mg/PLA composite materials, Lee et al. [45] employed a combination of the high-shear mixing method and the hot-pressing method to prepare cylindrical Mg/PLA composites for bone repair. The key steps involved the incorporation of Mg microparticles into the PLA melt through high-shear mixing, followed by further hot-pressing molding. When the Mg microparticles content in the composite material was 15 wt%, the compressive strength reached ~107 MPa, and the compressive modulus reached ~2.3 GPa, which was a significant improvement compared to the values of pure PLA materials (~69 MPa and ~1.6 GPa, respectively).

In addition to pursuing only high mechanical performance, multifunctional and personalized composite processing technologies (such as 3D printing) have also been developed in recent decades [46]. For instance, Dong et al. [47] combined Mg microparticles and PCL together and fabricated a Mg/PCL composite bone scaffold with a high porosity and connectivity rate using a fused deposition modeling (FDM) 3D printer. Compression test results showed that when the mass percentage of Mg microparticles was 5 wt% and the scaffold's porosity was 66.0 %, the compressive strength and modulus of the Mg/PCL scaffold were ~6.6 MPa and ~0.06 GPa, respectively. This matched the mechanical properties of human cancellous bone. In the preparation process of filament for FDM 3D printing, the colloidal route was also developed by Barrasa [48] to achieve uniform dispersion of Mg microparticles in composite filaments. To simplify the filament preparation step, low-temperature rapid prototyping technology was developed by Lai's group and it was applied to the preparation of Mg/polymer composites by mixed liquid slurry [49]. Mg/tricalcium phosphate/poly(L-lactide-*co*-glycolide) (Mg/TCP/PLGA) porous scaffold (porosity: ~65.8 %) with compressive strength and modulus as high as 3.7 MPa and 0.11 GPa was obtained, respectively [50].

For materials required for soft tissue repair, flexibility is prioritized over strength to accommodate soft tissue. To this end, Huang et al. utilized electrospinning technology [51] to combine Mg microparticles and PLGA, creating a Mg function-enhanced PLGA composite microfiber membrane with an elongation rate of up to 260 %. The micro-porous structure of the microfiber membrane, similar to the bionic structure of the extracellular matrix, provided good adhesion sites for human adipose stem cells. Additionally, the presence of Mg^{2+} further stimulated the rapid proliferation and differentiation of these stem cells.

The methods mentioned for processing composites aim to enhance the mechanical adaptability of BMPC based on the Mg reinforcement phase. However, these methods have their advantages and limitations. For example, injection molding and hot pressing can improve composite density and ensure isotropy, with limited impact on the mechanical properties of the polymer matrix. While methods such as ECAP, rolling, hot drawing, and stretching drawing, inspired by severe plastic deformation in metal processing, can simultaneously improve structural density, crystallinity, and polymer phase orientation, thereby enhancing the mechanical properties of composites a lot. However, it is important to note that these self-reinforcement methods can only improve the mechanical properties of BMPC in a specific direction, leading to anisotropic mechanical properties. Therefore, in practical applications, attention should be paid to the mechanical requirements of BMPC in multiple directions. Additionally, 3D printing and electrospinning are additive manufacturing methods that can customize the shape and porosity of BMPC according to requirements, offering greater operational flexibility and conserving raw materials. However, the cost is that the internally porous structure may result in weaker mechanical properties. For example, our previous study found that the compressive modulus of polymer-based porous scaffolds prepared using 3D printing technologies did not exceed 200 MPa (when the porosity was greater than 60 %) [47]. For cortical bone and trabecular bone, their compressive moduli are as high as 14.0–18.0 GPa and 2.0 GPa [52], respectively, while the modulus of scaffolds obtained by 3D printing is much lower than those of natural bone. This limits their use to only filling bone defects, rather than being able to serve as bone fixation devices with supportive functions. Therefore, when using 3D printing technology to prepare BMPC, it is necessary to balance the biocompatibility and mechanical performance of limited raw materials. In summary, the choice of processing technology depends on the physiological application scenario's demands for the mechanical performance and structural characteristics of BMPC.

2.3. Composite interfacial modification

The reinforcement mediated by Mg can improve the mechanical performance of composites on the condition that there is a good coupling between the Mg filler and the polymer matrix. It is believed that the higher the content of the reinforcing phase, the better the mechanical properties of the BMPC. However, there is a different phenomenon in our previous study. It found that when unmodified Mg microparticles were added to polymers to construct Mg/PLLA membranes [43] or Mg/PCL scaffolds [47], the tensile strength (or compressive strength) of the composite material gradually decreased as the Mg content exceeded 5 wt%, which was associated with the introduction of voids and other defects caused by the addition of Mg. Additionally, when applied in scenarios requiring high mechanical strength (e.g., bone fixation), the acidic hydrolysis products of the polymer matrix during degradation may hasten the corrosion of untreated Mg, leading to a rapid reduction in the composite mechanical strength. For example, in the study by Wan et al. [53] where Mg particle-reinforced PLLA composites were prepared using injection molding, it was found that although the addition of Mg particles could mitigate the problem of localized acidic environments formed due to PLLA degradation, it exacerbated the material's tensile performance, failing to meet the mechanical compatibility requirements of the composite. This was primarily attributed to the poor binding performance between Mg particles and PLLA. Therefore, the key to extending the applications of BMPC not only includes exploring new composite measures but also manipulating the interface and avoids defects between the two components. While enhancing the mechanical reinforcement effect, the control of degradation rates of each component can effectively regulate the overall performance decay speed, which holds significant implications for mechanical performance, degradation traits, and physiological functionality of the composites.

While interfacial modification methods in composites can enhance adhesion, it is crucial to consider another important aspect. When it comes to biomaterials, biocompatibility always takes top priority. Existing literature indicates that some composites incorporating organic surface modifiers like silane coupling agents exhibit favorable biocompatibility *in vitro* or *in vivo* [26,54]. However, some studies also demonstrated a dose-dependent cytotoxicity of these organic agents [55], and the long-term risks associated with their retention in the human body remained unknown. Therefore, the current interfacial modification should emphasize biocompatibility.

To enhance the interfacial bonding between Mg and polymers, our research team developed a variety of organic and inorganic surface modification strategies (including micro-arc oxidation (MAO) coating,

fluoride coating (HF), polydopamine coating, and KH550 silane coupling agent coating), as illustrated in Fig. 4A [56]. The effects of different interface processing on the mechanical properties of composites were investigated from the microscopic interface characteristics and interface bonding strength after the phase separation. Through the approach of molecular dynamics calculation, the microscopic mechanism influencing the composite's interface bonding was revealed at the atomic scale (Fig. 4B–D). The key reason for the strong bonding at the Mg-2Zn-MAO/PLA composite interface was found to be the intense electrostatic interaction between the carbonyl O atom in PLA and MgO (on the surface of Mg-2Zn-MAO). Moreover, the micropores formed on Mg-2Zn fiber after MAO also enhanced the coupling of Mg metal and PLA due to the mechanical interlocking force (rivet effect). Through the combined action of hot pressing at 170 °C under the pressure of 5 MPa for 10 min, the voids between the Mg-2Zn-MAO fibers and PLA were eliminated, resulting in the highest bending strength observed in the composites (Fig. 4E, F) [29]. Similar to MAO, the plasma-electrolytic oxidation (PEO) method was also capable of achieving composites with strong interface bonding, superior mechanical performance, and controllable degradation after the hot-pressing process at 170 °C [27]. This was attributed to the micropores formed on the surface of Mg fibers by the PEO process, which provided space for PLA infiltration and mechanical interlocking effects. Among the surface modification methods for Mg mentioned above, MAO, PEO, and fluoride coating treatments are considered relatively safe methods, as they introduce only essential inorganic elements required by the human body.

Additionally, natural surface modifiers such as phytic acid can chelate Mg^{2+} to form phytate, thereby enhancing the bonding between Mg and PLA and slowing down the degradation rate of the composite in bodily fluids. This coating can also provide beneficial properties such as antioxidant characteristics and blood glucose reduction functionality. For instance, Lee et al. [57] performed physical (polishing) and chemical surface (phytic acid) treatments on AZ31 Mg alloy fibers. To ensure the interlayer bonding strength within the BMPC and eliminate defects at the interface while reducing the extrusion of PLA from the interface, they obtained the optimal parameters of 180 °C, 10 min, and 1 MPa pressure through optimized experiments. Despite a reduction in diameter after polishing, the results of mechanical property tests showed significant improvements in tensile strength, Young's modulus, flexural strength, and flexural modulus for the Mg/PLA composite containing 47.3 % Mg fibers. These values were recorded as ~154 MPa, ~14.2 GPa, ~226 MPa, and ~11.6 GPa, respectively, compared to the original samples. The enhancement of these mechanical properties was related to the increased surface roughness of AZ31 Mg alloy fibers after mechanical grinding and the coupling effect of phytic acid on Mg^{2+} and PLA.

For chemically active Mg, the surface modification methods of materials such as fibers, plates, rods, etc. With relatively large sizes are relatively simple. However, for Mg particles at the micro and nanoscale,

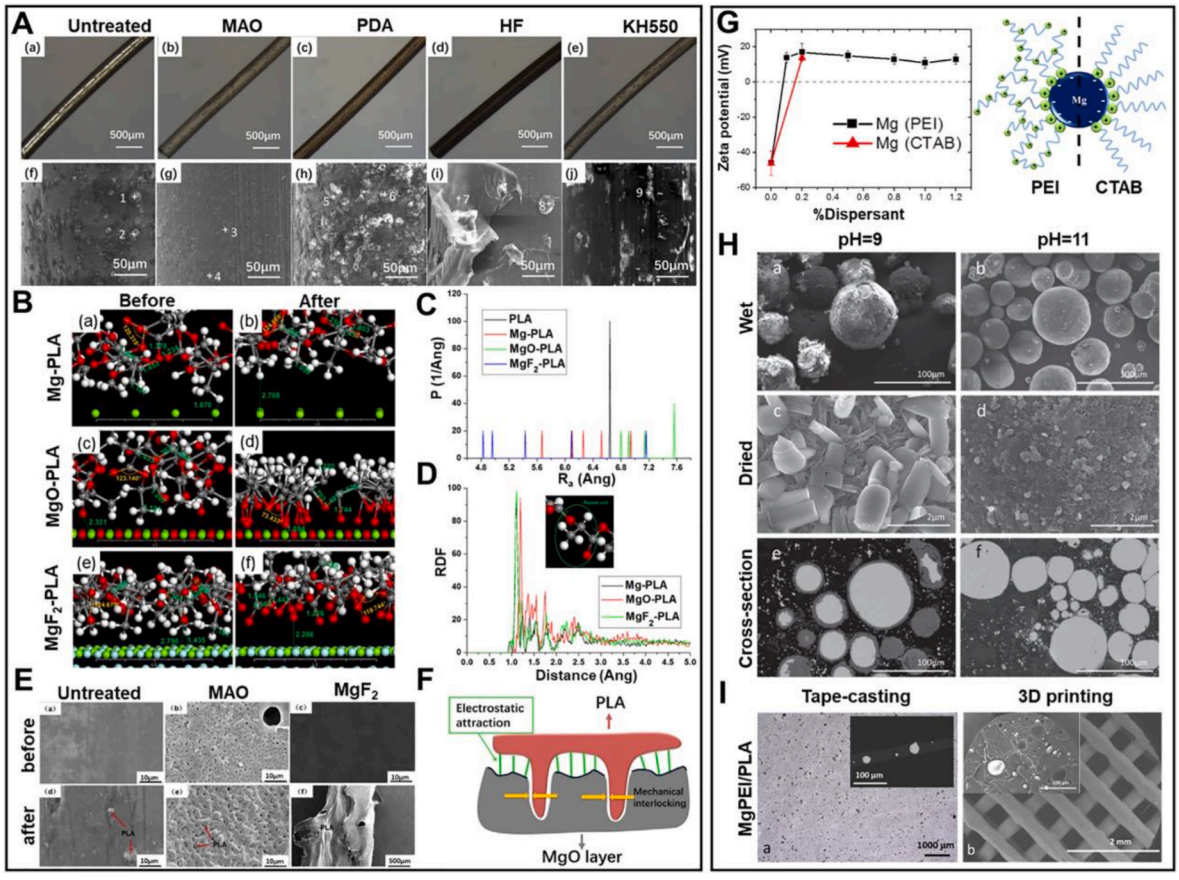

Fig. 4. Surface modification strategy of biodegradable Mg/polymer composite interface bonding. (A) Surface optical morphologies and SEM morphologies of Mg alloy fibers with different surface modifications after the pull-out experiments. (B) The changes in bond length, bond angle, as well as the distance from the PLA layer to the modified surface before and after molecular dynamic simulation. (C) Radius gyration (R_g) changes of PLA chains in the initial PLA structure and on the surface of Mg, MgO, and MgF_2 after dynamic simulation for 50,000 steps. (D) Radial distribution functions of PLA chains versus radial distance from Mg, MgO, and MgF_2 surface [56]. (E) SEM images of the surface morphology of Mg alloy with different surface modifications (Untreated, MAO, and MgF_2) before and after being combined with PLA after a shear test [29]. (F) Interface bonding mechanism between Mg alloy fibers and PLA matrix after MAO treatment [60]. (G) Evolution of the zeta potential of Mg suspension with the addition of PEI and CTAB, and illustrations of PEI and CTAB adsorption on Mg surface. (H) Surface micrographs and cross-section micrographs of Mg particles from aqueous suspensions at pH 9 and pH 11 [58]. (I) Surface micrographs and cross-section micrographs of MgPEI/PLA film (left: [26]) and scaffold with Mg addition of 10 wt% (right: [59]). Copyright 2018, 2019, 2020, Elsevier.

due to their larger specific surface area and tendency to readily react with water, surface modification in a neutral aqueous system is challenging. To tackle this problem, as depicted in Fig. 4G, Montero et al. [58] utilized cetyltrimethylammonium bromide (CTAB) and poly ethylenimine (PEI) respectively, as surface modifying agents for Mg microparticles under strongly alkaline conditions (pH > 11). Through the formation of ionic interactions between the dispersant and the matrix, modified Mg microparticles capable of stably suspending in Tetrahydrofuran, an organic solvent, were obtained. This was primarily due to the protective $Mg(OH)_2$ shell formed on the Mg microparticle surface under a strongly basic environment, preventing the Mg microparticles from becoming fully corroded (Fig. 4H). Furthermore, they utilized the tape casting method [26] and fused deposition modeling technique [59] to prepare Mg/PLA films and Mg/PLA porous scaffolds (Fig. 4I). The Mg microparticles modified with CTAB and PEI in the strongly basic environment were not only uniformly dispersed in PLA,

Table 1
Mechanical property comparison of BMPC.

Strategy	Mg/polymer	Mg content	Surface coating	Initial molecular weight ($\times 10^4$ g mol^{-1})	Tensile/Compressive modulus (GPa)	Tensile/Compressive strength (MPa)	Bending modulus (GPa)	Bending strength (MPa)	Elongation at break (%)	Shearing strength (MPa)	Ref.
Injection molding	AZ31 rod/PLA	37.2 vol%	–	6.0	–	69	–	199	–	–	[30,31]
		37.2 vol%	MAO	6.0	–	124–131	–	–	–	–	
		37.2 vol%	HF	6.0	–	108	–	245	–	–	
Hot pressing	AZ31 fiber/PLA	20 vol %	–	6.0	–	87	–	135	–	–	[61]
		50 vol %	–	9.0–12.0	12.9	164	12.3	245	–	–	[39]
		20 vol %	MAO	6.0	–	108	–	190	–	–	[61]
		50 vol %	Phytic acid	9.0–12.0	14.2	154	11.6	226	–	–	[57]
	BG fiber/AZ31 wire/PLA	30 vol %	–	9.0–12.0	13.4	137	–	–	–	–	[33]
	AZ31 network/PLA	10 vol %	–	6.0	–	68	–	–	–	80	[62]
		10 vol %	MAO	6.0	–	82	–	–	–	82.4	
	AZ31 sheet/PLA	70 vol %	–	5.5	–	90	–	219	–	70	[29]
		70 vol %	MAO	5.5	–	130	–	257	–	85	
		70 vol %	HF	5.5	–	116	–	230	–	75	
ECAP	—/PLA	0 %	–	6.0	–	–	4.5	168	–	–	[37]
Hot rolling	Mg particle/PLLA	5 wt%	–	7.8	2.6	104	–	–	53	–	[43]
Hot drawing	Mg-2Zn fiber/PLA	20 vol %	MAO	7.8	–	–	13.1	211	–	–	[40]
Forging and pressing/extrusion	—/PLLA	0 %	–	–	–	–	–	200–450	–	–	[44]
Strategy	Mg/polymer	Mg content	Surface coating	Initial molecular weight ($\times 10^4$ g mol^{-1})	Tensile/Compressive modulus (GPa)	Tensile/Compressive strength (MPa)	Bending modulus (GPa)	Bending strength (MPa)	Elongation at break (%)	Shearing strength (MPa)	Ref.
High-shear mixing + hot pressing	Mg particle/PLA	15 vol %	–	–	2.3	107	–	–	–	–	[45]
Electrospinning	Mg particle/PLGA	3 wt%	–	10.0	0.12	8.1	–	–	260	–	[51]
Colloidal route	Mg particle/PLA	5 wt%	PEI/PEG	18.2	3.6	40	–	–	–	–	[48]
3D printing	Mg particle/PCL	5 wt%	–	8.0	0.06	6.6	–	–	–	–	[47]
	Mg particle/TCP/PLGA	15 wt%	–	11.5	0.12	3.7	–	–	–	–	[50]
	Zn-1Mg particle/PLA	7 wt%	–	12.5–13.0	0.68	16	–	–	–	–	[25]

but also able to form covalent bonds with PLA at its melting temperature (165 °C) through PEI grafting on their surfaces. This approach might provide a new strategy for homogeneous and controllable degradation of Mg/polymer composites.

Although most of the current research about improving the interface of Mg/PLA composite materials focuses on enhancing the bonding between the composite components and extending the release period of Mg^{2+}, there are certain special requirements for specific physiological environments. For example, in the case of rapid bone formation, Mg^{2+} should be released in a controllable manner at a sufficient concentration to induce osteogenic differentiation of stem cells at an early stage and compensate for bone defects. An interesting experiment was conducted by Argentati et al. [35], where they subjected Mg particles to different surface treatments to improve the interface bonding, including heating in an oxidative atmosphere (TT) and surface modification using PEI. These modified Mg microparticles were then combined with PLA to extrude composite films, and the potential impact of these composites on the differentiation of human adipose-derived stem cells (hASCs) was investigated. The research findings revealed that among three Mg/PLA composite films containing 5 wt% Mg particles (untreated Mg/PLA, MgTT/PLA, and MgPEI/PLA), hASCs in the MgTT/PLA group exhibited the best osteogenic differentiation effect. The researchers attributed this to the faster release rate of Mg^{2+} from the composite films formed by Mg microparticles subjected to oxidative atmosphere heating, at a biologically safe concentration of Mg^{2+}.

Among the various interface modification methods mentioned above, they all can improve the bonding between Mg and polymer, focusing on enhancing either dispersion or interface bonding strength. However, they each have their advantages and limitations. Among them, the PEO and MAO methods are the most widely applicable and exhibit good biocompatibility after surface modification, but their drawback is that the implementation requires complex instruments. Organic surface modifiers such as KH550, PEI, and CTAB, although easy to implement, lack reliable verification of the biocompatibility of BMPC containing such surface modifiers. In contrast, surface modifiers such as phytic acid and HF are not only easy to implement but also can introduce beneficial elements into BMPC, making them a more favored means of interface modification.

To compare the efficacy of enhancing the mechanical properties of Mg/polymer composites through reinforcement measures, processing techniques, and interface modifications, we compiled the composites' comprehensive mechanical properties, as shown in Table 1, serving as a reference for future composite design and processing. Based on the previous context, it can be concluded that the main approaches to improve the mechanical properties of Mg/polymer composites are increasing the molecular weight of the polymer, increasing the proportion of Mg alloy, enhancing the interfacial bonding of composite components, and employing severe plastic deformation processing. Among these methods, interfacial modification and severe plastic deformation are undoubtedly the most cost-effective approaches.

2.4. Strengthening and toughening mechanism

Clarifying the "structure-function" relationship and toughening mechanisms between the microstructure and mechanical properties of existing BMPC is critically important for further developing materials with improved performance.

As mentioned in section 2.1, the incorporation of Mg can exploit their inherent strength advantage to enhance the overall strength of the composite. The mechanical properties of BMPC are mainly influenced by Mg metal in two aspects. One is the strength of Mg metal itself. Solid solution strengthening, precipitation hardening, stress strengthening, texture strengthening, and nanoscale additions can effectively improve the mechanical strength of Mg metal [63–65]. In the above processes, the main mechanism of Mg metal strengthening is through dislocation accumulation, grain refinement, deformation twinning, texture control, and dislocation pinning by solute atoms or nano-sized precipitates [66].

On the other hand, the relative content of Mg metal also plays a role. For BMPC composed of fibers, sheets, rods, etc., when the relative content of Mg metal increases, the mechanical properties of BMPC also increase accordingly, exhibiting mechanical properties closer to those of Mg metal. However, for BMPC composed of micro and nanoparticles or short fibers, a different trend is observed. For example, our previous work found that adding an appropriate amount of Mg microparticles to a polymer could improve the compressive or tensile strength of BMPC [43, 47]. However, excessive addition of particles can lead to aggregation, introducing more defects into the BMPC, which hinders crack propagation during the material deformation process, thereby reducing its mechanical properties.

In addition, as described in section 2.2, processing methods can be used to reorganize the aggregation morphology of molecular chains in the polymer (such as changes in molecular chain arrangement and crystallinity), thus achieving mechanical self-reinforcement. The mechanical properties of such self-reinforced polymer materials can be comparable to some alloys [67]. Taking the classic PLA as an example, Li et al. used a multistage stretching extrusion system to prepare self-reinforced and toughened PLA samples, finding a multitude of compact and well-ordered microfibrillar crystalline superstructures within. This structure greatly contributed to the mechanical properties of the PLA samples. On one hand, it acted as discontinuous fibers to self-reinforce the amorphous PLA. On the other hand, it also served as rivets to hinder the propagation of fiber-like cracks, leading to the formation of densely packed fiber cracks during the stretching process. This consumed a considerable amount of energy and transformed the failure mode of PLA from brittle to ductile [68].

Research on the toughening mechanisms and processing methods on polymers is more abundant, leading to the formation of various classic toughening theories, including microcrack theory, multiple crazing theory, shear yielding theory, crazing and shear band theory, hollowing theory, infiltration theory, and the theory of toughening by rigid particles. For specific reasons on how the Mg phase and processing measures enhance and toughen the polymer matrix, please refer to Table 2. Additionally, we present a schematic diagram in Fig. 5 to illustrate the process and mechanism by which the strength and toughness of Mg/polymer are simultaneously improved through self-reinforcement processing, using Mg particles as an example.

Although degradable Mg and polymers can be combined into composites in various ways to improve their mechanical properties, current studies on degradable composites remain inadequate. For instance, compared to some non-degradable materials, the mechanical performance of biodegradable composites used in biological applications is still lower, failing to meet the mechanical requirements of load-bearing parts of the human body. Hence, there is a need for the development of diversified composite processing techniques and interface modification methods, and further improve strength and toughness on the existing basis to meet the needs of different tissue repairs.

3. Factors affecting the degradation rate and degradation mechanism

Degradability is a crucial factor to be considered in the utilization of degradable composites for tissue repair functions. When the BMPC is immersed in physiological fluid environment, the following chemical reactions often occur:

$$Mg + 2H_2O = Mg^{2+} + H_2 + 2OH^- \quad \text{Eq. (1)}$$

$$R\text{-}COOH \rightarrow R\text{-}COO^- + H^+ \quad \text{Eq. (2)}$$

$$H^+ + OH^- = H_2O \quad \text{Eq. (3)}$$

This process induces a rapid rise in the pH of the medium, accompanied by the release of a large amount of hydrogen gas. However, due

Table 2
Representative strengthening and toughening theories of polymer-based composite.

	Theory	Key idea	Proposer	Ref.
Strengthening	Particle/fiber/network/rod/plate/mixed reinforcement theory	The second phase strengthens the polymer.	–	[29, 31, 40, 47, 62]
	Self-reinforcement theory	The polymer molecular chains become oriented, enhancing crystallinity during processing. Fibers formed within the polymer reinforce the amorphous region.	Li and et al.	[68]
Toughening	Microcrack theory	Microcracks form during polymer fracture, and the dispersed phase bridges the crack surfaces, halting further crack propagation.	Merz and et al.	[69]
	Multiple crazing theory	In response to external forces, the dispersed phase functions as a stress concentrator, prompting the polymer matrix to develop numerous crazings and dissipate energy. Additionally, it serves as a terminator for crazings, preventing their progression into cracks.	Bucknull and Smith	[70]
	Shear yielding theory	The energy absorbed by the polymer under external force results from shear deformation within the polymer matrix.	Newman and Strella	[71, 72]
	Crazing and shear band theory	Under external forces, both crazings and shear bands in the polymer collectively dissipate energy.	Bucknull and et al.	[73]
	Hollowing theory	When the Poisson's ratio and thermal expansion coefficient of the dispersed phase exceed those of the matrix, static tensile stress is induced in the surrounding matrix after processing and cooling. This external force, concentrated at the interface between the dispersed and continuous phases, may create cavities due to stress concentration. This phenomenon releases three-dimensional stress, transforming the matrix state from plane stress to one-dimensional stress. This one-dimensional stress state promotes the formation of shear bands, absorbing significant energy and effectively inhibiting polymer fracture.	Pearson and et al.	[74]
	Infiltration theory	As the concentration of dispersed phase particles increases, and their distance decreases, the stress fields around the particles overlap, forming infiltration channels. This phenomenon significantly strengthens the overall matrix stress field, enhances the plasticity of the matrix, and induces a brittle-to-tough transition in the material.	Wu and Margolina	[75, 76]
	Theory of toughening by rigid particles	During tensile deformation, the matrix polymer transfers stress to rigid particles. Differences in Poisson's ratio and elastic modulus lead to higher static pressure at the phase interface. This pressure induces yield deformation in rigid particles, absorbing significant energy and enhancing toughness.	Kurauchi and et al.	[77]

to the neutralization effect of polymer hydrolysis and the presence of calcium-phosphorus components in the physiological environment, the pH of the medium does not exceed 8.0 [78]. Regarding hydrogen gas, it is also a significant factor to consider in the design of BMCP. For Mg metal, a problem after implantation is the rapid evolution of hydrogen gas, leading to the formation of local hydrogen gas pockets that may hinder tissue healing due to delayed absorption. For biodegradable Mg/polymer composite (BMPC), hydrogen evolution remains a concern. Improper control can lead to the escape of hydrogen gas from the Mg surface, damaging the Mg-polymer interface and causing the separation and disintegration of Mg and polymer. Therefore, it is essential to regulate the interface and overall structure of BMPC to slow down the corrosion rate of Mg and the release rate of hydrogen gas. Taking Mg-MAO/PLA composite as an example, researchers have developed composite materials with matched degradation and hydrogen evolution rates through a combination of hot pressing and MAO treatment. This control is mainly achieved for the following reasons. (i) Composite materials reduce the proportion of Mg metal, thereby decreasing the overall amount of evolved hydrogen gas. (ii) After MAO treatment, the

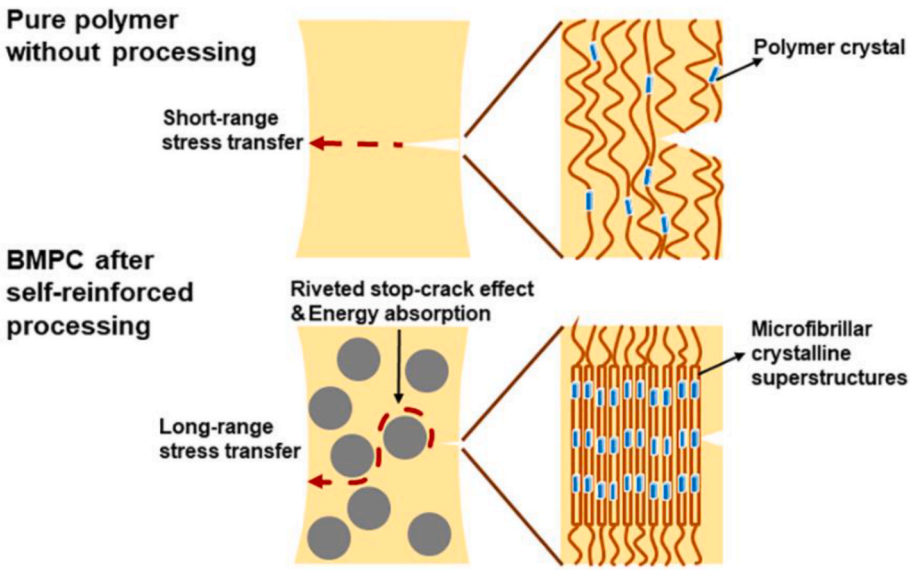

Fig. 5. Schematic diagram illustrating the mechanisms of Mg metal and self-reinforcement processing to enhance the strength and toughness of BMPC (Taking polymer reinforced by Mg particles as an example).

Mg surface is covered by a dense layer of MgO ceramic, which inhibits the penetration of corrosive ions in the degradation medium and reduces its self-corrosion current density [79]. (iii) When PLA is further coated to Mg-MAO, it acts as a barrier to block water and corrosive ions from entering the interior of BMPC and reacting with Mg. With this dual barrier effect, both the total amount and the hydrogen gas release rate from BMPC are effectively controlled, achieving a balance with the tissue's rate of hydrogen gas absorption [80]. In short, the study of controllable degradation of BMPC has always been a focus and a challenging issue.

Apart from hydrogen gas and ions release, the mechanical decay triggered by the degradation process also affects the bone healing process. The rational construction of a "mechanical-chemical" coupled degrading service environment and the accurate evaluation of the composites' degradation failure along with the biomechanical decay process have been the focal points for researchers over the years.

During degradation, factors that influence the degradation rate of composites can be classified into endogenous components and exogenous environmental factors based on their sources.

3.1. *Endogenous factors*

Compared to various exogenous factors, the physical and chemical states of the constituents of composites themselves largely determine their overall degradation rate in most physiological environments. In addition, during the degradation process, the constituents of composite materials may interact, potentially promoting or inhibiting further degradation. The following are some brief explanations.

3.1.1. *Composite component*

The composition of degradable Mg/polymer composite itself is of significant influence on the overall degradation and mechanical decay rates. Based on the inherent properties of the composite components, factors such as grain size and morphology of Mg alloy, intermetallic phase, alloying element composition, and apparent shape all constrain the overall degradation rate of the material. Furthermore, the molecular weight, structure of the polymer chains (including the molecular chain composition, size, structure and configuration, spatial shape, geometric shape, etc.), and the aggregation state structure (including the chain orientation and crystallinity) of the polymer as the matrix of the composite also affect the degradation rate of the composite a lot.

In terms of Mg component, first of all, the Mg content significantly affects the degradation rate of BMPC. With alkaline catalysis being the primary mechanism, the higher the relative content of Mg in BMPC, the more intense the alkaline catalysis effect during hydrolysis, leading to a higher weight loss rate [43]. Besides, as illustrated in Fig. 6A–D, Cifuentes et al. [81] studied the effect of the shape of Mg microparticles on the degradation behavior of Mg/(poly-(L,D-lactic) acid) (Mg/PDLA) composite cylinders. The results indicated that, under the same conditions except for particle size, the composite reinforced with spherical microparticles degraded slower than those with irregular flake-like particles, and their mechanical performance also decayed at a slower rate. This phenomenon was attributed to the relatively smaller specific surface area of the spherical microparticles. Moreover, the size of Mg particles also significantly affects the physical activity of BMPC. For instance, Liu et al. [82] used a one-pot reduction reaction to prepare different-sized Mg particles, including hexagonal nanosheets (80–320 nm), nano-flowers (100–250 nm), and small nanoparticles (average 65 nm). Those Mg particles were then encapsulated in pH-sensitive polymer polyethylene glycol-b-(poly(methyl methacrylate)-*co*-poly(4-vinylpyridine)) and applied in NIR-II photoacoustic and bubble-enhanced ultrasound imaging and cancer therapy. The study found that the nano-flowers, with their unique shape and suitable size (~100 nm), exhibited the optimal plasmonic resonance effect and superior accumulation rate, making them more suitable for specific tumor treatment.

The distribution of Mg within the polymer also influences the activity of the BMPC, thereby determining their application scenarios. For instance, BMPC comprising Mg uniformly dispersed within the polymer exhibits relatively sluggish reactivity, suitable for long-term tissue engineering therapies such as bone repair. In contrast, Mg existing as a separate phase within BMPC displays higher reactivity, suitable for short-term regenerative medical treatments such as bacterial or cancer therapies.

Considering polymer components, the commonly used polyesters include PLA, PGA, PCL, and PLGA, which are derived from different monomer homo-polymerization or copolymerization. Among them, due to the greater affinity of glycolide for water molecules, it is more prone to hydrolysis. Therefore, the higher the content of glycolide in the polymer, the faster its degradation rate [83]. At the same molecular weight, PCL with better hydrophobicity exhibits a slower degradation rate compared to PLA. This results in a corresponding slowdown in the degradation rate of the BMPC formed. According to statistics, PCL may

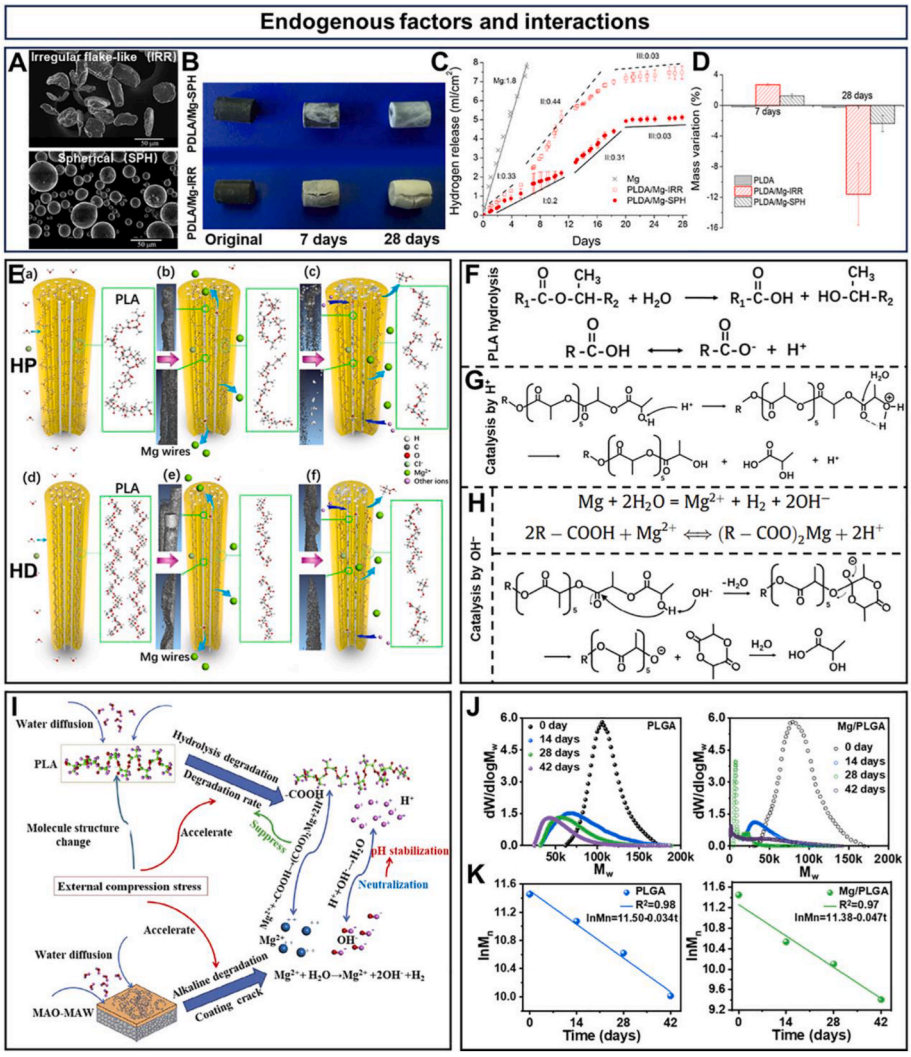

Fig. 6. Endogenous factors affecting the degradation rate of BMPC and the interaction of composite components during degradation. (A) SEM images of irregular flake-like and spherical Mg particles. (B) Photographs of the PLDA/Mg-IRR and PLDA/Mg-SPH cylinders as-processed and after immersion during 7 and 28 days in PBS solution. (C) Accumulated amount of hydrogen gas released as a function of immersion time. (D) Percentage of mass variation of dry specimens after 7 and 28 days of immersion [81]. (E) Illustration of degradation differences of the HP and HD Mg/PLA composite rods at different degradation time points detected by X-ray CT method [60]. Degradation mechanisms of PLA under different environments and interactions between Mg and PLA: (F) Hydrolysis of PLA in a neutral medium. (G) Hydrolysis of PLA catalysis by H^+. (H) Hydrolysis of PLA catalysis by OH^- [60]. (I) Schematic illustration of the synergistic degradation effects rendered by the Mg fillers [87]. (J) Gel permeation chromatography curves of PLGA matrix in PLGA microfibers and Mg/PLGA microfibers. (K) The fitted line of $\ln M_n$ as a function of degradation time [88]. Copyright 2016, 2017, 2019, 2024, Elsevier.

take 3–4 years to completely degrade, PGA degrades in 1.5–3 months, and PLLA degrades in 6–24 months [84]. In addition to monomer composition, the stereochemical structure of monomers in polyesters also affects their degradation rate. Taking PDLA for example, the percentage of D-lactyl units in a polymer affects its hydrolysis. Stereo-copolymer P(L/D)LA is proven to exhibit greater resistance to hydrolysis compared to PLLA and PLDA. Adding PDLA to PLLA leads to strong intermolecular interactions and the formation of stereo-copolymers. This interaction hindered water diffusion into the polymer and reduced the rate of hydrolytic degradation [85,86]. Therefore, considering the stronger interchain interactions between PLDA and PLLA chains, water diffusion within PLLA or PDLA is easier compared to P(L/D)LA. Hence, Mg/PLLA and Mg/PDLA composites degrade at a faster rate than Mg/P(L/D)LA composites when the content of Mg is the same.

Furthermore, the degradation properties of composites are closely related to the underlying polymer matrix, such as PLA. Both water and corrosive Cl^- can easily penetrate the amorphous regions of the orientated, irregular PLA chains and attack the local defect areas on degradable Mg fibers. However, the orientational and crystallinity enhancement of self-reinforced PLA substrates decelerated the diffusion of the degradation media in the composite rods, consequently slowing down the degradation rate of PLA and Mg alloy fibers [60]. Fig. 6E shows significant differences in the degradation behavior of PLA composite rods reinforced with 5 vol% Mg-2Zn alloy fibers prepared by two methods: hot pressing (HP) and hot drawing (HD). Compared to the HP sample, the HD composite rod displays notable corrosion of its internal Mg-2Zn alloy fibers after the same degradation time in Hank's balanced salt solution (HBSS) solution, even if the HD composite rod's diameter is smaller.

In addition, the interfacial bonding condition of the composites is another essential factor. For instance, Ali et al. [27] enhanced the interfacial shear strength of Mg/PLA composites from ~10.9 MPa to ~26.3 MPa by modifying the surface of WE43 Mg alloy fibers through PEO. After 180 days of degradation in simulated body fluid, unmodified Mg fibers nearly completely degraded, while surface-modified Mg fibers

exhibited a significantly slower corrosion rate with only a 3 % mass loss in 180 days. They suggested that the downward trend in interfacial strength was consistent with the interfacial corrosion mechanism. Without the PEO oxide layer, the corrosion was initiated by the degradation of Mg fibers, leading to the formation of inward and outward-growing corrosion layers. Concurrently, the circumferential stress induced by the expanding corrosion layer accelerated the degradation of PLA. On the other hand, the PEO oxide layer effectively suppressed the corrosion of Mg fibers and restricted the degradation of the PLA matrix at the interface.

3.1.2. Composite component interaction

Controversy exists regarding the interaction mechanism of the two components of the degradable Mg/polymer composite in the degradation process. For example, it is generally considered that PLA follows first-order degradation kinetics at the early stage of degradation. Li et al. [87] derived degradation rules for pure PLA and Mg/PLA composites based on this and concluded that the degradation rate of the PLA matrix in composites was much slower than that of pure PLA. Moreover, both the activation energy and pre-exponential factor of the PLA matrix in composites were higher than those of pure PLA, indicating that the composites slowed down the degradation rate of PLA. There were two reasons accounting for this outcome: (i) The alkaline ions (pH < 7.5) released from the degradation of Mg fibers neutralized the acidic substances released from the degradation of PLA, which stabilized the pH of the degradation medium and weakened the self-catalyzed hydrolysis of PLA. (ii) The crosslinking effect between Mg^{2+} and the carboxyl terminus of PLA also slowed down the degradation rate of PLA (Fig. 6F–I).

However, a quite different result in Mg functionally enhanced PLGA composites was obtained [88]. After soaking electrospun PLGA microfibers and Mg/PLGA composite microfibers in PBS, gel permeation chromatography tests revealed that the number-average molecular weight of the PLGA matrix in the composite microfibers declined faster, and the degradation rate of the Mg/PLGA composite microfibers (0.047 day^{-1}) exceeded that of the pure PLGA fibers (0.034 day^{-1}, Fig. 6J, K). This demonstrated that Mg significantly accelerated the hydrolysis of the PLGA matrix. Moreover, Cifuentes et al. [89] also confirmed that the presence of Mg microparticles in the polymer matrix increased the diffusion rate of water through the material, thereby enhancing the overall degradation rate of the composite. This was manifested by significantly higher water absorption and weight loss rates in the composite compared to the pure polymer.

The discrepancy between these two study outcomes might be attributed to the different shapes, interfacial bonding, and compositions of the composites. In composite with a larger specific surface area, water molecules can react faster with Mg, releasing a predominance of OH^-, establishing an alkaline degradation environment quickly. Furthermore, in the latter two cases, they used untreated Mg microparticles, which resulted in weaker interfacial bonding between Mg and the polymer. When immersed in an aqueous solution, the gaps between composite constituents provided a fast pathway for water molecule diffusion. Therefore, the trivial effect of a small amount of Mg^{2+} on the delayed polymer degradation induced by polymer crosslinking was inconsequential compared with the absolute predominance of alkali-catalyzed polymer degradation.

Given the diversified component compositions of BMPC, their physical forms also vary due to different processing methods. The proportion of material components, physical forms, and the interaction between the two components are all crucial factors in future studies on the degradation mechanisms.

3.2. Exogenous factors

The human body is a complex life system regulated by multiple factors to maintain internal homeostasis. Besides the composite components themselves, other exogenous factors in the physiological environment also influence the degradation rate. The reasons for degradation variability in degradable materials are analyzed sequentially from environmental factors such as degradation medium components, cells, microorganisms, temperature, stress, strain, light, oxygen concentration, etc.

3.2.1. Degradation medium component

Among various degradation media, representative examples include NaCl solution, PBS, Ringer's solution, simulated body fluid (SBF), HBSS, Earle's balanced salt solution (EBSS), cell culture medium, and protein-containing media [90–92]. It is worth noting that no single medium can be universally applied to all degradation test methods, given the diverse test conditions and human fluids involved. The degradation rate of Mg and its composites is influenced to different extents by factors such as pH, inorganic salts, proteins, small molecules, etc.

pH: The physiological environment of the human body is complex, with a wide range of pH values in different body parts. Tissues or organs under different pathological conditions present different pH levels. Local tissues show acidity under conditions of inflammation and bacterial infection. For instance, unlike the neutral body fluids, the digestive system represents a complex pH metabolic system. The pH range of gastric fluid is 1.0–3.0. In the small intestine, it is about 5.0–7.7. While in the colon, the pH is 8.3–8.4 (Fig. 7A). Therefore, when degradable materials are implanted in different tissue parts, there may be significant differences in degradation behavior. Zhang et al. [93] prepared Mg-2Zn wires with a diameter of 1.0 mm into anastomotic staples and studied their degradation behavior in the environment of gastric fluid and intestinal fluid. Electrochemical test results showed that the degradation rate of Mg-2Zn anastomotic staples was much slower in the simulated intestinal fluid environment (pH = 6.8) compared to the strongly acidic simulated gastric fluid environment (pH = 2.5), and its corrosion current density was just 26 % of that in the simulated gastric fluid environment (Fig. 7B). Besides Mg, the degradation rate of polymers also exhibits pH-dependency. It is reported that PLLA degrades the fastest in an alkaline environment, followed by an acidic environment. The degradation rate in deionized water is moderate, whereas the slowest degradation rate is found in a buffer solution with pH = 7.4 [94]. This is because both hydrate H^+ and OH^- catalyze the hydrolysis of PLLA crystalline residues, with OH^- exhibiting a significantly stronger catalytic effect on hydrolysis than hydrate H^+. However, buffer solutions often neutralize excessive H^+ or OH^-, thereby weakening the catalytic effect.

Inorganic ions: In physiological environments, especially for bone, inorganic ions such as Ca^{2+}, PO_4^{3-}, HPO_4^{2-}, HCO_3^-, SO_4^{2-}, and Cl^- commonly exist. Therein, Ca^{2+}, PO_4^{3-}, and HPO_4^{2-} can form protective Ca-P precipitates deposited on the Mg surface through chemical reactions, which in turn slow down the degradation rate of Mg [95]. Although HCO_3^- facilitates the degradation of Mg alloys due to the complexation effect as well as the formation of $MgCO_3$ [96], high concentrations of HCO_3^- can induce passivation at corrosion sites, thereby strongly inhibiting the expansion of pitting corrosion. SO_4^{2-} can accelerate the degradation of Mg alloys due to the instability of the corrosion product film it forms [97]. Besides, Cl^- is a well-known inorganic ion that can cause uneven local pitting on Mg, thus accelerating the degradation rate. In addition to affecting Mg within Mg/polymer composites, inorganic ions also influence the polymer. However, the influence of inorganic ions is not independent but rather coupled with the action of other factors. For example, Hegyesi et al. [98] found that increasing the concentration of Na_3PO_4-H_3PO_4 buffer in PBS (pH = 7.2) from 25 mM to 100 mM significantly reduced the degradation rate of PLA. This was attributed to the higher ion concentration reducing enzyme activity (lipase from *Candida rugosa* and proteinase K from *Tritirachium album*), indirectly decreasing the degradation rate of PLA.

Protein: Protein is the main bearer of physiological activities and plays an important role in physiological metabolism. Some studies showed that when degrading in HBSS solution containing fetal bovine

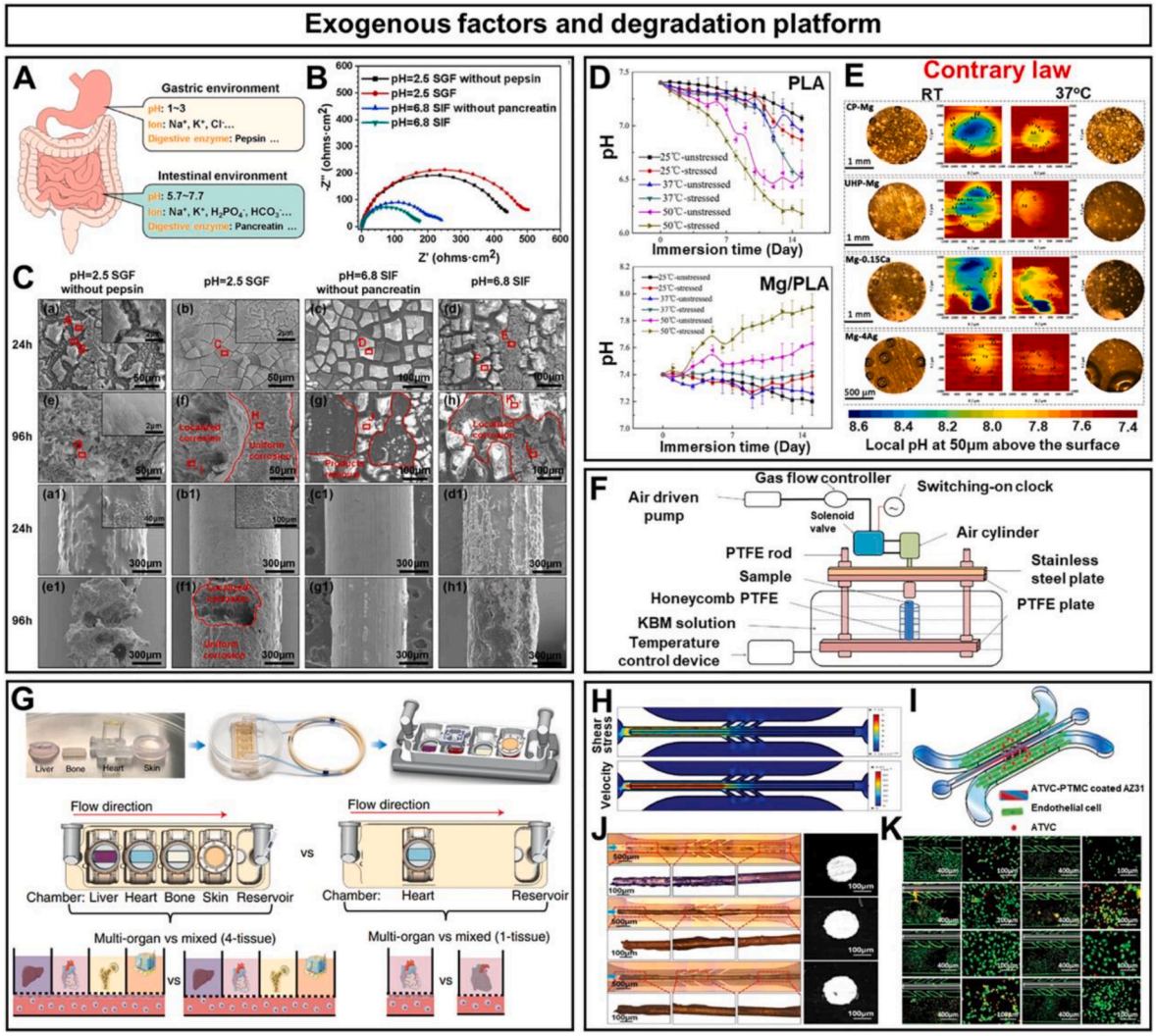

Fig. 7. Exogenous factors affecting the degradation rate of BMPC and novel degradation platforms based on microfluidic chips and organs-on-chips technologies. (A) The diagram of the gastric and intestinal environment. (B) Nyquist plots of Mg alloy wires immersed in different media. (C) SEM images of degraded surfaces after being immersed in different degradation media for 24 h [93]. (D) Degradation behavior of the pure PLA and Mg/PLA specimens as a function of compressive stress, immersion temperature, and time [87]. (E) The visual appearances and distributions of local pH above the surface of Mg alloys after 1 h of immersion in HBSS at room temperature (25 °C) or 37 °C under hydrodynamic conditions [78]. (F) Schematic illustration of the comprehensive apparatus used for Mg/polymer degradation test [124]. (G) Modular, multi-tissue platform components, assembly, and use of integrated multi-organ chip [131]. (H) Flow-induced shear stress on the Mg alloy wires and velocity in the microfluidic channels with the inlet flow rate of 10 μL min^{-1}. (I) Microfluidic chip models in dynamic platform. (J) Optical images of the surfaces and cross-sections of different samples in the microfluidics with the acyclic cell culture medium flow of 10 μL min^{-1} for 12 h degradation at 37 ± 0.5 °C. (K) Immunofluorescent images of apoptosis (red) endothelial cells in the chips implanted different samples after 12 h of culture [128]. Copyright 2017, 2022, Elsevier; 2022, Springer Nature; 2020, John Wiley and Sons.

serum, pure Mg surfaces adsorbed proteins, reducing the density of the passivation film on the Mg surface while increasing the thickness of the passivation layer, thereby slowing down the overall degradation rate of Mg [99]. Nevertheless, not all proteins inhibit the degradation rate of degradable materials. For example, enzymes, which are essentially proteins, have significant roles in different physiological environments. It was found that the corrosion rate of Mg-2Zn alloys was inhibited in simulated gastric fluid when pepsin was added, while it was increased in simulated intestinal fluid with the addition of trypsin [93]. The difference was because pepsin could be adsorbed onto the surface of Mg-2Zn alloys, acting as a physical barrier and suppressing pitting in the alloys in simulated gastric fluid. The trypsin adsorbed on the Mg-2Zn alloy surface affected the integrity of the magnesium hydrogen phosphate inorganic barrier layer, leading to uneven corrosion on the alloy surface (Fig. 7C). Not only does Mg in Mg/polymer composite materials respond to enzymes, but the polymer itself is also highly sensitive to enzymes. This is because, in the presence of enzymes, the polymer undergoes not only hydrolysis reactions but also accelerated disintegration catalyzed by the enzymes [100]. Currently, several enzymes are used to accelerate the degradation of PLA, including kutinase, lipase, protease, and esterase [101]. Different enzymes have varying degrees of catalytic effects on the degradation of PLA. Among them, protease appears to be the most effective enzyme in catalyzing PLA degradation to date.

Small molecules: Given the complexity of different parts of the human body, the degradation media often include inorganic salts, proteins, and various small-molecule substances to better fit the characteristics of the local microenvironment. Mei et al. [102] studied the separate and combined effects of 53 kinds of biological small-molecule organic compounds on the corrosion of pure Mg and Mg-0.8Ca alloys. The results demonstrated that amino acids, vitamins, and sugar molecules had little effect on the degradation rate of the two materials in SBF or cell culture media. Similarly, low concentrations of penicillin and streptomycin did not affect the degradation rate of the two materials in the cell culture medium, but high-concentration streptomycin

accelerated the degradation of both materials. Glucose, as the source of bio-energy, was found to slow down pure Mg's degradation rate as the glucose concentration increased in HBSS. This was mainly because glucose could be converted into gluconic acid, which chelated Ca^{2+} in the solution. Therefore, a Ca-P layer was formed on the sample surface, thus preventing the invasion of corrosive ions and delaying the corrosion of pure Mg [103].

In addition to influencing the degradation rate of Mg, those small molecules also have a significant impact on the degradation rate and surface properties of Mg/PLA composite materials. Agudo et al. [104] introduced 0.9 g L^{-1} of glucose and 1 mM of ketone bodies into SBF to modify the composition of the standard SBF solution. The study found that the addition of these substances directly affected the adsorption of salts on the surface of PLA and Mg/PLA films, thus accelerating the aging of PLA. Specifically, glucose (in the gluconate form) facilitated the formation of a CaP protective layer by coordinating with Ca^{2+} in the SBF. The presence of ketone bodies, especially the hydroxybutyrate anion, increased the surface hydrophilicity and Young's modulus of the degraded Mg/PLA films. Overall, as for the human body, the low physiological concentration of most small molecules results in little influence on the degradation rate.

At present, there is considerable research on the individual effects of the components in the above-mentioned degradation media on the degradation of Mg and polymers. However, there is limited research on Mg/polymer composite materials. In the future, it is worthwhile for researchers to dedicate more efforts to studying this aspect. With the deepened understanding of the impact of body fluid components, more intricate media have been employed or developed for degradation tests to mimic real-life conditions. Nevertheless, the lack of universally accepted test protocols often results in limited comparability among experimental results from different research groups. Hence, it is essential to categorize commonly used degradation media and define their respective applicability domains. Additionally, there is an urgent need to establish widely accepted degradation test standards to serve as guidelines for biodegradable materials.

3.2.2. Cells and microorganisms

Following the implantation of degradable materials, surrounding cells may be recruited to proliferate around the material and ultimately form tissue. The existence of cells also influences the degradation rate of materials. Zhang et al. [105] found that when Mg-2.1Nd-0.2Zn-0.5Zr alloy was co-cultured with macrophages, the corrosion rate of this alloy with macrophages was over twice than that of the group without macrophages. This was primarily because the reactive oxygen species (ROS) generated by macrophages diffused into the calcium/magnesium phosphate and $Mg(OH)_2$ corrosion product layer of Mg alloy, thereby promoting the formation of voids in the corrosion product protective layer and increasing the sensitivity and uniformity of corrosion.

Apart from cells, microorganisms such as bacteria also accelerate the degradation rate of Mg/polymer components, including Mg and polymer. Li et al. [106] found that for Mg-Li-Ca alloys in HBSS containing glucose and exposed to bacteria (*Pseudomonas* and *Enterobacter cloacae*), the pH value of the media did not rise but fell. This was because of the existence of glucose-stimulated bacterial activity, leading to the samples being covered by a bacteria biofilm within 48 h. The high-density bacteria around the Mg alloy samples were in an anaerobic environment, carrying out anaerobic respiration and yielding acidic substances. The bacterial activity changed the hydrogen evolution mode of the Mg alloy, significantly accelerating the degradation rate of the Mg-Li-Ca alloy in HBSS.

Biodegradable polymers are particularly sensitive to microbial reactions because polymers undergo both hydrolysis and enzymatic reactions in the presence of microorganisms, leading to an accelerated degradation rate. For example, in the case of PLA, the aqueous degradation rate of pure PLA is extremely low in natural environment (e.g. in water or soil). Even within 90 days, the weight loss rate does not exceed 5 % [107]. Bacterial strains with the ability to degrade PLA include *Bacillus safensis PLA1006*, *Nocardioides zeae EA12*, *Stenotrophonas pavanii EA33*, *Gordonia sulfurchicans EA63*, *Chitinophaga jiangningensis EA02*, etc [108]. These strains can form bacterial biofilms on PLA at ambient temperatures and accelerate the enzymatic degradation process of PLA through the secretion of proteases and lipases. In summary, the degradation rate of Mg/polymer composites can be accelerated by the action of cellular or microbial secretions, which may better reflect the actual degradation rate when they are *in vivo*.

3.2.3. Temperature

The normal physiological temperature of the human body is 37 °C, but under pathological or inflammatory conditions, the local tissue temperature will be higher than the average temperature. Relevant research [109] studied the degradation behavior of pure PLA and Mg/PLA composites in Kirkland's biocorrosion media at 25 °C, 37 °C, and 50 °C. The results showed that for pure PLA, the pH value declined more significantly as the temperature increased. However, for Mg/PLA composites, the pH value rose instead with increasing temperature (Fig. 7D). This was because the increased penetration speed of water molecules through the polymer substrate not only accelerated the degradation rate of the polymer but also promoted the corrosion of Mg, increasing in both the weight loss rate of composite and the pH value of the degradation fluid. Similarly, Ali's study also confirmed a phenomenon that elevated temperature accelerated the PLA and Mg degradation in Mg/PLA composite in PBS [39]. It was concluded that when the degradation temperature was below the glass transition temperature of the polymer, both polymer substrate in composites followed the Arrhenius equation (Eq.(4)), showing an exponential increase in degradation rate with temperature change [110].

$$k = k_0 \exp\left(-\frac{E_a}{RT}\right) \quad \text{Eq.(4)}$$

where k is the degradation rate, k_0 is the pre-exponential factor, E_a is the activation energy of polymer degradation, R is the gas constant, and T is the temperature. Therefore, when the temperature rises, the degradation speed of the polymer substrate in both pure PLA and Mg/PLA increases.

However, not all temperature increment result in accelerated degradation of biomaterials. Wang et al. [78] discovered that when various Mg and alloys (including pure Mg, ultra-high-purity Mg, Mg-0.15 wt% Ca, Mg-4 wt.% Ag) were immersed in Ca^{2+}-containing HBSS solution under hydrodynamic conditions, their degradation rate at 37 °C was lower than that at 25 °C. This discrepancy could be attributed to the differences in the reaction equilibrium constant of the "precipitation-dissolution" process of inorganic ions in HBSS at 25 °C and 37 °C. As a result, the formation of protective calcium-phosphate-rich precipitates and $Mg(OH)_2$ on Mg alloys was facilitated at 37 °C, forming denser structures that effectively shielded the Mg alloy from further corrosion. Moreover, accompanying Mg dissolution, the diffusion rate of participated ions including OH^- was higher at 37 °C than at 25 °C, all of these contributed to a quicker dynamic equilibrium and consumed the OH^- generated from the cathodic reactions to form Ca-P-containing products and $Mg(OH)_2$, leading to a slower corrosion rate and lower interfacial pH at 37 °C than at 25 °C (Fig. 7E).

The distinct rules in degradation rates with temperature between degradable Mg and its composites under different temperatures may be attributed to their varying degradation modes and the components of the degradation medium. In Li's research, the addition of some corrosion inhibitors (such as N-2-Hydroxyethylpiperazine-N-2-ethane sulfonic acid, and hydroxyethyl piperazine ethane sulfonic acid) to Kirkland's biocorrosion media delayed the formation of degradation by-products on material surfaces, thereby weakening the protective effect of these by-products [111]. Therefore, with increasing temperature, the degradation rate of both pure PLA and Mg/PLA composites accelerated. In addition, for composites, Mg was tightly enclosed by polymers, and the

resulting degradation products like Mg^{2+} and OH^- could only deposit on the composite surface after combining with inorganic ions in the Ca^{2+}-rich degradation media. Consequently, the protective effect on the Mg was ineffectual even with rising temperatures. In Mg alloys, pure metals benefited from calcium-phosphate-rich precipitates, which adhered well to the surface of Mg alloys, providing corrosion resistance.

3.2.4. Stress

During service, implanted materials inevitably undergo the impact of surrounding physiological loads. Different forms of external loads alter the materials' stress states, thereby changing their degradation rates [112]. The most common forms of physiological stress are tensile stress, compressive stress, bending stress, and shear stress.

Taking bone for example, stress not only acts on cells for mechanical conduction, impacting bone tissue healing, but the degradation rate changes and ion release of degradable implanted materials under stress can also influence the growth process of osteoblasts. Therefore, it is necessary to fully understand the degradation performance of materials under stress states. Li et al. [109] confirmed that in the early stage of degradation, applying 1 MPa of static compressive stress would simultaneously accelerate the degradation of the matrix in pure PLA and Mg/PLA composite by reducing the degradation activation energy and pre-exponential factor of PLA. They also established a numerical model and found that in composites, the degradation activation energy (E_a) and pre-exponential factor (K_b) of the PLA matrix were found to meet the following relationships with the stress value (δ):

$$E_a = E_0 - \alpha\delta \quad \text{Eq.(5)}$$

$$K_b = k_f \exp\left[-\frac{(E_0 - \alpha\delta)}{RT}\right] \quad \text{Eq.(6)}$$

where E_0 is the activation energy of the static sample, δ is the external stress value, α is the coefficient, k_f is the Arrhenius frequency factor, and k_b is the rate of bond rupture events.

Compared to static stress, dynamic stress aligns more with physiological conditions. Literature indicated that only dynamic stress could promote bone formation and growth, while static stress did not provide the effect [113]. Biomechanical research also showed that mechanical stimuli and transmission provided by dynamic loading affected the growth and development of bone cells, and assisted in bone tissue reconstruction [114]. Consequently, based on the initial work above, Li established a degradation platform under dynamic stress loading to study the impact of different compressive stress values (0.1–0.9 MPa) and loading frequencies (0.5–2.5 Hz) on the degradation rate of pure PLA and Mg/PLA composites. This platform could also integrate temperature factors to study the combined effects of temperature, stress, and load frequency on the composite degradation rate. The schematic of this platform is shown in Fig. 7F. Their findings revealed that an increase in load values and frequencies could accelerate the degradation rate of both pure PLA and Mg/PLA composites (Fig. 7D). For pure PLA, dynamic loading promoted the diffusion of acidic molecules from PLA, leading to a significant decrease in the pH value of the degradation medium. For the Mg/PLA composite, dynamic loading accelerated the destruction of the Mg fiber surface coating in the composite and facilitated the deposition of the Ca-P phase.

Unlike other tissues, human lumen structures (such as blood vessels, urethra, digestive tract, etc.) also endure the constant flushing of various body fluids and the effect of shear forces. Clinical statistics showed that the average shear stress experienced by an adult's coronary artery, ages 20–60, ranged from 1.1 Pa to 1.5 Pa. As age increased, the diameter of the coronary artery expanded, leading to a reduction in the average wall shear stress [115]. This necessitates the use of dynamic fluid platforms to study the degradation behavior of degradable materials within the lumen.

Shang et al. [116] utilized microfluidic technology to construct a dynamic degradation platform with an average flow-induced shear stress of 0.68 Pa. They studied the differences in the degradation rates of three degradable Mg wires, namely pure Mg, AZ31 Mg alloy, and Mg-Zn-Y-Nd alloy, under this platform. The results showed that the degradation rate of the three Mg under flow-induced shear stress was significantly higher than that under static conditions, and notably higher than the *in vivo* degradation rate. This was mainly due to the high fluid shear force limiting the formation of inorganic salt passivation layers, impeding their ability to protect the Mg alloy substrate, leading to the exposure of the Mg substrate to the degradation medium, accelerating the material transfer coefficient, ion diffusion, and charge transfer processes. The flowing body fluid environment could stabilize the pH around Mg to physiological values, causing further corrosion evolution. In contrast, ion diffusion was inhibited under static conditions, creating a microenvironment with high pH surrounding the sample, which inhibited subsequent Mg dissolution, thus reducing the degradation rate. This was also why the degradation rate enhanced with increasing shear stress.

Apart from Mg, degradable polymer materials are often used as surface coatings for Mg cardiovascular stents to alter their service life. Chu et al. [117] studied the differences in the degradation rates of PLGA films in deionized water under different fluid shear modes (steady, sinusoid, and square-wave fluid shear stress patterns). The results showed that although unstable shear stresses (sinusoid and square-wave fluid shear stress patterns) and stable shear stress had the same magnitude on average, the former accelerated the outward diffusion process of oligomers in the PLGA film in terms of its maximum shear stress and "window" of effectiveness, thereby accelerating the degradation rate *in vitro*.

We should mention that, in the context of stress, it is incorrect to assert that all stress magnitudes invariably escalate the degradation rate of degradable materials. The exact governing factors should be traced back to the intricate internal microstructure of these materials. In an exploratory study conducted by Wang et al. [118], it was observed that the degradation rate of the as-extruded Mg-4Li-1Ca alloy reacted distinctly to different levels of micro-compressive stress within 6 MPa. Specifically, under 0–3 MPa stress, the once strong basal texture of the as-extruded Mg alloys blurred, and internal stress gradients prompted grain boundary migration leading to grain growth. This phenomenon, combined with escalating compressive stress, sparked the genesis of second-phase particles and residual stress escalation, thus magnifying the corrosion rate via preferential corrosion. In contrast, as stress intensified, the second phase's volume fraction ascended, gaining ascendancy over the total corrosion rate, while the residual stress was released under compressive stress of 4.5–6 MPa. Consequently, the quickly synthesized surface corrosion product films beleaguered the microstructural impact on the corrosion behavior by forming robust physical barriers.

3.2.5. Strain

Strain also significantly impacts the degradation rates of degradable materials, as it can profoundly alter the material's surface energy, work function, and strain energy [119]. Generally, the degradation rate is accelerated with the increase of strain. Taking Mg alloy as an example, Wei et al. [120] investigated the impact of the scaled strain energy on the degradation kinetics of Mg alloys using density functional theory. The calculations revealed that both tensile and compressive strains could accelerate degradation by reducing the activation energy barrier. Moreover, the tensile or compressive strain also resulted in high-density dislocations and deformation twins within the Mg alloy, subsequently accelerating its corrosion rate [121]. However, the degradation mechanisms of Mg under compressive and tensile strains were quite different. This was because tensile strain tended to cause intergranular corrosion in Mg, while compressive deformation made the material denser, thereby inhibiting degradation reactions at grain boundaries. Besides tensile and compressive strains, the internal impacts of bending strain, biaxial elastic strain, hydrostatic strain, and the internal strain caused by

dislocation and twins are still worthy of further detailed analysis. The aforementioned strains have a significant impact on the degradation rate of Mg in composite constituents. However, for the polymer, its higher elasticity results in a lesser sensitivity to degradation rate variations under strain. Therefore, the degradation rate of Mg/polymer composites under strain is primarily governed by the Mg component.

3.2.6. Other factors

In addition to external factors, such as those mentioned above, light exposure also significantly affects the degradation rate of composites, especially for polymers. According to the bond energies of polymer chemical bonds, which are shown as follows: O-O bond energy (138.9 kJ mol^{-1}), C-C bond energy (347.7 kJ mol^{-1}), C-O bond energy (351.5 kJ mol^{-1}), C-H bond energy (413.4 kJ mol^{-1}), and O-H bond energy (462.8 kJ mol^{-1}) [122]. Taking ultraviolet light commonly used for implant sterilization as an example, the wavelength ranges from 200 to 400 nm with an energy range of 299–599 kJ. This energy is sufficient to break down polymers, thereby accelerating the degradation rate of BMPC.

Oxygen concentration also has a significant effect on the degradation rate of BMPC, which is manifested in several ways. During the processing of BMPC, especially in the air atmosphere, oxygen can weaken the bond energy of the polymer, leading to the formation of highly unstable peroxide structures. Polymers with peroxide structures have lower degradation activation energies, leading to accelerated degradation during subsequent use. Furthermore, oxygen also affects the proliferation of cells and bacteria in the environment, indirectly affecting the Mg and polymer in BMPC.

There are many factors influencing the degradation rate of BMPC. However, for different scenarios, researchers can typically design the composition of BMPC based on the duration time that the implant material needs to serve, aiming to meet the repair needs to the fullest extent. For example, in the gastrointestinal environment, an intestinal surgical staple needs to maintain the anastomosis state (strength) for at least 7 days, but Mg corrodes too quickly in the gastrointestinal environment. Therefore, researchers constructed Mg-MAO/PLLA composite anastomosis nails to meet the time scale compatibility [80]. For soft tissues such as urethral tissue, researchers tend to use the faster degrading PLGA50:50, with the addition of a moderate amount of Mg (less than 9 wt%) to allow it to degrade completely within 2–3 months, meeting the time scale compatibility for soft tissue repair [88]. For bone repair, as the healing process takes longer, usually requiring 6–12 months of repair period, researchers tend to choose slower degrading polymers such as PCL [47] and PLLA [43] as the polymer matrix. These polymers maintain the structural integrity and mechanical properties of BMPC during the first 3–6 months of degradation. After 6 months, BMPC can degrade and be absorbed relatively quickly, meeting the time scale compatibility for bone repair. In summary, when developing BMPC implants, researchers need to comprehensively consider the use scenario to meet the material's mechanical compatibility, time compatibility, and bio-performance requirements.

3.3. Mechanical property prediction during degradation

Aside from determining the degradation rates of the materials themselves, studying mechanical property alterations of composites in the early stages of degradation is crucial for body parts that require high mechanical requirements. For instance, during bone fracture repair, the mechanical properties of the implanted material should be maintained for at least 12 weeks [123] to ensure the healing of bone callus and stability of the fracture ends. Therefore, establishing a valid numerical model to predict early mechanical property evolution trends of degradable composites has significant implications for the effective assessment of bone fixation devices.

Using the Mg/PLA composites as an example, our group [60,124] established a numerical relationship between the bending strength and degradation time for pure PLA and Mg/PLA composites with different reinforcement phase contents, as shown in Eq. (7). This approach was based on the characteristic of PLA following first-order degradation kinetics in the early stage of degradation.

$$\ln M_n = \ln M_{n0} - kt \quad \text{Eq.(7)}$$

where M_{n0} and M_n represent the number-average molecular weight of PLA at time t_0 and t, respectively, and k is the degradation rate constant of PLA.

The relationship between the bending strength (S_b) and the number-average molecular weight (M_n) of PLA during the degradation process can be expressed as follows:

$$S_b = S_{b\infty} - \frac{B}{M_n} \quad \text{Eq.(8)}$$

where $S_{b\infty}$ is the bending strength at infinite molecular weight before degradation, and B is a constant.

Eq. (9) can be obtained by combining Eq. (7) and Eq. (8):

$$S_b = S_{b\infty} - \frac{B}{M_{n0}e^{-kt}} \quad \text{Eq.(9)}$$

By substituting the existing results into the obtained formula, a good fit result was achieved. Therefore, it was concluded that the degradation model accurately reflected the relationship between the bending strength, molecular weight, and degradation time of the Mg/PLA composites, thus providing a viable approach for designing degradable composites to meet future bone repair needs.

3.4. Establishment of in-time and ex-vivo degradation platform

The human body is a complex biochemical reaction entity, with vast microenvironmental differences across different parts, and the degradation process is influenced by multiple endogenous and exogenous factors. This results in significant variation in the degradation rates of the same degradable materials under different *in vivo* and *in vitro* conditions [125], making it challenging to infer the *in vivo* results from present *in vitro* degradation rates and processes. Therefore, one of the current research puzzles is to construct an *in-time* and "mechanical--chemical" coupled physiological environment for precise assessment of material degradation failure and biomechanical decay models in *ex-vivo* conditions.

To overcome this challenge and reduce the use of animal models, recently, researchers developed "micro-fluidic chips" [126] and "organ-on-chips" [127] technologies, which simulated the interaction function of multiple organs coupled biomaterials, living cells, local microenvironments, and biomechanics based on microfluidic technology (Fig. 7G). As a multidisciplinary convergence of frontier science and technology, it also allowed for the real-time observation of the interactions among biomaterials, cells, tissues, and organs during material degradation.

For instance, Ye et al. [128] developed a microfluidic model to simulate the microenvironment of early vascular stent implantation, aiming to reduce the cytocompatibility discrepancy between *in vitro* static culture and *in vivo* tests of Mg-based materials (Fig. 7H). This model investigated the response of endothelial cells to AZ31 Mg samples, poly (1,3-trimethylene carbonate (PTMC)-coated AZ31 Mg samples, and PTMC-atorvastatin calcium (ATVC)-coated AZ31 Mg samples (Fig. 7I). Compared to studies conducted in static cell culture environments, the dynamic environment established by microfluidic perfusion better mimicked the real corrosion behavior of various Mg samples in bodily fluids and their effects on endothelial cells, yielding results that were more representative of *in vivo* experiments (Fig. 7J, K). Additionally, Zhang et al. [129,130] developed a patterned biodegradable polymer vascular structure for implantation into micro-vessels. Based on this vascular structure, they also developed a 3D vascularized tissue

scaffold chip called “AngioChip”. With this platform, the blood circulation of artery-artery and artery-vein in the femoral vessel could be observed in real-time. In short, “micro-fluidic chips” and “organ-s-on-chips” technologies establish an advanced platform for the evaluation of biomaterial degradation and pave the way for precise capture of material degradation behavior in a *quasi-in vivo* environment without sacrificing the animal.

4. Composite physiological function and biological mechanism

4.1. Tissue repair functions

Mg is a necessary constant element in the human body and plays an important role in body development. Composites composed of Mg/polymer have broad application prospects in multiple human body parts. They have extensive applications in the brain, orthopedics, tendon, dentistry, skin, cardiovascular, neurological, urological, gastrointestinal, and digestive fields, which simultaneously require “structural support” and “physiological repair” functions. The active Mg^{2+} released from the composite is the main source of their biological viability and activity, while the polymer usually acts as a protective shield for Mg. Moreover, changes in pH in the medium can also significantly affect cell viability. pH value above ~8.4 or below ~6.0 significantly weakens the viability of many cell types [132]. Due to the multifunctionality of Mg, Mg^{2+} at different concentrations has been extensively reported to exhibit positive effects on cartilage regeneration, vascular repair, and neurogenesis. Fig. 8 summarizes the main application areas of the composites with Mg as the reinforced phase, suitable microenvironment medium condition for different scenarios, the key genes, proteins, and signaling pathways involved in the process of achieving tissue repair through inducing the differentiation of mesenchymal stem cells (MSCs).

Bone repair is a physiological process involving multiple signal transductions, typically accompanied by neurogenesis and vascular regeneration. MSCs are a vital cell source that can differentiate into various lineages, such as osteogenesis, chondrogenesis, angiogenesis, and neurogenesis [133]. For human bone MSC (hBMSC), that 5–10 mM of Mg^{2+} was most effective for proliferation [134]. Compared to MSCs, osteoblast precursor cells showed higher tolerance to Mg^{2+} while the hFOB1.19 osteoblast had a tolerance of up to 20 mM of Mg^{2+}. When Mg^{2+} concentration exceeds 20 mM, all functions of osteoblasts decline. Mg^{2+} at 10 mM significantly activated integrins [135] and focal adhesion kinase pathways [136] as well as enhanced the mineralization of the extracellular matrix by increasing the production of collagen and vascular endothelial growth factor (VEGF) [137], which were significant for osteogenesis. In BMSC osteogenic differentiation, the transient receptor potential cation channel, subfamily M, member 7 (TRPM7) was essential as the influx of Mg^{2+} upregulates the expression levels of runt-related transcription factor 2 (RUNX2), alkaline phosphatase (ALP), matrix metalloprotein-2 (MMP-2), Matrix metalloprotein-9 (MMP-9), and VEGF through the TRPM7/PI3K signaling pathway, ultimately promoting the recruitment, migration, mineralization of osteoblasts, and strengthening their resistance to alkaline stress [138]. When Mg-containing materials degrade in body fluids, inorganic products like Ca-P were usually adsorbed and precipitate on their surface, thus increasing the activity expression of COL-1, osteocalcin (OCN), osteopontin (OPN), RUNX2, ALP, and alizarin red S (ARS) proteins in MSCs. This also activated the MAP kinase activity (ERK1/ERK2), subsequently activating RUNX2, causing the osteogenic differentiation of MSCs. In addition, Mg^{2+} mediated PI3K/AKT, MAPK [139], and Wnt/β-catenin [140] signaling pathways were deeply involved in the survival and proliferation of MSCs.

Besides promoting bone repair, regulating the degradation and active ion release properties of Mg and its composites can also stimulate cartilage regeneration. Mg^{2+}-enriched hyaluronic acid has been approved in Europe for cartilage repair [141]. Compared to osteoblasts,

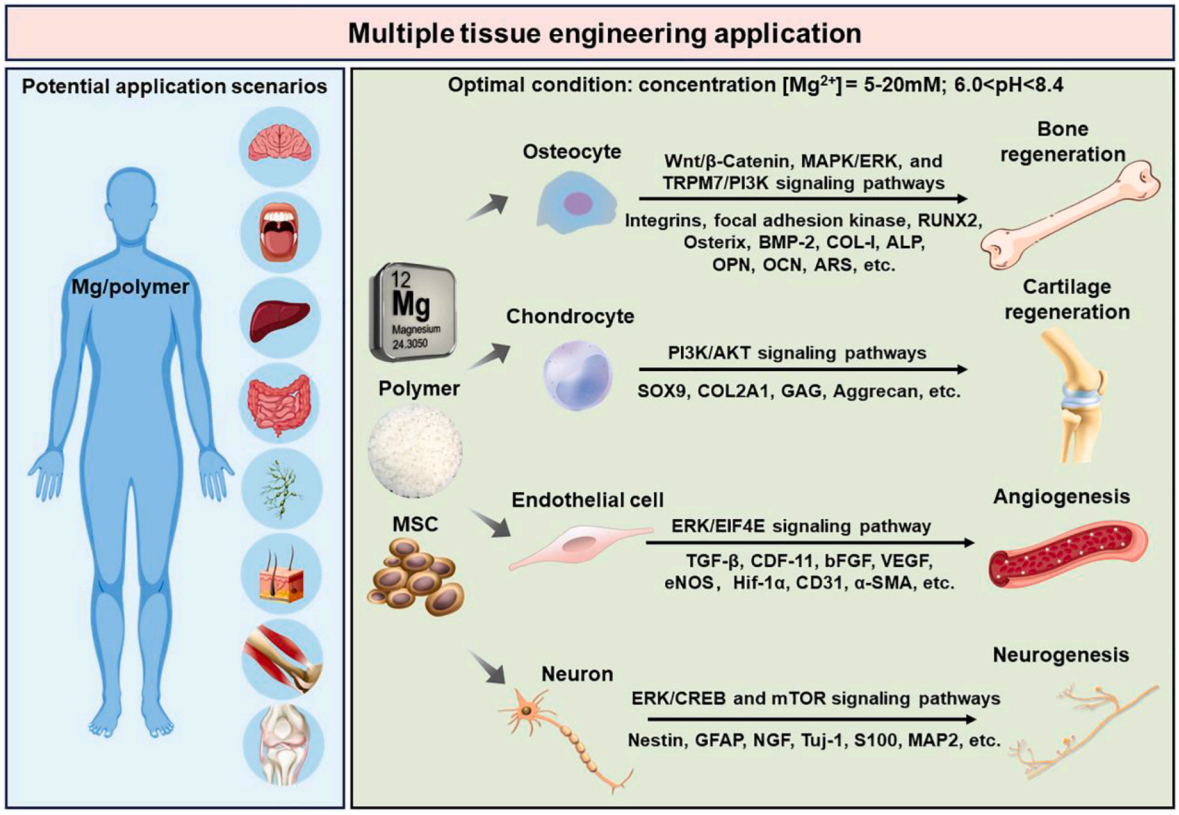

Fig. 8. Schematic illustration summarizing potential application scenarios of BMPC, important signaling pathways affecting MSC differentiation and multiple tissue regeneration processes. Created with Vecteezy.com.

chondrocytes exhibit a higher tolerance to Mg^{2+} due to Mg^{2+} inhibiting IL-1β-induced chondrocyte apoptosis by activating the PI3K/AKT pathway and enhancing extracellular matrix anabolism [142]. Within the tolerance range of cells to Mg^{2+}, higher concentrations of Mg^{2+} (no higher than 20 mM) more readily induce the differentiation of BMSCs towards chondrogenesis. For example, Gao et al. [143] constructed a bilayer scaffold simulating different pore sizes in the cartilage and subchondral bone regions, combined with the release of varying concentrations of Mg^{2+} in corresponding regions to modulate the chondrogenic/osteogenic differentiation of MSCs. They found that at higher concentrations (200–240 ppm), Mg^{2+} enhanced the secretion of chondrogenic-related proteins sex-determining region Y box protein 9 (SOX9) and Collagen type II (COL-II, especially COL2A1) by regulating cell adhesion, extracellular matrix (ECM) synthesis, PI3K/AKT signaling pathway, and MSC differentiation behavior. At lower concentrations (80–120 ppm), Mg^{2+} increased the secretion of osteogenic-related proteins ALP and COL-I by activating the Wnt/β-catenin signaling pathway. Furthermore, related research found that dopamine-coated Mg alloys could alleviate local inflammation responses, downregulated the NF-κB signaling pathway, and regulated the local immune environment. Thereafter, the sample recruited hBMSCs and promoted their differentiation towards chondrogenesis, leading to increased expression of chondrocyte markers such as SOX9, COL-II, Aggrecan, and glycosaminoglycan (GAG) [144].

Additionally, bone repair often involves concurrent vascular regeneration. Mg^{2+} can promote vascular regrowth. Some research found that the growth differentiation factor-11 (GDF-11) protein played a crucial role in mediating Mg^{2+} vascular regeneration. GDF-11 could promote MSC differentiation into endothelial cells, thus stimulating angiogenesis by activating transforming growth factor-β (TGF-β) receptors and the downstream ERK/EIF4E pathway [145]. Furthermore, GDF-11 expression driven VEGF expression, highlighting the importance of GDF-11 and VEGF in the vascular genesis of MSCs. Some Mg alloy vascular stents carrying erosion-resistant polymer coatings also played a crucial role in repairing narrowed vessels. Vascular endothelialization repair was highly associated with Mg^{2+} activating high vitality epidermal growth factor (EGF), basic fibroblast growth factor (bFGF), hypoxia-inducible factor-1α (HIF-1α), endothelial nitric oxide synthase (eNOS) and angiopoietin-4 (ANGPT4) proteins in endothelial cells or stem cells [146]. Simultaneously, Mg^{2+} and Cu^{2+} released from the stent activated the NLRP3/IL1β signaling pathway, inhibiting over proliferation of vascular smooth muscle cells, thereby aiding in alleviating neointimal hyperplasia and restenosis [147].

Mg^{2+} also has a positive regulatory effect on nerve growth, and its elevation in the brain can enhance memory and synaptic plasticity *in vivo*. Notably, neuro-regeneration peaked within 24 h after a bone fracture, preceding vascular formation, ossification, and mineralization, and initiated bone defect regeneration. This implied that early supplementation of Mg^{2+} could promote the reconstruction of neural networks, thereby benefiting the subsequent bone repair process. Compared with bone and blood vessels, nerve repair required a lower concentration of Mg^{2+}. In the range of 0.6–1.0 mM, Mg^{2+} elevation promoted neural differentiation, possibly via extracellular signal-regulated kinase (ERK)-induced cyclic adenosine monophosphate (cAMP) response element-binding protein (CREB) activation, while suppressing glial cell differentiation [148]. During the neural innervation in primordial osteogenic center formation and bone regeneration processes, nerve growth factor (NGF)-responsive tropomyosin receptor kinase A (TrkA) was the representative signaling pathway [149]. Gelatin methacrylate hydrogel containing Mg was also proven capable of accelerating MSC-derived calcitonin gene-related peptide (CGRP) nerve fiber secretion from rat cranial periosteum, thereby inducing cranial bone regeneration [150]. Moreover, significant up-regulation of marker proteins such as Nestin, glial fibrillary acidic protein (GFAP), NGF, Tuj-1 (known as β-tubulin III), soluble protein-100 (S100), microtubule-associated protein 2 (MAP2) could be observed in highly neural differentiated MSCs [151].

In addition to mediating various signaling pathways, Mg^{2+} and drug release kinetics in BMPC also play a vital role in tissue repair. Taking bone repair as an example, Lin et al. [152] designed and prepared composite microspheres loaded with Mg^{2+} using a microfluidic capillary device. By first constructing a first layer of PLGA shell outside Mg^{2+} as a reservoir, and then further constructing a layer of sodium alginate physical barrier based on this PLGA shell. Adjusting the surface microporous network of the above-mentioned double-layer shell microspheres could achieve a continuous delivery of Mg^{2+} at a rate of 50 ppm per day for more than 2 weeks, avoiding the adverse situation of burst release of single-layer shell microspheres at the beginning (exceeding 550 ppm on the first day) and then a release rate of 0 ppm in the following 14 days. The results of rat femoral defect experiments confirmed that even under the same Mg loading amount, the double-layer shell composite microspheres showed higher bone regeneration rate and Young's modulus of new bone than the single-layer shell composite microspheres. Furthermore, Yang et al. [153] utilized the water-in-oil-in-water (w/o/w) double-emulsion solvent extraction/evaporation technique to fabricate composite microspheres (PLLA matrix) encapsulating varying contents and sizes of Mg particles and bovine serum albumin (BSA) solutions. *In vitro* release studies demonstrated that altering the content or size of Mg particles changed the internal connectivity of the composite microspheres during degradation. Specifically, increasing the Mg content (from 0 wt% to 10 wt%) accelerated the release of Mg^{2+} and BSA, resulting in the highest pH increase in PBS medium to ~8.8 (for 10 wt% content), and concurrently led to an increase in the number of surface and internal micropores, cracks, and cavities, laying the foundation for the second burst release of BSA. Besides regulating Mg content, their study also found that, at the same content, composite microspheres with larger Mg particles (~31.02 μm) exhibited a slower BSA release rate compared to those with smaller Mg particles (~9.68 μm), attributed to the denser internal structure of microspheres with larger Mg particles. These results suggested that this composite microsphere system could manipulate drug release kinetics by adjusting the content or size of Mg within the microspheres. Further *in vitro* and *in vivo* studies confirmed that incorporating Mg into the composite microspheres could alleviate PLLA-induced macrophage infiltration and expression of inflammatory cytokines, presenting potential applications in various drug- and protein-mediated tissue regeneration.

BMPC has considerable biological functions. However, the efficacy of BMPC also depends on the relative Mg content, cell species, and the specific body site. For bone and its surrounding tissues, they exhibit higher tolerance to the Mg content in BMPC. BMPC with higher Mg content is more prone to form biomineralized surfaces in body fluids, facilitating the adhesion of bone cells and bone integration. However, in soft tissues, their tolerance to Mg content is lower. This is because soft tissues lack minerals, and an excessive amount of Mg forming insoluble corrosion products can lead to tissue rejection of the implanted BMPC. For instance, the presence of excessive Mg^{2+} in the urethral environment can easily induce the formation of the precursor to urinary calculi ($Mg(NH_4)PO_4{\cdot}6H_2O$), which is detrimental to tissue healing. Therefore, it is necessary to flexibly design the composition of BMPC according to different tissue environments.

As an implant, BMPC has both advantages and limitations from a biological perspective. Taking bone repair as an example, its advantages lie in available material composition and structure design according to the application scenario. The design of BMPC slows down the corrosion rate of internal Mg, avoiding adverse effects due to local ion concentration and high pH. Furthermore, the polymer acts as a protective layer for Mg, slowing down the rate of hydrogen gas release and preventing the hindering effect of hydrogen gas cavities induced by rapid hydrogen gas release on bone reconstruction. However, BMPC also has some disadvantages. For example, due to the encapsulation effect of the polymer, BMPC cannot create as many binding sites with Ca-P compounds in the body fluid as Mg metal, resulting in a much lower formation of

hydroxyapatite on the surface compared to Mg metal, which is not conducive to the rapid construction of a bio-mineralized surface. Subsequently, in the later stages of bone repair, once the protective layer is breached, this may be accompanied by the overflow of a large amount of Mg^{2+}. The above may result in an insufficient rate of bone regeneration in the early stages of bone repair, and the excessive escape of Mg^{2+} in the later stages. It contributes nothing to the activity of osteoblasts and antagonizes with Ca^{2+} in the body fluids, leading to adverse phenomena such as bone resorption [154].

In summary, bone repair is known to be a complex process that involves simultaneous repair of cartilage, blood vessels, and nerves. BMPC plays significant roles at different stages of bone repair, but the demand for Mg^{2+} varies at each stage. Therefore, designing BMPC with tailored Mg^{2+} release characteristics is a worthwhile research topic in future studies of neurovascular bone repair. Some studies also indicate that composites composed of multiple metals (such as Zn or Fe) exhibit superior effects in bone repair compared to single Mg-containing composites. Consequently, it is of remarkable scientific value to further investigate the individual and synergistic roles of these diverse metal ions in tissue repair.

4.2. Cell cross-talking and cascade response

The physiological process of tissue regeneration after injury comprises four stages: hemostasis, inflammation, proliferation, and remodeling. Once an implant is introduced into the body, immune cells, such as neutrophils and macrophages, are the first responders to foreign materials and play a crucial role in determining the biocompatibility or failure of the implant. When these immune cells are recruited to the defect site, they differentiate into two types: pro-inflammatory cells (including monocytes, M1 macrophages, and auxiliary TH cells) and anti-inflammatory cells (such as M2 macrophages and TH2 cells). Therein, pro-inflammatory cells are responsible for wound cleaning, while anti-inflammatory cells tend to favor tissue remodeling and promote tissue maturation [155].

The ideal degradable biomaterials should suppress excessive inflammatory response and stimulate endogenous cells to express functional proteins associated with tissue repair when performing their physiological functions. Many studies reported that during the inflammatory phase, the active ions released by Mg, Zn and their composites could promote the M2 phenotype of macrophages, expressing anti-inflammatory markers such as CD206, interleukin-10 (IL-10) and transforming growth factor-β (TGF-β) in macrophages, and inhibit the expression of pro-inflammatory markers such as interleukin-1β (IL-1β) and CC chemokine receptor 7 (CCR7) [156–158], thereby speeding up the transition of injured tissue from the inflammatory phase to the proliferation and remodeling phase. This cascade functions among these cations and immune cells and functional cells are a complex physiological process. For example, research results from Qiao et al. [154] demonstrated that, at the early stage of the inflammatory phase, Mg^{2+} promoted the upregulation of TRPM7 expression, leading to TRPM7-dependent Mg^{2+} influx in the monocyte-macrophage lineage, causing cleavage and nuclear accumulation of the TRPM7 cleavage kinase part (M7CKs). This subsequently triggered the phosphorylation of Histone H3 at serine 10 on the promoter of inflammation cytokine genes dependent on TRPM7, which resulted in the formation of an osteogenic

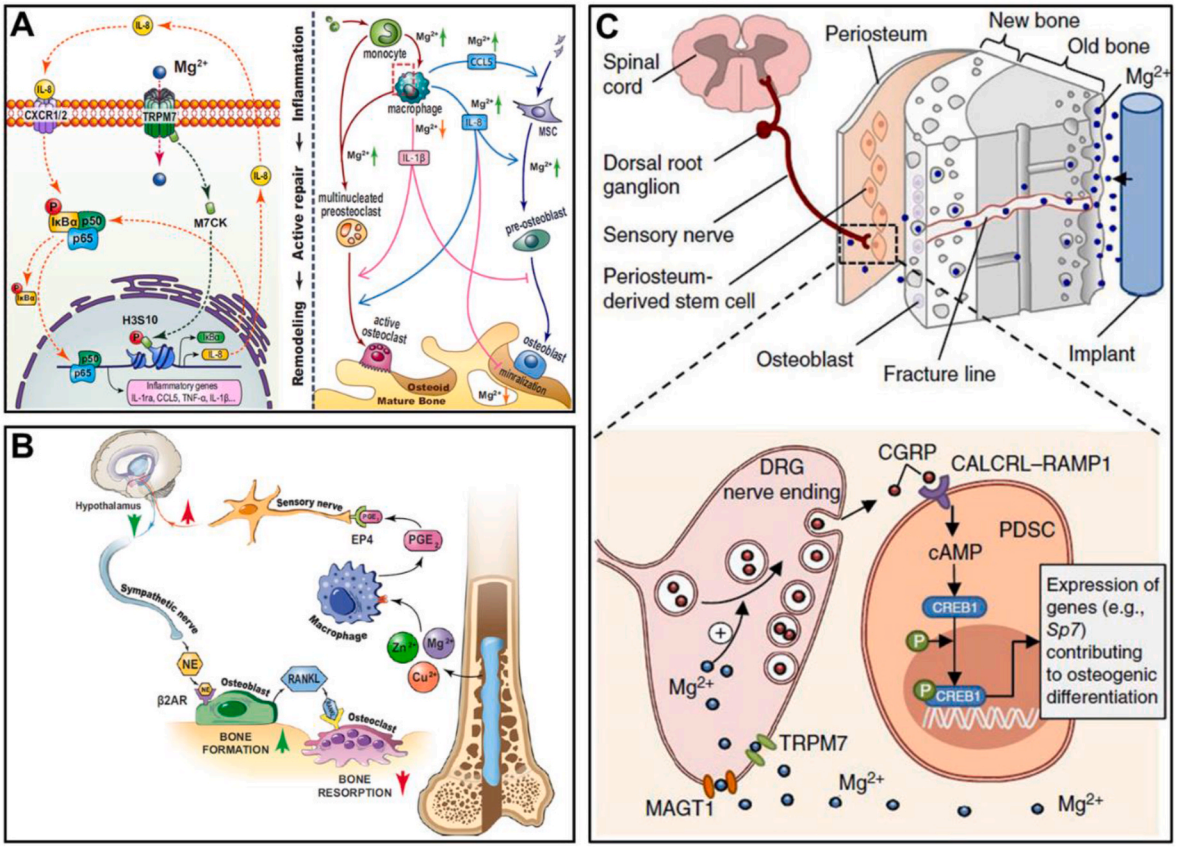

Fig. 9. (A) The mechanism in which Mg^{2+} modulates macrophages, nerve cells, and MSCs in the bone healing process [154]. (B) A schematic diagram of the divalent cations triggered the production of PGE2 from macrophages, which activated the EP4 at the sensory nerve to tune down sympathetic tones via the CREB signaling in the VMH, resulting in increased osteogenesis and decreased osteoclastogenesis in the periosteum [159]. (C) Illustration of Mg^{2+} promoting the secretion of CGRP in the rat dorsal root ganglion, thereby enhancing the signaling pathway of osteogenic differentiation of periosteum-derived stem cells [160]. Copyright 2016, 2021, 2022 Springer Nature.

immune microenvironment. This activated the high expression of bone morphogenetic protein-2 (BMP-2) and vascular endothelial growth factor A proteins associated with new bone and vascular regeneration in human MSCs (Fig. 9A).

In addition to inducing tissue regeneration by activating macrophages in the microenvironment, the active cations released from Mg and its composites can also interact in a cascade with other cells, thereby mediating the tissue repair process. Further research by Qiao et al. [159] found that Mg^{2+} and Zn^{2+} could stimulate periosteum sensory by promoting the secretion of prostaglandin E2 (PGE2) from macrophages. This immune response was accompanied by the sprouting and dendritic budding of CGRP-α and nerve fibers. Subsequently, the nerve fibers perceived inflammation clues through the PGE2 receptor 4 and transmitted the interosensory signals to the central nervous system, which downregulated sympathetic neural tension for new bone formation, thereby promoting bone generation, as shown in Fig. 9B. Zhang et al. [160] also found that the increase in extracellular Mg^{2+}-induced magnesium transporter 1 (MAGT1) and TRPM7-dependent Mg^{2+} influx, as well as an increase in intracellular adenosine triphosphate and vesicle accumulation in the nerve endings of rat dorsal root ganglion neurons *in vitro*. Ultimately, CGRP-induced calcitonin receptor-like receptor (CALCRL) and receptor activity-modifying protein 1 (RAMP1)-dependent activation of cAMP-responsive element binding protein 1 (CREB1) and Sp7 transcription factor in periosteal stem cells derived from rats *in vitro*, thereby enhancing the osteogenic differentiation of periosteal MSCs (Fig. 9C).

Despite the burgeoning number of biological studies on biodegradable Mg and its composites, currently, we know little about how these materials drive cellular cascading responses and induce their physiological functions. Therefore, it is necessary to further investigate and clarify their intrinsic mechanisms to optimize their healing effects.

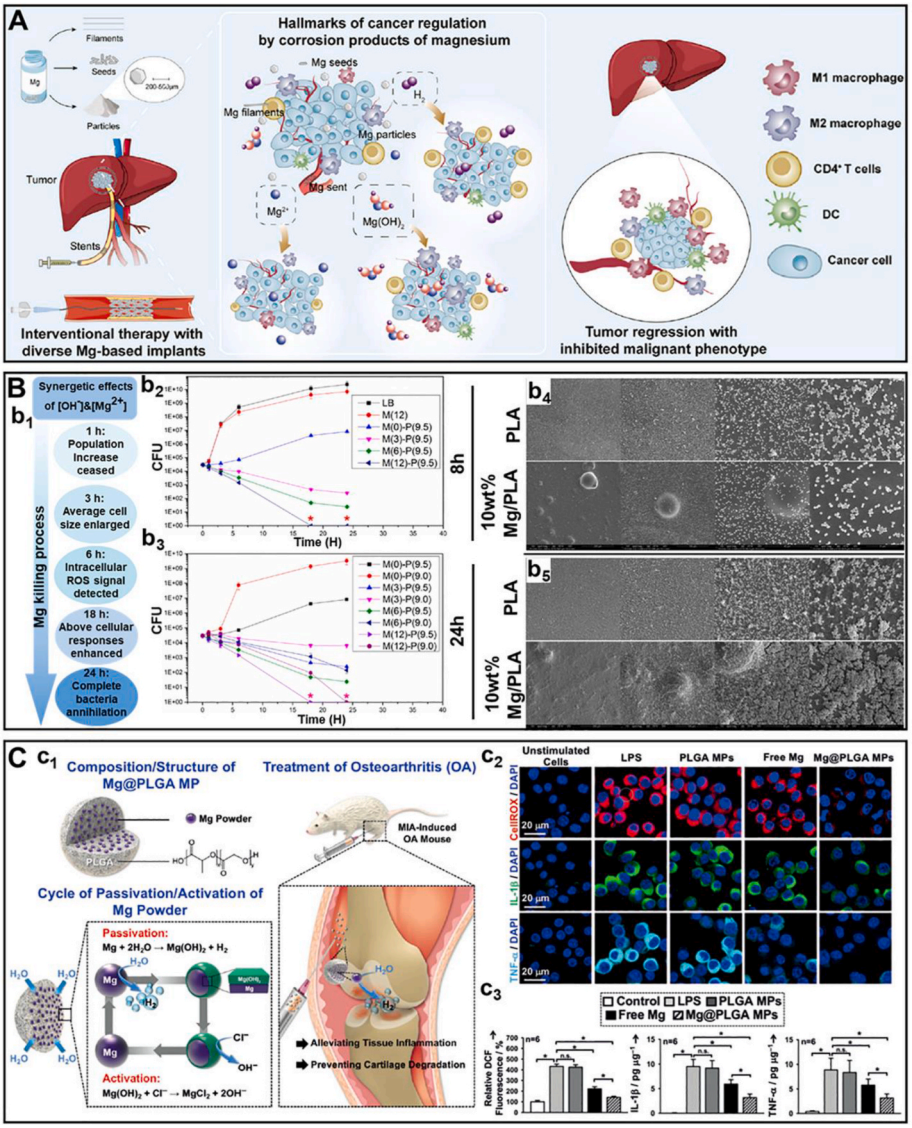

Fig. 10. Other biological functions of BMPC. (A) The antitumor applications in diverse physical forms for interventional therapy and antitumor mechanism [161]. (B) Antibacterial mechanism of Mg: (b_1) Schematic showing the bacteria-killing process and cellular response in 24 h. (b_2-b_3) Antibacterial ability of Mg^{2+} and alkalinity alone and in combination [165]. (b_4-b_5) SEM images of *S. epidermidis* biofilm on PLA and PLA/Mg films after 8 h and 24 h of incubation [166]. (C) Mg@PLGA composite microparticles inflammation inhibition effect and molecular mechanism of osteoarthritis: (c_1) Mechanism of the evolution of H_2 gas in situ from composite microparticles, suppressing tissue inflammation and degradation of cartilage in mice with osteoarthritis. (c_2) Laser confocal microscope images of cellular ROS, IL-1β, and TNF-α and (c_3) their corresponding intensities in lipopolysaccharide stimulated RAW264.7 cells following various treatments [171]. Copyright 2020, 2023, Elsevier; 2016, American Chemical Society; 2018, John Wiley and Sons.

4.3. Other biological functions

The biological functions of BMPC are mainly dependent on the corrosion products of the Mg in the composite, including intermediate and end products. During degradation, BMPC release active cations, except for this, inorganic compounds, alkaline microenvironment, hydrogen gas, transient reactive oxygen species, and other reactive intermediate species are also associated with regeneration. The effects of these products on tissues should not be overlooked. In addition to repairing damaged tissues, these products can also work in conjunction with Mg^{2+} to combat pathogens or tumors/cancer and play an antioxidant and anti-inflammation role in some inflammatory tissues.

4.3.1. Anti-tumor/cancer function

Mg and its composites are widely reported materials with anti-tumor effects. Materials containing Mg can produce three effective anti-tumor products during degradation, including $Mg(OH)_2$, H_2, and Mg^{2+} (Fig. 10A) [161]. The anti-tumor process of an Mg-containing implant involved three stages. First, during tumor proliferation, vigorous cell glycolysis produced excess lactate, leading to an acidic microenvironment (pH = 6.8 is optimal for tumor cell proliferation). Mg and its composites could produce $Mg(OH)_2$ during degradation, which continuously alkalizes the tumor microenvironment, significantly inhibiting tumor cell proliferation. Secondly, Mg and its composites underwent a reduction reaction, continuously producing H_2 with significant anti-inflammatory and antioxidant effects, effectively suppressing oxidative stress and enhancing the sensitivity of conventional anti-tumor drugs. Finally, tumor patients often had concurrent hypomagnesemia, affecting tissue cell enzymatic reactions and metabolic functions, accelerating the malignancy of the tumor. The continuous high concentration of Mg^{2+} produced during the degradation of Mg and its composites could remodel the tumor microenvironment, inhibit the malignant development of tumor cells, and improve the overall body condition of the patient.

To uncover the local anti-tumor effects of Mg-containing materials, Zan et al. [162] conducted in-depth research on the molecular mechanism of H_2 release from Mg-induced apoptosis in human colon carcinoma HCT116 cells. Genomic and proteomic studies revealed that the localized release of H_2 increased the expression levels of the P53 tumor suppressor protein. Subsequently, the P53 protein disrupted the mitochondrial membrane potential of HCT116 cells, activated autophagy, and inhibited reactive oxygen species within the cells, ultimately leading to tumor suppression. Furthermore, they validated the anti-tumor efficacy of Mg-containing materials in a subcutaneous tumor model in mice and obtained compelling data indicating that the lowest hydrogen concentration capable of inducing apoptosis in a large number of tumor cells was 91.2 μL mm^{-3} day^{-1}. Additionally, biodegradable Mg alloy and its composite can locally ablate tumor cells by photothermal or eddy current thermal effect, with significantly killed tumors.

4.3.2. Antibacterial function

The antimicrobial properties are crucial for BMPC. BMPC may be susceptible to bacterial infections during tissue repair, surgery, or post-surgery, potentially causing delayed tissue healing if the infection is not cleared promptly. It has been reported that adjusting the Mg content in BMPC can inhibit bacterial adhesion and biofilm formation, as well as maintain cell compatibility [163]. The antimicrobial mechanism of BMPC is mainly attributed to the positively charged Mg^{2+} released, disrupting the charge balance of negatively charged bacterial cell membranes. Additionally, an increase in ion concentration leads to an elevation in bacterial extracellular osmotic pressure, resulting in cellular dehydration. A significant increase in pH also causes bacterial acid-base imbalance and death.

While numerous studies reported on the antibacterial properties of pure Mg metals or BMPC, there remains considerable controversy regarding their antibacterial efficacy and biocompatibility. This is due to a lack of consistency in the culture protocols employed for antibacterial and cell experiments in such research [164]. Further validation is needed for studies concurrently relying on Mg to achieve both the antibacterial function and biological compatibility. According to the study reported by Feng et al. [165], the antibacterial effect of Mg-containing materials depended on the combined effect of the released Mg^{2+} and OH^-. Only when the local environment reached a Mg^{2+} concentration of 300 ppm and a pH above 9.5, could Mg-containing materials exhibit significant antibacterial properties. The bacteria-killing process and cellular response in 24 h is presented in Fig. 10B. However, below this critical condition, bacterial colonization on the surface of Mg/PLA composite materials could even promote the further development of bacterial biofilms, leading to a more mature biofilm formation on Mg/PLA films compared to PLA films alone [166]. For BMPC, relying solely on increasing the Mg content to achieve antibacterial purposes is not reliable. This is because exceeding the critical condition for Mg antibacterial properties can lead to reduced cell tolerance (e.g. cell lines including L929, NIH 3T3, MC3T3-E1, and ECV304, exhibit intolerance to Mg^{2+} concentrations over 240 ppm and pH level over 8.8 [167]). Lee et al. [168] also found that Mg/PLA composite materials containing 15 vol% Mg exhibited a significant improvement in enhancing cell adhesion and proliferation. However, the composite materials with 30 vol% Mg showed a deterioration in cell proliferation and differentiation due to the rapid degradation of Mg particles. Even in Mg/PLA materials containing as high as 30 vol% Mg, many bacteria still thrived on the material surface. This was because the Mg^{2+} concentration and pH of the Mg/PLA composite materials at this content within 24 h of degradation did not exceed 300 ppm and 7.8, respectively, failing to meet the antimicrobial requirements. At this moment, 300 ppm already far exceeded the tolerance of MC3T3-E1 cells to Mg^{2+}.

To address the inconsistent tolerance of bacteria and cells to the degradation products of BMPC, many researchers introduce additional antibacterial components such as Zn (antibacterial threshold <100 μM), Cu (antibacterial threshold <100 μM), and Ag (antibacterial threshold <1 μM), which are metallic elements with stronger antibacterial properties and bacterial-targeting [169], to develop BMPC that possess both antibacterial activity and biocompatibility. Furthermore, adjunctive photothermal therapy can help rapidly kill bacteria within minutes, thereby enhancing the antibacterial efficacy of BMPC. In sum, in the development of antibacterial BMPC, there is a need to balance the demands of antibacterial properties and biocompatibility.

4.3.3. Antioxidant and anti-inflammation function

Mg and its composites also exhibit remarkable antioxidant and anti-inflammation functions due to their bioactive degradation by-product. On one hand, Mg and its composites release hydrogen gas during degradation. As hydrogen is a reductive gas, this confers Mg with an antioxidative capacity unavailable in the other biodegradable metal types (Zn and Fe). Recent years have seen this hydrogen gas therapy deployed in the treatment of inflamed tissues, such as osteoarthritis [170]. Manifestations of osteoarthritis included the activation of highly concentrated ROS in the joint and subsequent inflammation, which induced significant oxidative damage and apoptosis in chondrocytes. Hydrogen therapy mitigated excessive ROS, alleviated oxidative stress, reduced inflammation, and protected chondrocytes and joints. However, the direct application of hydrogen gas therapy encountered challenges due to its low solubility and easy diffusion, leading to poor bioavailability. To overcome this, Wan et al. [171] designed a localized delivery system based on Mg@PLGA composite microparticles. *In vivo* studies in mouse osteoarthritis knee joints demonstrated that, through the passivation/activation cycles of Mg in body fluids and under concentrations exceeding the hydrogen therapy threshold, this system gradually evolved into gaseous hydrogen, effectively ameliorating tissue inflammation, preventing cartilage destruction, and halting the progression of osteoarthritis (Fig. 10C). On the other hand, Mg^{2+} in extracts of Mg

alloys could inhibit the translocation of p65 to the cell nucleus induced by lipopolysaccharide and improve immune microenvironment. This inhibition suppressed ROS generation, matrix metalloproteinase expression, and NF-κB signaling, effectively reducing local inflammation response and ultimately treating osteoarthritis [144].

In summary, all the function strongly relies on the release of Mg^{2+} and gas, alteration of the pH of the microenvironment, or other reactive intermediates. However, the inevitable harm to normal cells, disruption of microenvironment homeostasis, and induced inflammatory responses during tissue repair are often neglected or not well-researched. Therefore, comprehensive considerations are needed to balance pathogen eradication and tissue regeneration when designing such functional materials in the future.

4.4. Progress in clinical application of Mg-containing medical devices

Currently, several Mg metals and their composites have been successfully translated and clinically applied in orthopedic or cardiovascular implantable devices worldwide. However, most BMPC remains in the laboratory or preclinical stages. For example, in 2013, the Magmaris Mg alloy screw (Mg-Y-RE-Zr alloy) produced by Syntellix (Germany) became the first Mg alloy bone implant to receive CE certification in the European Union. In 2015, the KMET Mg screw (Mg-Ca alloy) produced by the South Korean company U&I also received approval from the South Korean Food and Drug Administration for use in hand fracture internal fixation surgery. In 2016, BIOTRONIK (Germany) released the absorbable cardiovascular scaffold Magmaris BRS (BIOSOLVE-II) for commercial use. This stent is composed of Mg as the matrix, supplemented with a PLLA drug-eluting coating. The stent has a thickness of 150 μm and adopts a 6-crown 2-link design. In 2021, BIOTRONIK announced the clinical study results of the absorbable cardiovascular stent Magmaris BRS in 123 patients over a 5-year follow-up period. The composite stent demonstrated safety and efficacy, significantly reducing the occurrence of in-stent restenosis postoperatively, and no stent thrombosis was found. In 2024, BIOTRONIK announced again that its self-developed Freesolve™ bioresorbable Mg stent (Mg stent with PLLA coating and drug loading) has received FDA Breakthrough Device designation for the treatment of below-the-knee peripheral artery disease.

Additionally, in China, policies regarding the approval and registration of Mg-containing implants have been issued, focusing on key issues such as the devices' corrosion resistance, controllable degradation rate, and risk assessment standards for *in vivo* Mg degradation. In 2023, the National Medical Products Administration of China approved the registration application for the innovative product of Mg metal clips from Suzhou Aoruiji Medical Technology Co., Ltd. Moreover, Mg alloy screws developed by Dongguan Yian Technology Co., Ltd., and the Mg-Nd-Zn-Zr (JDBM) Mg alloy bone plates and screws developed through a collaboration between Shanghai Jiao Tong University and an enterprise, are leading the way. 3D-printed PLGA/TCP/Mg composite bone repair scaffolds, jointly incubated by the Shenzhen Institutes of Advanced Technology (Chinese Academy of Sciences), have been awarded special approval for innovative medical devices by the National Medical Products Administration of China. It has already completed preclinical registration testing. At present, it is currently in a multicenter clinical trial phase. Although clinical research on BMPC is limited, the positive results achieved worldwide in the development and clinical research of Mg-containing medical devices are expected to drive the clinical application of BMPC devices.

5. Stimuli-responsive therapy platform based on Mg/polymer composite

It is generally believed that the physiological function of BMPC relies on the bioactive products released by Mg degradation. In addition to these, the composite itself can be designed to possess stimuli-responsive functionality, enhancing the biological performance of the composite. The composite can trigger self-physical or chemical changes after implantation, thus selectively initiating tissue repair functions by releasing various substances to induce microenvironment changes (pH and Mg^{2+} concentration variation), or under external stimuli (such as light, magnetic field, ultrasound, microwave, stress, etc.). Combining biodegradable composites with stimuli-responsive therapeutic platforms can maximize the treatment effectiveness beyond the composites themselves while reducing side effects. Due to these advantages, such stimuli-responsive therapeutic platforms are gaining increasing attention from researchers. The following section will introduce several design and application scenarios of stimuli-responsive BMPC.

5.1. pH responsiveness

pH-sensitive materials are a type of materials that undergo changes in their volume, shape, or chemical bond breakage as a response to the local environment pH. They contain functional groups sensitive to H^+ or OH^- within their molecules, enabling them to change the intra- or intermolecular forces with external pH variations, leading to various macroscopic property changes, and consequently achieving controlled "drug" release from the carrier during the therapeutic process. As it happens, BMPC can also rapidly alter the pH surrounding the medium during degradation.

In most cases, researchers only consider the effects of localized changes in material acidity or alkalinity on tissues, while neglecting the material's responsiveness and the interaction between "material-cell/tissue". Distinct from other soft tissue repair materials, our previous study [88] found that Mg/PLGA microfiber membranes prepared by electrospinning exhibited a spontaneous micro/nano-hierarchical porous morphology when immersed in PBS or cell culture medium (Fig. 11A), since the Mg microparticles degraded and elevated the medium pH to around 8.5. Analysis of the composition of the composite revealed that the micro-phase separation was caused by the differential reaction sensitivity of LA and GA monomers in the PLGA copolymer in response to OH^-. Inspired by this, we conducted genomic and proteomic studies on the pH-responsive composite microfibers and found that the micro/nano-hierarchical porous microfibers enhanced endothelial cell adhesion, spreading, and proliferation, as well as activated endothelial cell angiogenic capacity through the release of Mg^{2+} via the bFGF/bFGFR signaling pathway. Furthermore, two soft tissue defect models were established, one for refractory healing urethral tissue defects and the other for easily healing skin defects, confirming the pH-responsive fibrous membrane could promote tissue integration and facilitate soft tissue vascularized repair.

After a significant increase in pH, vast changes occur not only in the physical form of the polymer but also in the morphology of Mg itself. Dong et al. [172] found that when the easily corroded Mg was coated with dicalcium phosphate dihydrate, the material could rapidly revert to its original form in simulated human body fluid even if the protective layer was damaged. This was because the dicalcium phosphate dihydrate protective coating exhibited high pH sensitivity, especially in an alkaline environment. When the corroded area caused a local rise in pH after the protective layer was damaged, it stimulated the release of Ca^{2+} and PO_4^{3-} from dicalcium phosphate dihydrate in a feedback reaction, leading to the reformation of inorganic deposited at the damage site, thus facilitating the self-healing process.

Although the current technology for the *in vitro* application of these pH-sensitive materials is relatively mature, their further *in vivo* application still poses challenges. This is mainly due to the differences between the degradation rate *in vitro* and *in vivo*. In non-dynamic *in vitro* environments, the rapid degradation of Mg and its composites can induce rapid changes in the surrounding medium pH, triggering the materials' pH-responsive behavior. However, *in vivo* experiments, unlike closed *in vitro* environments, involve significant material exchange and ion transport processes. The degradation products of the materials are

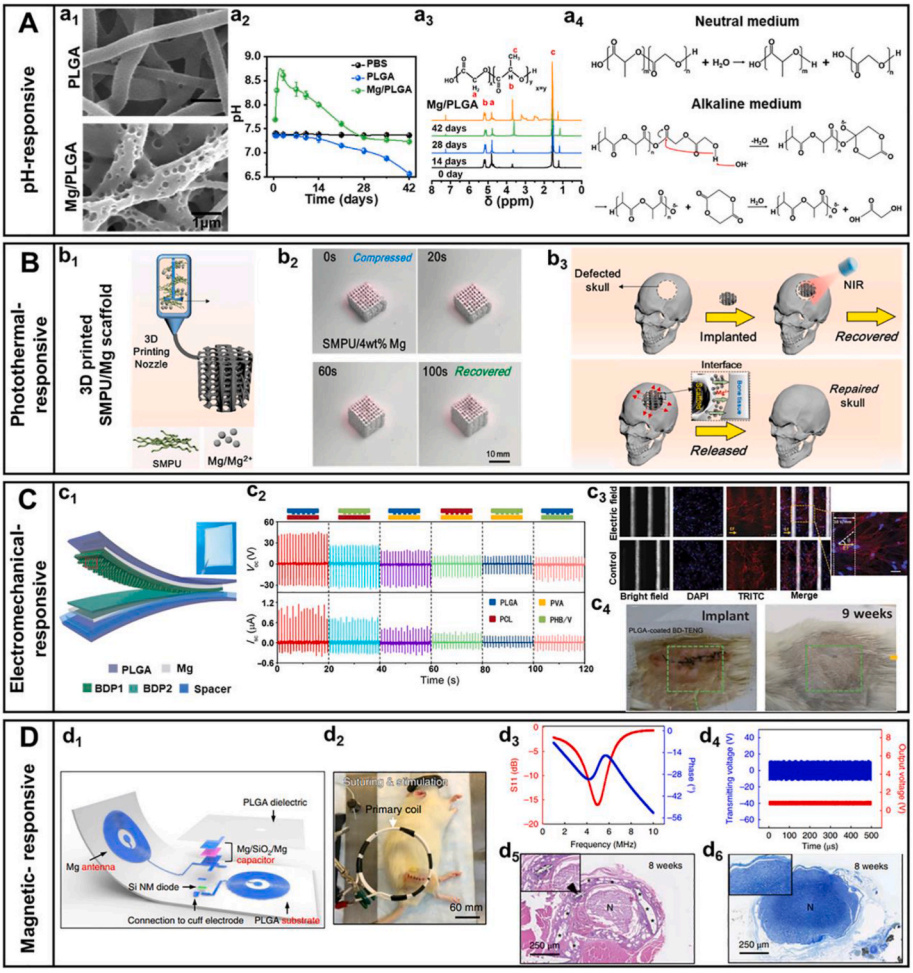

Fig. 11. Design and application scenarios of stimuli-responsive BMPC. (A) Design and application of pH-responsive Mg/PLGA microfibers for soft tissue repair [88]: (a_1) Typical microstructure of the two kinds of microfibers after degradation in PBS. (a_2) pH changes of PLGA and Mg/PLGA microfibers. (a_3) ^{1}H NMR spectra of residual polymer matrix in Mg/PLGA microfibers with time. (a_4) The scission mechanism of PLGA molecular chains in neutral and alkaline degradation medium. (B) Design and application of 3D-printed NIR-responsive SMPU/Mg scaffolds with tight contact for robust bone regeneration [174]: (b_1) 3D printed SMPU/Mg scaffold. (b_2) Photographs of the shape recovery process in the air of the regular SMPU/Mg scaffold irradiated by the 808 nm laser. (b_3) After implantation, the compressed scaffold recovered in NIR light, resulting in the supporting stimulus at the interface between the scaffold and tissue. (C) Design and application of biodegradable TENG (BD-TENG) composed of Mg and polymer layers including PLGA, PVA, PCL, and PHB/V [178]: (c_1) Schematic diagram of BD-TENG. (c_2) Electric output performance of BD-TENG with different friction polymer layers. (c_3) Orientation and distribution of nerve cells cultured on the electrodes with/without electric field stimulation (TRITC, tetramethyl rhodamine isothiocyanate). (c_4) Images of an implanted BD-TENG located in the subdermal dorsal region of an SD rat after surgery and 9 weeks, respectively. (D) Design and application of the magnetic responsive devices [180]: (d_1) The component of the magnetic responsive system including a wireless receiver, inductor, a radio frequency diode, a Mg/SiO_2/Mg capacitor, and a PLGA substrate interconnected with Mg deposited by sputtering (left). (d_2) The electrical stimulation activated with a transmitting coil under a wireless magnetic field. (d_3) Radiofrequency behavior of the stimulator (red, S11; blue, phase, resonance frequency ~5 MHz). (d_4) Example output waveform (stimulator, red) wirelessly generated by an alternating current (sine wave) applied to the transmission coil (transmitter, blue). (d_5-d_6) H&E-stained sections and Toluidine blue-stained sections obtained at the interface between the metallic electrodes of the nerve cuff and the sciatic nerve. Copyright 2022, 2024 Elsevier; 2016 Science AAAS; 2018, Springer Nature.

likely metabolized to other locations in a short time, which may prevent these pH-responsive materials from reaching the required pH range to trigger the response. Therefore, future research should focus on studying the effectiveness of the pH responsiveness of materials in environments that more accurately reflect *in vivo* conditions.

5.2. Photothermal responsiveness

Apart from the stimuli-responsiveness induced by chemical reactions in Mg/polymer composites, their inherent physical properties can also respond to external stimuli. In recent years, bio-materials with photo-sensitive characteristics have received wide attention from researchers, particularly in the repair of infected and tumorous tissues. Phototherapy (such as photothermal treatment) is flexibly applied due to its temporal and spatial controllability, as heat can directly or indirectly affect cellular behavior. High temperatures could cause protein unfolding and aggregation, DNA damage, and irreversible protein denaturation, resulting in cell damage or even death, which had an important role in bacterial killing and tumor therapy. Alternatively, mild heat could enhance membrane permeability without affecting cellular vitality, promoting the influx of functional materials or biomolecules into the cytoplasm for specific cellular function activation [173].

Bulk Mg or polymer materials themselves do not possess photo-responsive capabilities. To confer it with photo responsiveness to composites, a feasible approach is to change the size of the Mg to the micro or nanoscale to endow it with localized surface plasmon resonance ability, thereby generating a photo-thermal conversion. For example, as shown in Fig. 11B, Zhang et al. [174] combined Mg microparticles with shape-memory polyurethane (SMPU) to fabricate a porous bone repair scaffold using low-temperature rapid prototyping 3D printing

technology. This scaffold could be heated and activated within 60 s to restore the original porous form from a compressed form based on the shape memory ability of SMPU when exposed to near-infrared (NIR) light. After thermal activation of the scaffold, the gentle NIR-induced photothermal effect could further stimulate the osteogenic differentiation of MSCs, accelerating the healing of bone defects, and providing new ideas for minimally invasive intervention therapy for bone repair.

Additionally, photosensitizers can be introduced into the polymer part of the composite. For example, Zhao et al. [175] constructed mesoporous silica microcapsules loaded with simvastatin on the surface of Mg alloy and then used layer-by-layer self-assembly technology to modify the Mg alloy surface with the photo-sensitive dopamine and poly (ε-caprolactone-*co*-diacrylate) bi-molecular hybrid coating. This hybrid coating exhibited rapid, stable, and cyclic self-healing capability. Under NIR light exposure, the composite showed excellent antibacterial properties, cell compatibility, bone regeneration, and vascularization due to the synergistic effects of high temperature, reactive oxygen species (ROS), and simvastatin release.

Although significant advances in therapeutic platforms based on photo-responsive materials (including Mg/polymer composite) are made, there are still several bottleneck issues that urgently need to be addressed. First, normal tissues also experience some damage from a laser, leading to factors such as water, hemoglobin, and light scattering causing laser attenuation. Therefore, photothermal therapy (or photodynamic therapy) is limited by its relatively low penetration depth. Even though the use of photosensitizers with excitation wavelengths within the biological window (the first biological window: 650–900 nm (NIR-I) and the second biological window: 900–1700 nm (NIR-II) [176]) could achieve some tissue penetration, it still could not reach deep into human tissues. There is still an urgent need to develop novel platforms with high penetrability, non-invasiveness, and controllability to promote their clinical application. Second, in photothermal therapy for killing pathogens such as bacteria or tumor cells, the local tissue temperature needs to be maintained around 50 °C for several minutes, which can lead to overheating and thermal damage to normal tissues during the treatment process. Reducing this damage is also currently one of the hotspots in research on photosensitive materials.

5.3. Electromechanical responsiveness

Electromechanical responsiveness usually refers to the process of converting mechanical signals of materials into electrical signals. Mg and its alloys themselves do not possess electromechanical responsiveness. In some natural or synthetic polymer materials, internal dipoles could be displaced under stress, causing a non-coincidence of positive and negative charge centers, and thus displaying an electric charge [177]. Upon implantation into the body, these mechanical-sensitive nanomaterials, apart from substances released by their degradation, could also convert excessive physiological stress in the body into electrical signals. This further stimulated tissue regeneration through mediating bioelectrical signal transduction processes. These energy-producing devices are known as piezoelectric nanogenerators (PENG). Additionally, combining two or more materials can couple electrical signals produced by mutual friction and electrostatic induction, releasing external electrical signals. These energy devices, composed of multiple materials, are referred to as triboelectric nanogenerators (TENG). This unique mode of operation allows the application of TENG under movement and physiological conditions, collecting biomechanical energy such as body movement, respiration, and heartbeats. Electrical signals produced by electromechanical conversion could be used to enhance the neural differentiation of MSCs in the field of tissue engineering.

For instance, the team led by Zhong Lin Wang [178] constructed a frictional component assembled from two types of degradable polymer layers (including PLGA, poly (vinyl alcohol) (PVA), PCL, and poly (3-hydroxybutyric acid-*co*-3-hydroxyvaleric acid) (PHB/V)) with a nano-surface structure, and introduced a spacer layer (200 μm) between these frictional layers to generate an effective separation space. A layer of Mg film with a thickness of 50 nm was also deposited on one side of each frictional layer as an electrode layer. The entire biodegradable TENG (BD-TENG) was finally packaged with biodegradable polymers. It was found that when the two polymer friction layers were composed of PLGA and PCL, the entire BD-TENG had the maximum frictional voltage and current output. However, as the whole TENG was degradable, the BD-TENG substrate and the friction voltage gradually disappeared after 21 days of degradation. Due to its excellent biocompatibility and ability to generate electricity through friction, this BD-TENG could stimulate neurons to align in the direction of the electric field and promote accelerated wound healing in rats (Fig. 11C).

Although these types of degradable power generation devices based on composite can currently utilize excess energy from the human body to promote tissue repair functions, there are some difficulties faced for their further transformation. One factor that needs particular consideration is their reliance on cumbersome and complex equipment and wires to collect and conduct electrical signals. Hence, the development of portable, wireless, universal, operable electromechanical-driven strategies may be one of the key developmental directions for future electromechanically responsive degradable materials.

5.4. Magnetic responsiveness

Possessing strong tissue penetration ability and painless, non-invasive characteristics, magnetic fields have broad clinical applications. Magnetic-responsive materials are mainly composed of magnetic microparticles and nanoparticles. Taking degradable magnetic particles as an example, which are primarily composed of Fe metal and its oxides, these magnetic materials themselves have both *in vivo* magnetic resonance imaging and therapeutic functions. At present, they have been widely applied in the biomedical field, such as in controlled drug release and tissue engineering [179]. Apart from Fe and its composites that can respond to magnetic fields, other non-magnetic degradable metals can also be combined with semiconductor devices to form degradable composite devices with magnetic induction capabilities. For instance, Rogers' team [180] invented a wireless biodegradable composite electronic system that could generate continuous electrical stimulation for nerve regeneration therapy. This implantable device, encapsulated by PLGA, included a Mg loop antenna, Si radio frequency diode, and Mg/SiO_2/Mg capacitor. It used magnetic induction-coupled power transmission to obtain radio frequency power, aiming to deliver electrical stimulation signals inside the body for peripheral nerve repair. When applied to the rat sciatic nerve injury model, the device could regulate the intensity of electrical stimulation by adjusting the external magnetic field intensity or receiving parameters of the Mg coil to achieve the purpose of on-demand repairs (Fig. 11D).

Magnetic-responsive composite treatment platforms also exhibit excellent capabilities in areas such as lesion targeting, enhancing biomembrane permeability, and magnetic thermal effects. Nevertheless, there are notable drawbacks to magnetic responsive materials. On one hand, when using nanomagnetic particles in a biological body or cells, once escaping from a biodegradable material substrate, nanoparticles smaller than 50 nm can pass through the bio-membrane, inducing inflammation, generating reactive oxygen species, hindering DNA functions, and inducing cell apoptosis leading to detrimental effects on tissue function. Therefore, evaluating the biocompatibility of magnetic responsive materials is vital before application. On the other hand, devices composed of magnetic responsive composites for tissue repair also face the issue of relying on cumbersome and complex equipment and wires to collect and conduct signals. Hence, the development of wireless, biologically safe, and effective magnetic induction degradable materials may be an important direction for future functional material development.

5.5. Other responsiveness

The aforementioned stimulus-responsive therapy platforms mainly rely on the physicochemical properties of Mg. In addition, common polymers such as poly-3-hydroxybutyrate (PHB) and PLLA have been found to exhibit good piezoelectric performance due to the existence of polar carbonyl functional groups (C=O). Therein, reducing the molecular weight of PHB decreases its piezoelectric structure domain, thereby weakening the piezoelectric effect [181]. Further increasing the proportion of 3-hydroxyvalerate (3-HV), a co-monomer of PHB, leads to a decrease in crystallinity and the loss of piezoelectric response. For PLLA, improvements in orientation and crystallinity due to stretching, annealing, and supercritical CO_2 treatment also enhance its piezoelectric effect [182]. Besides the piezoelectric effect, PLA and PLLA can utilize its glass transition temperature as a transformation point for the shape memory effect [183,184], enabling reversible transition between the glassy state and rubbery state, thus facilitating minimally invasive delivery of drugs or medical devices. Inspired by these, it is expected that more stimulus-responsive therapy platforms based on these polymers and Mg will be developed to broaden the application of BMPC.

In conclusion, stimuli-responsive platforms pave the way for innovative applications of BMPC in the realm of tissue engineering. Despite these responsive treatment platforms demonstrating superior therapeutic effects at a laboratory scale, the aforementioned side-effect challenges must be addressed before their clinical utilization. Given the swift progressions in both material science and life sciences, these limitations could potentially be overcome in time. It is projected that stimuli-responsive treatment platforms could soon provide effective solutions for tissue repair.

6. Conclusion and perspectives

BMPC, owing to its favorable mechanical properties and biodegradability, has garnered substantial scholarly attention. The composite concept mitigates not only the risk of Mg corrosion and localized environmental alkalization but also weakens the acidic stimuli of polymer degradation by-products on tissues. Herein, based on the discussion of the whole paper, we briefly summarize the basic criteria that need to be met for the preparation and application of BMPC from the perspectives of composition design, surface modification, mechanical properties, biodegradability, biological performance, and stability, as illustrated in Fig. 12.

Currently, some BMPCs demonstrate outstanding therapeutic effects at the laboratory scale, but the development and evaluation of clinically applicable composites present challenges. Herein, we present future perspectives based on the above criteria.

(i) Organic surface modifiers enhance the interfacial bonding and mechanical properties of composite materials but also introduce potential safety hazards. Future development should focus more on safe and efficient surface modification strategies.
(ii) The physiological environment is a complex and multifactorial coupled system. To accurately predict the real-life performance of degradable materials like BMPC in this environment, establishing a multi-field coupled *in vitro* degradation platform based on "microfluidic chips" and "organs-on-chips" is of great

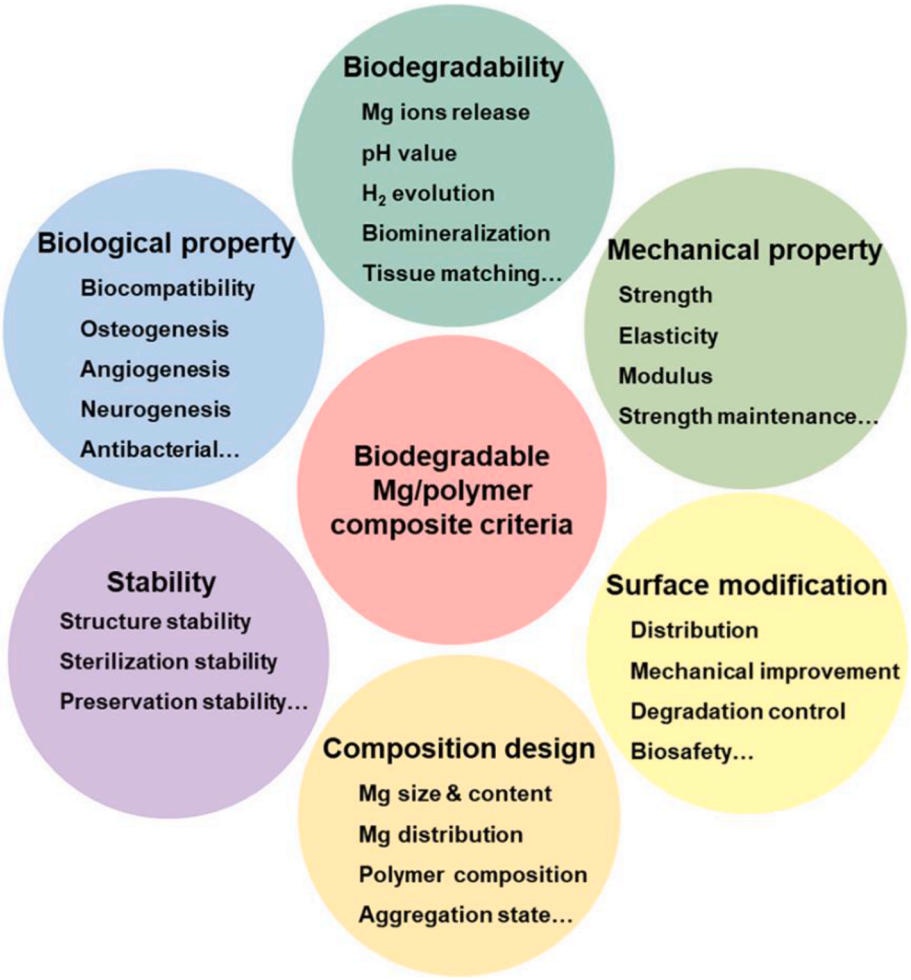

Fig. 12. Schematic diagram of the main criteria that an ideal BMPC should fulfill.

significance for the comprehensive and real-time evaluation of the efficacy of all biomaterials.

(iii) Early in degradation, BMPC can effectively control degradation rates through interface modification and processing. However, risks in the later stages, such as premature detachment, disintegration, or large fragment entry into body fluids or cavities, can cause secondary damage or cavity obstruction. Therefore, further tracking of the full-stage degradation changes to several years of BMPC is necessary for preclinical studies.

(iv) The process of tissue regeneration mediated by biomaterials such as BMPC is complex, involving hemostasis, inflammation (immune response), proliferation, remodeling, and interactions with surrounding tissues. However, research on BMPC in this area is limited, indicating the need for further in-depth studies.

(v) The "stimulus-responsiveness" endows BMPC with powerful functions beyond their own performance. However, this comes at the cost of adverse, potentially irreversible effects on surrounding normal tissues. Therefore, the development of gentle yet effective multifunctional composite materials and related intelligent therapeutic platforms is crucial.

Ethics approval and consent to participate

Ethics approval and consent to participate does not apply to this review manuscript.

CRediT authorship contribution statement

Xianli Wang: Writing – original draft, Investigation, Funding acquisition, Formal analysis, Conceptualization. **Cheng Wang:** Writing – review & editing, Supervision, Funding acquisition, Formal analysis, Data curation. **Chenglin Chu:** Supervision, Resources, Methodology, Formal analysis, Conceptualization. **Feng Xue:** Validation, Supervision, Resources, Project administration, Investigation, Funding acquisition, Formal analysis. **Jun Li:** Writing – review & editing, Supervision, Resources, Investigation, Formal analysis. **Jing Bai:** Writing – review & editing, Validation, Supervision, Resources, Project administration, Funding acquisition, Formal analysis, Data curation, Conceptualization.

Declaration of competing interest

The authors declare that they have no known competing financial interests or personal relationships that could have appeared to influence the work reported in this paper.

Acknowledgments

This work was supported by the Science and Technology Project of Jiangsu Province (BE2023719), Suzhou Science and Technology Project (SYC2022135, SJC2023005, SZS2023023), the Open Research Fund of Jiangsu Key Laboratory for Advanced Metallic Materials (AMM2024A01, AMM2023B03), Jiangsu Key Laboratory for Light Metal Alloys (LMA202403), and Jiangsu Key Laboratory of Advanced Structural Materials and Application Technology (ASMA202304). Ms. X. Wang thanks the China Scholarship Council for the award of fellowship and fundings (No. 202306090175).

References

[1] A.K. Gaharwar, I. Singh, A. Khademhosseini, Engineered biomaterials for in situ tissue regeneration, Nat. Rev. Mater. 5 (2020) 686–705.
[2] Y. Liu, Y. Zheng, X.H. Chen, J.A. Yang, H. Pan, D. Chen, L. Wang, J. Zhang, D. Zhu, S. Wu, K.W.K. Yeung, R.C. Zeng, Y. Han, S. Guan, Fundamental theory of biodegradable metals-definition, criteria, and design, Adv. Funct. Mater. 29 (2019) 1805402.
[3] H. Shi, C. Xu, X. Hu, W. Gan, K. Wu, X. Wang, Improving the Young's modulus of Mg via alloying and compositing-A short review, J. Magnesium Alloys 10 (2022) 2009–2024.
[4] Y. Qin, H. Yang, A. Liu, J. Dai, P. Wen, Y. Zheng, Y. Tian, S. Li, X. Wang, Processing optimization, mechanical properties, corrosion behavior and cytocompatibility of additively manufactured Zn-0.7Li biodegradable metals, Acta Biomater. 142 (2022) 388–401.
[5] H. Yang, B. Jia, Z. Zhang, X. Qu, G. Li, W. Lin, D. Zhu, K. Dai, Y. Zheng, Alloying design of biodegradable zinc as promising bone implants for load-bearing applications, Nat. Commun. 11 (2020).
[6] S. Wu, X. Liu, K.W.K. Yeung, C. Liu, X. Yang, Biomimetic porous scaffolds for bone tissue engineering, Mat. Sci. Eng. R. 80 (2014) 1–36.
[7] D. Katti, S. Lakshmi, R. Langer, C. Laurencin, Toxicity, biodegradation and elimination of polyanhydrides, Adv. Drug Deliv. Rev. 54 (2002) 933–961.
[8] C. Mukherjee, D. Varghese, J.S. Krishna, T. Boominathan, R. Rakeshkumar, S. Dineshkumar, C.V.S. Brahmananda Rao, A. Sivaramakrishna, Recent advances in biodegradable polymers – properties, applications and future prospects, Eur. Polym. J. 192 (2023) 112068.
[9] J. Muldoon, C.B. Bucur, T. Gregory, Fervent hype behind magnesium batteries: an open call to synthetic chemists-electrolytes and cathodes needed, Angew. Chem. Int. Ed. 129 (2017) 12232–12253.
[10] J. Xie, J. Zhang, Z. You, S. Liu, K. Guan, R. Wu, J. Wang, J. Feng, Towards developing Mg alloys with simultaneously improved strength and corrosion resistance via RE alloying, J. Magnesium Alloys 9 (2021) 41–56.
[11] P. Tong, L. Chen, X. Sun, H. Li, Y. Feng, J. Li, S. Guan, Surface modification of biodegradable magnesium alloy with poly (L-lactic acid) and sulfonated hyaluronic acid nanoparticles for cardiovascular application, Int. J. Biol. Macromol. 237 (2023) 124191.
[12] Z. Xue, X. Sun, H. Li, M. Iqbal, L. Qi, F. Wang, Y. Hou, J. Li, S. Guan, Composite coatings of S-HA nanoparticles and Schiff base on ZE21B alloy for stronger corrosion resistance and biological performance, J. Magnesium Alloys 12 (2024) 1102–1116.
[13] M.N. Collins, G. Ren, K. Young, S. Pina, R.L. Reis, J.M. Oliveira, Scaffold fabrication technologies and structure/function properties in bone tissue engineering, Adv. Funct. Mater. 31 (2021) 2010609.
[14] Y. Yuan, Y. Xu, Y. Mao, H. Liu, M. Ou, Z. Lin, R. Zhao, H. Long, L. Cheng, B. Sun, S. Zhao, M. Zeng, B. Lu, H. Lu, Y. Zhu, C. Chen, Three birds, one stone: an osteo-microenvironment stage-regulative scaffold for bone defect repair through modulating early osteo-immunomodulation, middle neovascularization, and later osteogenesis, Adv. Sci. 11 (2024) 2306428.
[15] J. Kong, B. Wei, T. Groth, Z. Chen, L. Li, D. He, R. Huang, J. Chu, M. Zhao, Biomineralization improves mechanical and osteogenic properties of multilayer-modified PLGA porous scaffolds, J. Biomed. Mater. Res. A 106 (2018) 2714–2725.
[16] Y. Lu, Y. Liu, Y. Dai, Y. Yan, K. Yu, Effects of extrusion and rolling processes on the microstructure and mechanical properties of Zn-Li-Ag alloys, Metals 12 (2022) 520.
[17] Y. Qin, H. Yang, A. Liu, J. Dai, P. Wen, Y. Zheng, Y. Tian, S. Li, X. Wang, Processing optimization, mechanical properties, corrosion behavior and cytocompatibility of additively manufactured Zn-0.7Li biodegradable metals, Acta Biomater. 142 (2022) 388–401.
[18] B. Venkateswarlu, B.R. Sunil, R.S. Kumar, Magnesium based alloys and composites: revolutionized biodegradable temporary implants and strategies to enhance their performance, Materialia 27 (2023) 101680.
[19] H. Huang, G. Li, Q. Jia, D. Bian, S. Guan, O. Kulyasova, R.Z. Valiev, J.V. Rau, Y. Zheng, Recent advances on the mechanical behavior of zinc based biodegradable metals focusing on the strain softening phenomenon, Acta Biomater. 152 (2022) 1–18.
[20] Z. Wei, J. Zhang, R. Bao, R. Wu, H. Zhang, Achieving high strength in a Mg-Li-Zn-Y alloy by α-Mg precipitation, Mat. Sci. Eng. A.-Struct. 846 (2022) 143272.
[21] E. Malikmammadov, T.E. Tanir, A. Kiziltay, V. Hasirci, N. Hasirci, PCL and PCL-based materials in biomedical applications, J. Biomater. Sci. Polym. Ed. 29 (2018) 863–893.
[22] P.K. Samantaray, A. Little, D.M. Haddleton, T. McNally, B. Tan, Z. Sun, W. Huang, Y. Ji, C. Wan, Poly(glycolic acid) (PGA): a versatile building block expanding high performance and sustainable bioplastic applications, Green Chem. (2020) 4055–4081.
[23] J. Gao, Y. Su, Y. Qin, Calcium phosphate coatings enhance biocompatibility and degradation resistance of magnesium alloy: correlating in vitro and in vivo studies, Bioact. Mater. 6 (2021) 1223–1229.
[24] Y. Lai, H. Cao, X. Wang, S. Chen, M. Zhang, N. Wang, Z. Yao, Y. Dai, X. Xie, P. Zhang, X. Yao, L. Qin, Porous composite scaffold incorporating osteogenic phytomolecule icariin for promoting skeletal regeneration in challenging osteonecrotic bone in rabbits, Biomaterials 153 (2018) 1–13.
[25] C. Pascual-González, J. de la Vega, C. Thompson, J.P. Fernández-Blázquez, D. Herráez-Molinero, N. Biurrun, I. Lizarralde, J.S. Del Río, C. González, J. Llorca, Processing and mechanical properties of novel biodegradable poly-lactic acid/Zn 3D printed scaffolds for application in tissue regeneration, J. Mech. Behav. Biomed. 132 (2022) 105290.
[26] A. Ferrández-Montero, M. Lieblich, J.L. González-Carrasco, R. Benavente, V. Lorenzo, R. Detsch, A.R. Boccaccini, B. Ferrari, Development of biocompatible and fully bioabsorbable PLA/Mg films for tissue regeneration applications, Acta Biomater. 98 (2019) 114–124.
[27] W. Ali, M. Echeverry-Rendón, A. Kopp, C. González, J. Llorca, Effect of surface modification on interfacial behavior in bioabsorbable magnesium wire reinforced poly-lactic acid polymer composites, Npj Mat. Degrad. 7 (2023) 14–65.
[28] X. Li, C. Chu, L. Zhou, J. Bai, C. Guo, F. Xue, P. Lin, P.K. Chu, Fully degradable PLA-based composite reinforced with 2D-braided Mg wires for orthopedic implants, Compos. Sci. Technol. 142 (2017) 180–188.

[29] H. Cai, X. Li, C. Chu, F. Xue, C. Guo, Q. Dong, J. Bai, Insight into the effect of interface on the mechanical properties of Mg/PLA composite plates, Compos. Sci. Technol. 183 (2019) 107801.
[30] M.S. Butt, J. Bai, X. Wan, C. Chu, F. Xue, H. Ding, G. Zhou, Mg alloy rod reinforced biodegradable poly-lactic acid composite for load bearing bone replacement, Surf. Coating. Technol. 309 (2017) 471–479.
[31] M.S. Butt, J. Bai, X. Wan, C. Chu, F. Xue, H. Ding, G. Zhou, Mechanical and degradation properties of biodegradable Mg strengthened poly-lactic acid composite through plastic injection molding, Mat. Sci. Eng. C-Mater. 70 (2017) 141–147.
[32] X. Wang, P. Shen, N. Gu, Y. Shao, M. Lu, C. Tang, W. Cheng, C. Chu, F. Xue, J. Bai, Dual Mg-reinforced PCL membrane with a Janus structure for vascularized bone regeneration and bacterial elimination, ACS Biomater. Sci. Eng. 10 (2023) 537–549.
[33] W. Ali, A. Mehboob, M. Han, S. Chang, Novel biodegradable hybrid composite of polylactic acid (PLA) matrix reinforced by bioactive glass (BG) fibres and magnesium (Mg) wires for orthopaedic application, Compos. Struct. 245 (2020) 112322.
[34] M. Wu, Q. Ren, X. Zhu, W. Li, H. Luo, F. Wu, L. Wang, W. Zheng, P. Cui, X. Yi, Super toughened blends of poly(lactic acid) and poly(butylene adipate-co-terephthalate) injection-molded foams via enhancing interfacial compatibility and cellular structure, Int. J. Biol. Macromol. 245 (2023) 125490.
[35] C. Argentati, F. Dominici, F. Morena, M. Rallini, I. Tortorella, A. Ferrandez-Montero, R.M. Pellegrino, B. Ferrari, C. Emiliani, M. Lieblich, L. Torre, S. Martino, I. Armentano, Thermal treatment of magnesium particles in polylactic acid polymer films elicits the expression of osteogenic differentiation markers and lipidome profile remodeling in human adipose stem cells, Int. J. Biol. Macromol. 223 (2022) 684–701.
[36] F. Bouaksa, C.O. Rodas, F. Za Ri, G. Stoclet, M. Na T-Abdelaziz, J.M. Gloaguen, T. Tamine, J.M. Lefebvre, Molecular chain orientation in polycarbonate during equal channel angular extrusion: experiments and simulations, Comput. Mater. Sci. 85 (2014) 244–252.
[37] H. Li, Z. Wu, F. Xue, J. Bai, C. Chu, Influence of equal channel angular pressing on the properties of polylactic acid, Polym. Eng. Sci. 58 (2018) 665–672.
[38] X. Li, C.L. Chu, L. Liu, X.K. Liu, J. Bai, C. Guo, F. Xue, P.H. Lin, P.K. Chu, Biodegradable poly-lactic acid based-composite reinforced unidirectionally with high-strength magnesium alloy wires, Biomaterials 49 (2015) 135–144.
[39] W. Ali, A. Mehboob, M. Han, S. Chang, Experimental study on degradation of mechanical properties of biodegradable magnesium alloy (AZ31) wires/poly (lactic acid) composite for bone fracture healing applications, Compos. Struct. 210 (2019) 914–921.
[40] H. Cai, Y. Zhang, X. Li, J. Meng, F. Xue, C. Chu, L. Tao, J. Bai, Self-reinforced biodegradable Mg-2Zn alloy wires/polylactic acid composite for orthopedic implants, Compos. Sci. Technol. 162 (2018) 198–205.
[41] H. Shi, H. Cheng, C. Han, Y. Yu, M. Yu, Y. Zhang, Uniaxial stretching and properties of miscible poly(L-lactide)/poly(vinyl acetate) blends, J. Therm. Anal. Calorim. 148 (2023) 6819–6832.
[42] L. Wang, J. Qiu, E. Sakai, Microstructures and mechanical properties of polylactic acid prepared by a cold rolling process, J. Mater. Process. Technol. 232 (2016) 184–194.
[43] X. Wang, Y. Qian, S. Wang, M. Wang, K. Sun, Z. Cheng, Y. Shao, S. Zhang, C. Tang, C. Chu, F. Xue, L. Tao, M. Lu, J. Bai, Accumulative rolling Mg/PLLA composite membrane with lamellar heterostructure for enhanced bacteria inhibition and rapid bone regeneration, Small 19 (2023) 202301638.
[44] Z. Chenguang, Z. Guang, High-Strength Absorbable Internal Fixation Bone Screw for Fracture, 2017. United States Patent, Patent No. US11607257B2, Date of Patent: Mar 21 2019.
[45] H. Lee, D.Y. Shin, Y. Na, G. Han, J. Kim, N. Kim, S. Bang, H.S. Kang, S. Oh, C. Yoon, J. Park, H. Kim, H. Jung, M. Kang, Antibacterial PLA/Mg composite with enhanced mechanical and biological performance for biodegradable orthopedic implants, Biomater. Adv. 152 (2023) 213523.
[46] F. Badkoobeh, H. Mostaan, M. Rafiei, H.R. Bakhsheshi-Rad, S. RamaKrishna, X. Chen, Additive manufacturing of biodegradable magnesium-based materials: design strategies, properties, and biomedical applications, J. Magnesium Alloys 11 (2023) 801–839.
[47] Q. Dong, M. Zhang, X. Zhou, Y. Shao, J. Li, L. Wang, C. Chu, F. Xue, Q. Yao, J. Bai, 3D-printed Mg-incorporated PCL-based scaffolds: a promising approach for bone healing, Mat. Sci. Eng. C-Mater. 129 (2021) 112372.
[48] J. Orellana-Barrasa, A. Ferrández-Montero, A.R. Boccaccini, B. Ferrari, J. Y. Pastor, The mechanical, thermal, and chemical properties of PLA-Mg filaments produced via a colloidal route for fused-filament fabrication, Polymers-Basel 14 (2022) 5414.
[49] W. Yu, R. Li, J. Long, P. Chen, A. Hou, L. Li, X. Sun, G. Zheng, H. Meng, Y. Wang, A. Wang, X. Sui, Q. Guo, S. Tao, J. Peng, L. Qin, S. Lu, Y. Lai, Use of a three-dimensional printed polylactide-coglycolide/tricalcium phosphate composite scaffold incorporating magnesium powder to enhance bone defect repair in rabbits, J Orthop. Transl 16 (2019) 62–70.
[50] Y. Lai, Y. Li, H. Cao, J. Long, X. Wang, L. Li, C. Li, Q. Jia, B. Teng, T. Tang, J. Peng, D. Eglin, M. Alini, D.W. Grijpma, G. Richards, L. Qin, Osteogenic magnesium incorporated into PLGA/TCP porous scaffold by 3D printing for repairing challenging bone defect, Biomaterials 197 (2019) 207–219.
[51] L. Huang, X. Wang, Y. Zhang, Z. Cheng, F. Xue, Y. Guo, Y. Deng, C. Chu, L. Tao, J. Bai, Electrospun Mg/poly(lactic-co-glycolic acid) composite scaffold for urethral reconstruction, J. Mater. Sci. 55 (2020) 13216–13231.
[52] S. Preethi Soundarya, A. Haritha Menon, S. Viji Chandran, N. Selvamurugan, Bone tissue engineering: scaffold preparation using chitosan and other biomaterials with different design and fabrication techniques, Int. J. Biol. Macromol. 119 (2018) 1228–1239.
[53] P. Wan, C. Yuan, L. Tan, Q. Li, K. Yang, Fabrication and evaluation of bioresorbable PLLA/magnesium and PLLA/magnesium fluoride hybrid composites for orthopedic implants, Compos. Sci. Technol. 98 (2014) 36–43.
[54] B. Chen, Z. Lin, Q. Saiding, Y. Huang, Y. Sun, X. Zhai, Z. Ning, H. Liang, W. Qiao, B. Yu, K.W.K. Yeung, J. Shen, Enhancement of critical-sized bone defect regeneration by magnesium oxide-reinforced 3D scaffold with improved osteogenic and angiogenic properties, J. Mater. Sci. Technol. 135 (2023) 186–198.
[55] A.M.P. Dupraz, S.A.T.V.D. Meer, J.R. De Wijn, J.H. Goedemoed, Biocompatibility screening of silane-treated hydroxyapatite powders, for use as filler in resorbable composites, J. Mater. Sci. Mater. Med. 7 (1996) 731–738.
[56] H. Cai, Y. Zhang, J. Meng, X. Li, F. Xue, C. Chu, L. Tao, J. Bai, Enhanced fully-biodegradable Mg/PLA composite rod: effect of surface modification of Mg-2Zn wire on the interfacial bonding, Surf. Coating. Technol. 350 (2018) 722–731.
[57] H. Lee, S. Chang, Thermoforming of partially biodegradable hybrid thermoplastic composites for bone plate applications, Compos. Part B-Eng. 270 (2024) 111123.
[58] A. Ferrandez-Montero, M. Lieblich, R. Benavente, J.L. González-Carrasco, B. Ferrari, New approach to improve polymer-Mg interface in biodegradable PLA/Mg composites through particle surface modification, Surf. Coating. Technol. 383 (2020) 125285.
[59] A. Ferrández-Montero, M. Lieblich, R. Benavente, J.L. González-Carrasco, B. Ferrari, Study of the matrix-filler interface in PLA/Mg composites manufactured by Material Extrusion using a colloidal feedstock, Addit. Manuf. 33 (2020) 110142.
[60] H. Cai, J. Meng, X. Li, F. Xue, C. Chu, C. Guo, J. Bai, In vitro degradation behavior of Mg wire/poly(lactic acid) composite rods prepared by hot pressing and hot drawing, Acta Biomater. 98 (2019) 125–141.
[61] X. Li, C.L. Chu, L. Liu, X.K. Liu, J. Bai, C. Guo, F. Xue, P.H. Lin, P.K. Chu, Biodegradable poly-lactic acid based-composite reinforced unidirectionally with high-strength magnesium alloy wires, Biomaterials 49 (2015) 135–144.
[62] X. Li, C. Chu, L. Zhou, J. Bai, C. Guo, F. Xue, P. Lin, P.K. Chu, Fully degradable PLA-based composite reinforced with 2D-braided Mg wires for orthopedic implants, Compos. Sci. Technol. 142 (2017) 180–188.
[63] C. Ling, Q. Li, Z. Zhang, Y. Yang, W. Zhou, W. Chen, Z. Dong, C. Pan, C. Shuai, Influence of heat treatment on microstructure, mechanical and corrosion behavior of WE43 alloy fabricated by laser-beam powder bed fusion, Int. J. Extrem. Manuf. 6 (2024) 15001.
[64] H. Xu, J. Jiang, G. Bi, S. Meng, X. Zhang, Y. Li, T. Chen, Microstructure and mechanical properties of extruded and rolled Mg–Y–Zn–Ni–Co alloy, J. Mater. Res. Technol. 27 (2023) 8323–8333.
[65] S. Abazari, A. Shamsipur, H.R. Bakhsheshi-Rad, J.W. Drelich, J. Goldman, S. Sharif, A.F. Ismail, M. Razzaghi, Magnesium-based nanocomposites: a review from mechanical, creep and fatigue properties, J. Magnesium Alloys 11 (2023) 2655–2687.
[66] T. Xin, Y. Zhao, R. Mahjoub, J. Jiang, A. Yadav, K. Nomoto, R. Niu, S. Tang, F. Ji, Z. Quadir, D. Miskovic, J. Daniels, W. Xu, X. Liao, L. Chen, K. Hagihara, X. Li, S. Ringer, M. Ferry, Ultrahigh specific strength in a magnesium alloy strengthened by spinodal decomposition, Sci. Adv. 7 (2021) f3039.
[67] S. Goutianos, L. Van der Schueren, J. Beauson, Failure mechanisms in unidirectional self-reinforced biobased composites based on high stiffness PLA fibres, Compos. Part. A-Appl. S. 117 (2019) 169–179.
[68] C. Li, T. Jiang, J. Wang, H. Wu, S. Guo, X. Zhang, J. Li, J. Shen, R. Chen, Y. Xiong, In situ formation of microfibrillar crystalline superstructure: achieving high-performance polylactide, ACS Appl. Mater. Interfaces 9 (2017) 25818–25829.
[69] E. Merz, G. Claver, M. Baer, Studies on heterogeneous polymeric systems, J. Polym. Sci. 22 (1956) 325–341.
[70] C.B. Bucknall, R.R. Smith, Stress-whitening in high-impact polystyrenes, Polymer 6 (1965) 437–446.
[71] S. Newman, S. Strella, Stress-strain behavior of rubber-reinforced glassy polymers, J. Appl. Polym. Sci. 9 (1965) 2297–2310.
[72] S. Strella, Rubber reinforcement of glassy polymers, J. Polym. Sci., Part A: Polym. Phys. 4 (1966) 527.
[73] C. Bucknall, J. Reid, W. Stevens, Fracture behavior of high-impact polystyrene under an aggressive environment, Abstr. Am. Chem. Soc. 173 (1977) 9.
[74] A. Yee, R. Pearson, Toughening mechanisms in elastomer-modified epoxies, J. Mater. Sci. 21 (1986) 2462–2474.
[75] M. Alia, W. Souheng, Percolation model for brittle-tough transition in nylon/rubber blends, Polymer 29 (1988) 2170–2173.
[76] S. Wu, Chain structure, phase morphology, and toughness relationships in polymers and blends, Polym. Eng. Sci. 30 (1990) 753–761.
[77] T. Kurauchi, T. Ohta, Energy absorption in blends of polycarbonate with ABS and SAN, J. Mater. Sci. 19 (1984) 1699–1709.
[78] C. Wang, C. Song, D. Mei, L. Wang, W. Wang, T. Wu, D. Snihirova, M. L. Zheludkevich, S.V. Lamaka, Low interfacial pH discloses the favorable biodegradability of several Mg alloys, Corrosion Sci. 197 (2022) 110059.
[79] C. Li, X. Fan, L. Cui, R. Zeng, Corrosion resistance and electrical conductivity of a nano ATO-doped MAO/methyltrimethoxysilane composite coating on magnesium alloy AZ31, Corrosion Sci. 168 (2020) 108570.
[80] Y. Zhang, J. Cao, M. Lu, Y. Shao, K. Jiang, X. Yang, X. Xiong, S. Wang, C. Chu, F. Xue, Y. Ye, J. Bai, A biodegradable magnesium surgical staple for colonic anastomosis: in vitro and in vivo evaluation, Bioact. Mater. 22 (2023) 225–238.
[81] S.C. Cifuentes, R. Gavilán, M. Lieblich, R. Benavente, J.L. González-Carrasco, In vitro degradation of biodegradable polylactic acid/magnesium composites: relevance of Mg particle shape, Acta Biomater. 32 (2016) 348–357.

[82] L. Liu, Y. Wu, J. Ye, Q. Fu, L. Su, Z. Wu, J. Feng, Z. Chen, J. Song, Synthesis of magnesium nanoparticle for NIR-II-photoacoustic-imaging-guided synergistic burst-like and H2 cancer therapy, Chem 8 (2022) 2990–3007.
[83] Z. Mohamadnia, E. Ahmadi, M. Rafienia, H. Mirzadeh, H. Mobedi, Investigation of drug release and 1H-NMR analysis of the insitu forming systems based on poly (lactide-co-glycolide), Polym. Adv. Technol. 20 (2009) 48–57.
[84] M.N. Collins, G. Ren, K. Young, S. Pina, R.L. Reis, J.M. Oliveira, Scaffold fabrication technologies and structure/function properties in bone tissue engineering, Adv. Funct. Mater. 31 (2021) 2010609.
[85] H. Tsuji, C.A. Del Carpio, In vitro hydrolysis of blends from enantiomeric poly (lactide)s. 3. Homocrystallized and amorphous blend films, Biomacromolecules 4 (2003) 7–11.
[86] H. Tsuji, Autocatalytic hydrolysis of amorphous-made polylactides: effects of l-lactide content, tacticity, and enantiomeric polymer blending, Polymer (Guilford) 43 (2002) 1789–1796.
[87] X. Li, C. Chu, Y. Wei, C. Qi, J. Bai, C. Guo, F. Xue, P. Lin, P.K. Chu, In vitro degradation kinetics of pure PLA and Mg/PLA composite: effects of immersion temperature and compression stress, Acta Biomater. 48 (2017) 468–478.
[88] X. Wang, X. Li, N. Gu, Y. Shao, Y. Guo, Y. Deng, C. Chu, F. Xue, L. Huang, L. Tao, J. Bai, pH-responsive, self-sculptured Mg/PLGA composite microfibers for accelerated revascularization and soft tissue regeneration, Biomater. Adv. 158 (2024) 213767.
[89] S.C. Cifuentes, M. Lieblich, L. Saldaña, J.L. González-Carrasco, R. Benavente, In vitro degradation of biodegradable polylactic acid/Mg composites: influence of nature and crystalline degree of the polymeric matrix, Materialia 6 (2019) 100270.
[90] D. Mei, S.V. Lamaka, X. Lu, M.L. Zheludkevich, Selecting medium for corrosion testing of bioabsorbable magnesium and other metals-A critical review, Corrosion Sci. 171 (2020) 108722.
[91] A. Kahlberg, Y. Tshomba, D. Baccellieri, L. Bertoglio, E. Rinaldi, V. Ardita, E. Colombo, U. Moscato, G. Melissano, R. Chiesa, Renal perfusion with histidine-tryptophan-ketoglutarate compared with Ringer's solution in patients undergoing thoracoabdominal aortic open repair, J. Thorac. Cardiovasc. Surg. 165 (2023) 569–579.
[92] Z. Wang, J. Chen, X. Wu, D. Ma, X. Zhang, R. Li, C. Han, H. Liu, X. Yin, Q. Du, D. Tong, Y. Huang, PCV2 targets cGAS to inhibit type I interferon induction to promote other DNA virus infection, PLoS Pathog. 17 (2021) e1009940.
[93] Y. Zhang, J. Cao, X. Wang, H. Liu, Y. Shao, C. Chu, F. Xue, J. Bai, The effect of enzymes on the in vitro degradation behavior of Mg alloy wires in simulated gastric fluid and intestinal fluid, Bioact. Mater. 7 (2022) 217–226.
[94] H. Tsuji, K. Ikarashi, In vitro hydrolysis of poly(l-lactide) crystalline residues as extended-chain crystallites, Polym. Degrad. Stabil. 85 (2004) 647–656.
[95] Q. Dong, X. Zhou, Y. Feng, K. Qian, H. Liu, M. Lu, C. Chu, F. Xue, J. Bai, Insights into self-healing behavior and mechanism of dicalcium phosphate dihydrate coating on biomedical Mg, Bioact. Mater. 6 (2021) 158–168.
[96] H. Liu, X. Li, H. Yao, P. Sun, Enhanced strategies for phosphate recovery from urine by magnesium galvanic process, Water Res. 245 (2023) 120669.
[97] C. Zhao, F. Cao, G. Song, Corrosivity of haze constituents to pure Mg, J. Magnesium Alloys 8 (2020) 150–162.
[98] N. Hegyesi, Y. Zhang, A. Kohári, P. Polyák, X. Sui, B. Pukánszky, Enzymatic degradation of PLA/cellulose nanocrystal composites, Ind. Crop. Prod. 141 (2019) 111799.
[99] R. Hou, F. Feyerabend, H. Helmholz, V.M. Garamus, R. Willumeit-Römer, Effects of proteins on magnesium degradation - static vs. dynamic conditions, J. Magnesium Alloys 11 (2023) 1332–1342.
[100] X. Qi, Y. Ren, X. Wang, New advances in the biodegradation of Poly(lactic) acid, Int. Biodeterior. Biodegrad. 117 (2017) 215–223.
[101] P. Rytlewski, M. Stepczyńska, U. Gohs, R. Malinowski, B. Budner, M. Żenkiewicz, Flax fibres reinforced polylactide modified by ionizing radiation, Ind. Crop. Prod. 112 (2018) 716–723.
[102] D. Mei, S.V. Lamaka, C. Feiler, M.L. Zheludkevich, The effect of small-molecule bio-relevant organic components at low concentration on the corrosion of commercially pure Mg and Mg-0.8Ca alloy: an overall perspective, Corrosion Sci. 153 (2019) 258–271.
[103] W. Yan, Y. Lian, Z. Zhang, M. Zeng, Z. Zhang, Z. Yin, L. Cui, R. Zeng, In vitro degradation of pure magnesium–the synergetic influences of glucose and albumin, Bioact. Mater. 5 (2020) 318–333.
[104] V. Luque-Agudo, J.M. Casares-López, M.L. González-Martín, A.M. Gallardo-Moreno, M. Hierro-Oliva, PLA-Mg film degradation under in vitro environments supplemented with glucose and/or ketone bodies, Polym. Test. 127 (2023) 108189.
[105] J. Zhang, S. Hiromoto, T. Yamazaki, J. Niu, H. Huang, G. Jia, H. Li, W. Ding, G. Yuan, Effect of macrophages on in vitro corrosion behavior of magnesium alloy, J. Biomed. Mater. Res. A 104 (2016) 2476–2487.
[106] L. Li, Z. Han, R. Zeng, W. Qi, X. Zhai, Y. Yang, Y. Lou, T. Gu, D. Xu, J. Duan, Microbial ingress and in vitro degradation enhanced by glucose on bioabsorbable Mg-Li-Ca alloy, Bioact. Mater. 5 (2020) 902–916.
[107] M. Yao, L. Liu, C. Ma, H. Zhang, Y. Zhang, R. Song, Z. Fang, P. Song, A lysine-derived flame retardant for improved flame retardancy, crystallinity, and aqueous-phase degradation of polylactide, Chem. Eng. J. 462 (2023) 142189.
[108] Y. Wang, T. Hu, W. Zhang, J. Lin, Z. Wang, S. Lyu, H. Tong, Biodegradation of polylactic acid by a mesophilic bacteria Bacillus safensis, Chemosphere 318 (2023) 137991.
[109] X. Li, C. Chu, Y. Wei, C. Qi, J. Bai, C. Guo, F. Xue, P. Lin, P.K. Chu, In vitro degradation kinetics of pure PLA and Mg/PLA composite: effects of immersion temperature and compression stress, Acta Biomater. 48 (2017) 468–478.
[110] L. Yang, W. Zhen, Poly(lactic acid)/p-phenylenediamine functionalized graphene oxidized nanocomposites: preparation, rheological behavior and biodegradability, Eur. Polym. J. 121 (2019) 109341.
[111] S.V. Lamaka, J. Gonzalez, D. Mei, F. Feyerabend, R. Willumeit Römer, M. L. Zheludkevich, Local pH and its evolution near Mg alloy surfaces exposed to simulated body fluids, Adv. Mater. Interfac. 5 (2018).
[112] X. Li, C. Chu, P.K. Chu, Effects of external stress on biodegradable orthopedic materials: a review, Bioact. Mater. 1 (2016) 77–84.
[113] X. Li, Y. Wang, C. Chu, L. Han, J. Bai, F. Xue, A study on Mg wires/poly-lactic acid composite degradation under dynamic compression and bending load for implant applications, J. Mech. Behav. Biomed. Mater. 105 (2020) 103707.
[114] Q. Ma, Z. Miri, H.J. Haugen, A.M. Loca, L. Dagnjia, Significance of mechanical loading in bone fracture healing, bone regeneration, and vascularization, J. Tissue Eng. 14 (2023) 1778662877.
[115] S.K. Samijo, J.M. Willigers, R. Barkhuysen, P.J.E.H. Kitslaar, R.S. Renemaan, P. J. Brands, A.P.G. Hoeks, Wall shear stress in the human common carotid artery as function of age and gender, Cardiovasc. Res. 39 (1998) 515–522.
[116] T. Shang, K. Wang, L. Zhang, L. Zhou, L. Liu, C. Liu, H. Zhang, X. Li, Y. Zhao, J. Wang, A microfluidic system simulating physiological fluid environment for studying the degradation behaviors of magnesium-based materials, J Sci.-Adv. Mater. Dev. 8 (2023) 100590.
[117] Z. Chu, X. Li, Y. Li, Q. Zheng, C. Feng, M. Guo, X. Ding, W. Feng, Y. Gao, J. Yao, X. Chen, L. Wang, Y. Fan, Effects of different fluid shear stress patterns on the in vitro degradation of poly(lactide-co-glycolide) acid membranes, J. Biomed. Mater. Res. 105 (2017) 23–30.
[118] Y. Wang, C. Liu, Z. Jiao, L. Cai, C. Sun, D. Wang, L. Cui, C. Wen, R. Zeng, Corrosion behavior and mechanical property of Mg-4Li-1Ca alloys under micro-compressive stress, J. Mater. Sci. Technol. 175 (2024) 170–184.
[119] B. Wei, D. Legut, S. Sun, H.T. Wang, Z.Z. Shi, H.J. Zhang, R.F. Zhang, An improved electrochemical model for strain dependent electrochemical polarization and corrosion kinetics, Mater. Des. 202 (2021) 109555.
[120] B. Wei, D. Legut, S. Sun, H.T. Wang, Z.Z. Shi, H.J. Zhang, R.F. Zhang, Synergistic effect of solute and strain on the electrochemical degradation in representative Zn-based and Mg-based alloys, Corrosion Sci. 188 (2021) 109539.
[121] I.P. Etim, W. Zhang, Y. Zhang, L. Tan, K. Yang, Microstructural evolution and biodegradation response of Mg–2Zn–0.5Nd alloy during tensile and compressive deformation, Acta Metall. Sin. 34 (2021) 834–844.
[122] R.H. Rubinstein, Polymer physics, Polymer Physics (2003), https://doi.org/10.1093/oso/9780198520597.001.0001.
[123] D.H.K. Chow, J. Wang, P. Wan, L. Zheng, M.T.Y. Ong, L. Huang, W. Tong, L. Tan, K. Yang, L. Qin, Biodegradable magnesium pins enhanced the healing of transverse patellar fracture in rabbits, Bioact. Mater. 6 (2021) 4176–4185.
[124] X. Li, C. Qi, L. Han, C. Chu, J. Bai, C. Guo, F. Xue, B. Shen, P.K. Chu, Influence of dynamic compressive loading on the in vitro degradation behavior of pure PLA and Mg/PLA composite, Acta Biomater. 64 (2017) 269–278.
[125] N. Zhou, P. Li, H. Qiu, J. Wang, N. Huang, A. Zhao, J. Wang, Comparison of in vascular bioreactors and in vivo models of degradation and cellular response of Mg-Zn-Mn stents, Ann. Biomed. Eng. 49 (2021) 1551–1560.
[126] L.A. Damiati, M. El-Yaagoubi, S.A. Damiati, R. Kodzius, F. Sefat, S. Damiati, Role of polymers in microfluidic devices, Polymers-Basel 14 (2022) 5132.
[127] B. Zhang, A. Korolj, B.F.L. Lai, M. Radisic, Advances in organ-on-a-chip engineering, Nat. Rev. Mater. 3 (2018) 257–278.
[128] C. Ye, J. Wang, A. Zhao, D. He, M.F. Maitz, N. Zhou, N. Huang, Atorvastatin eluting coating for magnesium-based stents: control of degradation and endothelialization in a microfluidic assay and in vivo, Adv. Mater. Technol. 5 (2020).
[129] B. Zhang, M. Montgomery, M.D. Chamberlain, S. Ogawa, A. Korolj, A. Pahnke, L. A. Wells, S. Massé, J. Kim, L. Reis, A. Momen, S.S. Nunes, A.R. Wheeler, K. Nanthakumar, G. Keller, M.V. Sefton, M. Radisic, Biodegradable scaffold with built-in vasculature for organ-on-a-chip engineering and direct surgical anastomosis, Nat. Mater. 15 (2016) 669–678.
[130] B. Zhang, B.F.L. Lai, R. Xie, L. Davenport Huyer, M. Montgomery, M. Radisic, Microfabrication of AngioChip, a biodegradable polymer scaffold with microfluidic vasculature, Nat. Protoc. 13 (2018) 1793–1813.
[131] K. Ronaldson-Bouchard, D. Teles, K. Yeager, D.N. Tavakol, Y. Zhao, A. Chramiec, S. Tagore, M. Summers, S. Stylianos, M. Tamargo, B.M. Lee, S.P. Halligan, E. H. Abaci, Z. Guo, J. Jacków, A. Pappalardo, J. Shih, R.K. Soni, S. Sonar, C. German, A.M. Christiano, A. Califano, K.K. Hirschi, C.S. Chen, A. Przekwas, G. Vunjak-Novakovic, A multi-organ chip with matured tissue niches linked by vascular flow, Nat. Biomed. Eng. 6 (2022) 351–371.
[132] M. Echeverry-Rendón, F. Echeverria, H. Buikema, M.C. Harmsen, G. Krenning, Endothelial function after the exposition of magnesium degradation products, Biomater. Adv. 134 (2022) 112693.
[133] H. Hanna, L.M. Mir, F.M. Andre, In vitro osteoblastic differentiation of mesenchymal stem cells generates cell layers with distinct properties, Stem Cell Res. Ther. 9 (2018).
[134] Y. Leem, K. Lee, J. Kim, H. Seok, J. Chang, D. Lee, Magnesium ions facilitate integrin alpha 2- and alpha 3-mediated proliferation and enhance alkaline phosphatase expression and activity in hBMSCs, J. Tissue Eng. Regen. M. 10 (2016) E527–E536.
[135] X. Nie, X. Sun, C. Wang, J. Yang, Effect of magnesium ions/Type I collagen promote the biological behavior of osteoblasts and its mechanism, Regen. Biomater. 7 (2020) 53–62.
[136] J. Wang, J. Xu, B. Song, D.H. Chow, P. Shu-hang Yung, L. Qin, Magnesium (Mg) based interference screws developed for promoting tendon graft incorporation in bone tunnel in rabbits, Acta Biomater. 63 (2017) 393–410.

[137] Y. Yan, Y. Wei, R. Yanga, L. Xia, C. Zhao, B. Gao, X. Zhang, J. Fu, Q. Wang, N. Xu, Enhanced osteogenic differentiation of bone mesenchymal stem cells on magnesium-incorporated titania nanotube arrays, Colloids Surf., B 179 (2019) 309–316.
[138] X. Zhang, H. Zu, D. Zhao, K. Yang, S. Tian, X. Yu, F. Lu, B. Liu, X. Yu, B. Wang, W. Wang, S. Huang, Y. Wang, Z. Wang, Z. Zhang, Ion channel functional protein kinase TRPM7 regulates Mg ions to promote the osteoinduction of human osteoblast via PI3K pathway: in vitro simulation of the bone-repairing effect of Mg-based alloy implant, Acta Biomater. 63 (2017) 369–382.
[139] L. Qi, X. Fang, J. Yan, C. Pan, W. Ge, J. Wang, S.G. Shen, K. Lin, L. Zhang, Magnesium-containing bioceramics stimulate exosomal miR-196a-5p secretion to promote senescent osteogenesis through targeting Hoxa7/MAPK signaling axis, Bioact. Mater. 33 (2024) 14–29.
[140] C. Hung, A. Chaya, K. Liu, K. Verdelis, C. Sfeir, The role of magnesium ions in bone regeneration involves the canonical Wnt signaling pathway, Acta Biomater. 98 (2019) 246–255.
[141] L. Zhou, V.O. Gjvm, J. Malda, M.J. Stoddart, Y. Lai, R.G. Richards, K. Ki Wai Ho, L. Qin, Innovative tissue-engineered strategies for osteochondral defect repair and regeneration: current progress and challenges, Adv. Healthcare Mater. 9 (2020).
[142] L. Zheng, S. Zhao, Y. Li, J. Xu, W. Yan, B. Guo, J. Xu, L. Jiang, Y. Zhang, H. Wei, Q. Jiang, Engineered MgO nanoparticles for cartilage-bone synergistic therapy, Sci. Adv. 10 (2024) k6084.
[143] C. Gao, W. Dai, X. Wang, L. Zhang, Y. Wang, Y. Huang, Z. Yuan, X. Zhang, Y. Yu, X. Yang, Q. Cai, Magnesium gradient-based hierarchical scaffold for dual-lineage regeneration of osteochondral defect, Adv. Funct. Mater. 33 (2023).
[144] J. Zhao, H. Wu, L. Wang, D. Jiang, P. Jia, W. Jia, The beneficial potential of magnesium-based scaffolds to promote chondrogenesis through controlled Mg2+ release in eliminating the destructive effect of activated macrophages on chondrocytes, Biomater. Adv. (2022) 112719.
[145] C. Zhang, Y. Lin, Q. Liu, J. He, P. Xiang, D. Wang, X. Hu, J. Chen, W. Zhu, H. Yu, Growth differentiation factor 11 promotes differentiation of MSCs into endothelial-like cells for angiogenesis, J. Cell Mol. Med. 24 (2020) 8703–8717.
[146] L. Huang, X. Wang, Y. Zhang, Z. Cheng, F. Xue, Y. Guo, Y. Deng, C. Chu, L. Tao, J. Bai, Electrospun Mg/poly(lactic-co-glycolic acid) composite scaffold for urethral reconstruction, J. Mater. Sci. 55 (2020) 13216–13231.
[147] L.Y. Li, Z. Yang, X.X. Pan, B.X. Feng, R. Yue, B. Yu, Y.F. Zheng, J.Y. Tan, G. Y. Yuan, J. Pei, Incorporating copper to biodegradable magnesium alloy vascular stents via a Cu(II)-Eluting coating for synergistic enhancement in prolonged durability and rapid Re-endothelialization, Adv. Funct. Mater. 32 (2022) 2205634.
[148] W. Liao, M. Jiang, M. Li, C. Jin, S. Xiao, S. Fan, W. Fang, Y. Zheng, J. Liu, Magnesium elevation promotes neuronal differentiation while suppressing glial differentiation of primary cultured adult mouse neural progenitor cells through ERK/CREB activation, Front. Neurosci. 11 (2017), https://doi.org/10.3389/fnins.2017.00087.
[149] Z. Li, C.A. Meyers, L. Chang, S. Lee, Z. Li, R. Tomlinson, A. Hoke, T.L. Clemens, A. W. James, Fracture repair requires TrkA signaling by skeletal sensory nerves, J. Clin. Invest. 129 (2019) 5137–5150.
[150] X. Jing, C. Xu, W. Su, Q. Ding, B. Ye, Y. Su, K. Yu, L. Zeng, X. Yang, Y. Qu, K. Chen, T. Sun, Z. Luo, X. Guo, Photosensitive and conductive hydrogel induced innerved bone regeneration for infected bone defect repair, Adv. Healthcare Mater. 12 (2023) 2201349.
[151] Y. Xia, X. Jing, X. Wu, P. Zhuang, X. Guo, H. Dai, 3D-printed dual-ion chronological release functional platform reconstructs neuro-vascularization network for critical-sized bone defect regeneration, Chem. Eng. J. 465 (2023) 143015.
[152] Z. Lin, J. Wu, W. Qiao, Y. Zhao, K.H.M. Wong, P.K. Chu, L. Bian, S. Wu, Y. Zheng, K.M.C. Cheung, F. Leung, K.W.K. Yeung, Precisely controlled delivery of magnesium ions thru sponge-like monodisperse PLGA/nano-MgO-alginate core-shell microsphere device to enable in-situ bone regeneration, Biomaterials 174 (2018) 1–16.
[153] F. Yang, X. Niu, X. Gu, C. Xu, W. Wang, Y. Fan, Biodegradable magnesium-incorporated poly(L-lactic acid) microspheres for manipulation of drug release and alleviation of inflammatory response, ACS Appl. Mater. Interfaces 11 (2019) 23546–23557.
[154] W. Qiao, K.H.M. Wong, J. Shen, W. Wang, J. Wu, J. Li, Z. Lin, Z. Chen, J. P. Matinlinna, Y. Zheng, S. Wu, X. Liu, K.P. Lai, Z. Chen, Y.W. Lam, K.M. C. Cheung, K.W.K. Yeung, TRPM7 kinase-mediated immunomodulation in macrophage plays a central role in magnesium ion-induced bone regeneration, Nat. Commun. 12 (2021) 2885.
[155] M. He, Q. Wang, Y. Feng, X. Gao, C. He, J. Li, W. Zhao, W. Tian, C. Zhao, Spatiotemporal management of the osteoimmunomodulation of fibrous scaffolds by loading a novel amphiphilic, Nanomedicine. ACS Appl. Mater. Interfaces 14 (2022) 13991–14003.
[156] U. Adhikari, X. An, N. Rijal, T. Hopkins, S. Khanal, T. Chavez, R. Tatu, J. Sankar, K.J. Little, D.B. Hom, N. Bhattarai, S.K. Pixley, Embedding magnesium metallic particles in polycaprolactone nanofiber mesh improves applicability for biomedical applications, Acta Biomater. 98 (2019) 215–234.
[157] J. Tan, S. Li, C. Sun, G. Bao, M. Liu, Z. Jing, H. Fu, Y. Sun, Q. Yang, Y. Zheng, X. Wang, H. Yang, A dose-dependent spatiotemporal response of angiogenesis elicited by Zn biodegradation during the initial stage of bone regeneration, Adv. Healthcare Mater. 13 (2023) 2302305.
[158] L. Sun, X. Li, M. Xu, F. Yang, W. Wang, X. Niu, In vitro immunomodulation of magnesium on monocytic cell toward anti-inflammatory macrophages, Regen. Biomater. 7 (2020) 391–401.
[159] W. Qiao, D. Pan, Y. Zheng, S. Wu, X. Liu, Z. Chen, M. Wan, S. Feng, K.M. C. Cheung, K.W.K. Yeung, X. Cao, Divalent metal cations stimulate skeleton interoception for new bone formation in mouse injury models, Nat. Commun. 13 (2022) 535.
[160] Y. Zhang, J. Xu, Y.C. Ruan, M.K. Yu, M. O'Laughlin, H. Wise, D. Chen, L. Tian, D. Shi, J. Wang, S. Chen, J.Q. Feng, D.H.K. Chow, X. Xie, L. Zheng, L. Huang, S. Huang, K. Leung, N. Lu, L. Zhao, H. Li, D. Zhao, X. Guo, K. Chan, F. Witte, H. C. Chan, Y. Zheng, L. Qin, Implant-derived magnesium induces local neuronal production of CGRP to improve bone-fracture healing in rats, Nat. Med. 22 (2016) 1160–1169.
[161] B. Xu, Y. Song, K. Yang, Y. Li, B. Chen, X. Liao, Q. Jia, Magnesium metal and its corrosion products: promising materials for tumor interventional therapy, J. Magnesium Alloys 11 (2023) 763–775.
[162] R. Zan, H. Wang, W. Cai, J. Ni, B.J.C. Luthringer-Feyerabend, W. Wang, H. Peng, W. Ji, J. Yan, J. Xia, Y. Song, X. Zhang, Controlled release of hydrogen by implantation of magnesium induces P53-mediated tumor cells apoptosis, Bioact. Mater. 9 (2022) 385–396.
[163] R. Ma, Y. Lai, L. Li, H. Tan, J. Wang, Y. Li, T. Tang, L. Qin, Bacterial inhibition potential of 3D rapid-prototyped magnesium-based porous composite scaffolds–an in vitro efficacy study, Sci. Rep. 5 (2015).
[164] H. Lee, D.Y. Shin, S. Bang, G. Han, Y. Na, H.S. Kang, S. Oh, C. Yoon, S. Vijayavenkataraman, J. Song, H. Kim, H. Jung, M. Kang, A strategy for enhancing bioactivity and osseointegration with antibacterial effect by incorporating magnesium in polylactic acid based biodegradable orthopedic implant, Int. J. Biol. Macromol. 254 (2024) 127797.
[165] H. Feng, G. Wang, W. Jin, X. Zhang, Y. Huang, A. Gao, H. Wu, G. Wu, P.K. Chu, Systematic study of inherent antibacterial properties of magnesium-based biomaterials, ACS Appl. Mater. Interfaces 8 (2016) 9662–9673.
[166] M.C. Fernández-Calderón, D. Romero-Guzmán, A. Ferrández-Montero, C. Pérez-Giraldo, J.L. González-Carrasco, M. Lieblich, R. Benavente, B. Ferrari, M. L. González-Martín, A.M. Gallardo-Moreno, Impact of PLA/Mg films degradation on surface physical properties and biofilm survival, Colloids Surf., B 185 (2020) 110617.
[167] X. Gu, Y. Zheng, Y. Cheng, S. Zhong, T. Xi, In vitro corrosion and biocompatibility of binary magnesium alloys, Biomaterials 30 (2009) 484–498.
[168] H. Lee, D.Y. Shin, Y. Na, G. Han, J. Kim, N. Kim, S. Bang, H.S. Kang, S. Oh, C. Yoon, J. Park, H. Kim, H. Jung, M. Kang, Antibacterial PLA/Mg composite with enhanced mechanical and biological performance for biodegradable orthopedic implants, Biomater. Adv. 152 (2023) 213523.
[169] Y. Feng, S. Zhu, L. Wang, L. Chang, Y. Hou, S. Guan, Fabrication and characterization of biodegradable Mg-Zn-Y-Nd-Ag alloy: microstructure, mechanical properties, corrosion behavior and antibacterial activities, Bioact. Mater. 3 (2018) 225–235.
[170] W. Zhang, L. Zeng, H. Yu, Z. He, C. Huang, C. Li, Y. Nie, L. Li, F. Zhou, B. Liu, Y. Zhang, Z. Yao, W. Zhang, L. Qin, D. Chen, Q. He, Y. Lai, Injectable spontaneous hydrogen-releasing hydrogel for long-lasting alleviation of osteoarthritis, Acta Biomater. 158 (2023) 163–177.
[171] W.L. Wan, Y.J. Lin, P.C. Shih, Y.R. Bow, Q. Cui, Y. Chang, W.T. Chia, H.W. Sung, An in situ depot for continuous evolution of gaseous H2 mediated by a magnesium passivation/activation cycle for treating osteoarthritis, Angew. Chem. Int. Ed. 57 (2018) 9875–9879.
[172] Q. Dong, X. Zhou, Y. Feng, K. Qian, H. Liu, M. Lu, C. Chu, F. Xue, J. Bai, Insights into self-healing behavior and mechanism of dicalcium phosphate dihydrate coating on biomedical Mg, Bioact. Mater. 6 (2021) 158–168.
[173] Y. Qu, K. Lu, Y. Zheng, C. Huang, G. Wang, Y. Zhang, Q. Yu, Photothermal scaffolds/surfaces for regulation of cell behaviors, Bioact. Mater. 8 (2022) 449–477.
[174] Y. Zhang, C. Li, W. Zhang, J. Deng, Y. Nie, X. Du, L. Qin, Y. Lai, 3D-printed NIR-responsive shape memory polyurethane/magnesium scaffolds with tight-contact for robust bone regeneration, Bioact. Mater. 16 (2022) 218–231.
[175] Y. Zhao, P. He, J. Yao, M. Li, B. Wang, L. Han, Z. Huang, C. Guo, J. Bai, F. Xue, Y. Cong, W. Cai, P.K. Chu, C. Chu, pH/NIR-responsive and self-healing coatings with bacteria killing, osteogenesis, and angiogenesis performances on magnesium alloy, Biomaterials 301 (2023) 122237.
[176] Z. Chen, L. Su, Y. Wu, J. Liu, R. Wu, Q. Li, C. Wang, L. Liu, J. Song, Design and synthesis of a small molecular NIR-II chemiluminescence probe for in vivo-activated H2S imaging, Proc. Natl. Acad. Sci. USA 120 (2023) e2089781176.
[177] Z. Liu, X. Wan, Z.L. Wang, L. Li, Electroactive biomaterials and systems for cell fate determination and tissue regeneration: design and applications, Adv. Mater. 33 (2021) 2007429.
[178] Q. Zheng, Y. Zou, Y. Zhang, Z. Liu, B. Shi, X. Wang, Y. Jin, H. Ouyang, Z. Li, Z. L. Wang, Biodegradable triboelectric nanogenerator as a life-time designed implantable power source, Sci. Adv. 2 (2016) e1501478.
[179] A. Pardo, M. Gómez-Florit, S. Barbosa, P. Taboada, R.M.A. Domingues, M. E. Gomes, Magnetic nanocomposite hydrogels for tissue engineering: design concepts and remote actuation strategies to control cell fate, ACS Nano 15 (2021) 175–209.
[180] J. Koo, M.R. MacEwan, S. Kang, S.M. Won, M. Stephen, P. Gamble, Z. Xie, Y. Yan, Y. Chen, J. Shin, N. Birenbaum, S. Chung, S.B. Kim, J. Khalifeh, D.V. Harburg, K. Bean, M. Paskett, J. Kim, Z.S. Zohny, S.M. Lee, R. Zhang, K. Luo, B. Ji, A. Banks, H.M. Lee, Y. Huang, W.Z. Ray, J.A. Rogers, Wireless bioresorbable electronic system enables sustained nonpharmacological neuroregenerative therapy, Nat. Med. 24 (2018) 1830–1836.
[181] R.V. Chernozem, I.O. Pariy, A. Pryadko, A.P. Bonartsev, V.V. Voinova, V. A. Zhuikov, T.K. Makhina, G.A. Bonartseva, K.V. Shaitan, V.V. Shvartsman, D. C. Lupascu, K.N. Romanyuk, A.L. Kholkin, R.A. Surmenev, M.A. Surmeneva,

A comprehensive study of the structure and piezoelectric response of biodegradable polyhydroxybutyrate-based films for tissue engineering applications, Polym. J. 54 (2022) 1225–1236.
[182] C. Zhao, J. Zhang, Z.L. Wang, K. Ren, A poly(l-lactic acid) polymer-based thermally stable cantilever for vibration energy harvesting applications, Adv. Sustain. Syst. 1 (2017) 1700068.
[183] Y. Ren, X. Hu, Y. Chen, L. Liu, R. Qu, H. Xu, X. Song, A drug-loaded amphiphilic polymer/poly(l-lactide) shape-memory system, Int. J. Biol. Macromol. 217 (2022) 1037–1043.
[184] X. Wang, Y. Zhang, P. Shen, Z. Cheng, C. Chu, F. Xue, J. Bai, Preparation of 4D printed peripheral vascular stent and its degradation behavior under fluid shear stress after deployment, Biomater. Sci. 10 (2022) 2302–2314.